EFFECTS OF ADDITIVES ON ANALYTE MIGRATION BEHAVIOR IN CAPILLARY ELECTROPHORESIS

by

ANDREA R. KRANACK

B.Sc., University of New Brunswick, 1995

A THESIS SUBMITTED IN PARTIAL FULFILLMENT OF
THE REQUIREMENTS FOR THE DEGREE OF
MASTER OF SCIENCE

in

THE FACULTY OF GRADUATE STUDIES
Department of Chemistry

We accept this thesis as conforming
to the required standard

THE UNIVERSITY OF BRITISH COLUMBIA

March 1998

In presenting this thesis in partial fulfilment of the requirements for an advanced degree at the University of British Columbia, I agree that the Library shall make it freely available for reference and study. I further agree that permission for extensive copying of this thesis for scholarly purposes may be granted by the head of my department or by his or her representatives. It is understood that copying or publication of this thesis for financial gain shall not be allowed without my written permission.

Department of Chemistry

The University of British Columbia
Vancouver, Canada

Date April 8 /98

DE-6 (2/88)

Abstract

The aim of this work is to study the effects of additives on the analyte migration behavior in capillary electrophoresis (CE). The first part of this thesis presents an investigation into the interaction between the analytes and the additives in both the liquid and gas phase. β-Cyclodextrin (β-CD) was used as the additive and several nitrophenols were employed as analytes to compare the trends of the binding affinity in the gas and liquid phase. It was demonstrated that the trend of the equilibrium constants (K) in the aqueous phase determined by CE was the same as in the gaseous phase determined by electrospray mass spectrometry. It was also concluded that ammonium ions were bound to β-CD in the gas phase. The second part of this thesis presents a quantitative study of ion-pairing interactions in CE. The ion-pairing agents dodecyltrimethylammonium bromide (DTAB) and tetramethylammonium bromide (TMAB) were used as additives in several separation buffers to examine the relationship between the analytes and the additives in aqueous and nonaqueous CE. It was concluded that the interaction between the analytes and the additives in this study was mainly due to ion-pairing and that hydrophobic interactions played a minor role. In the final part of this thesis, the effects of multicomponent additives were studied. Sulfobutylether-β-CD (SBE-β-CD) and hydroxypropyl-β-CD (HP-β-CD) were used as differently charged additives. Once the interaction between the analytes with each additive was understood, the effects of a mixture of the two differently charged additives were examined.

Table of Contents

List of Tables

List of Figures

Acknowledgments

I would like to thank my supervisor, Dr. David Chen, for sponsoring this work and for his advice and encouragement throughout my research. I am grateful to Dr. Shouming He in Dr. Steven Withers laboratory for his help with the mass spectrometry analyses. I also appreciate the generosity of Beckman Instruments, for supplying a second CE instrument as well as for the donation of several neutral eCAP capillaries, and of CyDex, Inc., for the donation of the SBE-β-CD. I want to thank my lab mates, Xuejun Peng, Philip Britz-McKibbin and Michael Bowser, for their helpful comments pertaining to this thesis and for sharing their knowledge about CE. I am especially grateful to Dr. Gwendolyn Bebault for sharing her experience and for her continued support throughout my research. I would like to extend my utmost gratitude to Craig McCormick for his patience, friendship and for helping me to understand what it means to enjoy science. Finally, I would like to thank my parents for all of their encouragement throughout the years, for teaching me the meaning of hard work and endurance and for showing me how to appreciate and enjoy life through their example!

Chapter I Introduction

1.1 General Introduction to Capillary Electrophoresis

"It is not unusual in science that formulation of new concepts and analytical techniques predate their widespread acceptance in the scientific community by periods as long as decades" [1]. Capillary electrophoresis (CE), the analytical separative tool generally described as the study of the migration of charged substances in solution under the influence of an applied electric field in a narrow bore silica capillary, is no exception. Although zone electrophoresis in free solution using large tubes was first introduced in 1967 by Hjertén [2], CE literature did not begin to rise exponentially until 1980 and commercial instruments have only become available in the last decade. Acceptance of CE required the adaptation of attributes from three existing fields, that is, conventional electrophoresis, gas chromatography (GC) and high performance liquid chromatography (HPLC). Drawing on the strengths from each of these fields, CE is a successful separation technique like conventional electrophoresis, uses inexpensive silica tubing as in GC and reaches low levels of detection from highly sensitive optical detectors like HPLC [1]. With the conversion of these three scientific tools into components customized for CE, the field rapidly advanced between 1980 and 1990, as scientists realized the need for a reproducible, quantitative, microscale separation technique, which could not be met by other established methods.

Electrophoresis, the differential movement of charged species (ions) by attraction or repulsion in an electric field, has long been an important technique in scientific laboratories. First introduced in 1937, Arne Tiselius discovered that by placing protein mixtures between buffer solutions in a tube and applying an electric field, sample components migrated in a direction and at a rate determined by their charge and their size [3]. This separation technique in free solution was limited by both thermal diffusion and convection. Therefore, in order to separate and analyze ionic substances, nearly all forms of electrophoresis required some type of anti-convective media to carry out the electromigration of the analytes of interest. Whether this support was in the form of paper for the separation of small organic molecules, or as an agarose

or polyacrylamide gel, for the separation of proteins and DNA/RNA, the need for high resolution analysis of complex systems has been an essential part of thousands of research projects to date.

Although conventional slab gel electrophoresis is one of the most widely used separation techniques, this method generally requires long analysis times and has often proved to be difficult with regard to detection and automation. The use of narrow bore capillaries as an alternative to the slab gel format, gives the scientist a unique separation method which offers several advantages. Since the narrow capillaries are anti-convective in themselves, gel media is not required for most of the separations performed. Fused silica capillaries used in CE have a high surface-to-volume ratio, which allows for the effective dissipation of the Joule heating generated from the applied field. With typical CE capillary dimensions ranging from 20 to 100 μm in inner diameter and from 20 to 100 cm in length, the volumes required to fill the capillary are in the microlitre (μL) range. Therefore, the volume of buffer and analyte that are required are also in the order of microlitres . This is not only helpful when studying small samples, such as DNA and proteins where minute amounts of analyte are available, but also minimizes the use of toxic reagents, thereby reducing the detrimental effects to the environment.

1.2 Experimental Set-up

Whether CE is carried out using a "homemade" or a commercial instrument, the basic instrumental design is the same. Figure 1.1 is a schematic representation of the five main components of a CE instrument. A fused silica capillary filled with separation buffer is arranged between two buffer reservoirs. A third reservoir, containing the analytes of interest dissolved in the same separation buffer, is available for injection by replacing the inlet buffer reservoir with the sample vial. Quantitative sample injection can be accomplished either electrokinetically or hydrodynamically. For separation, an electric field is applied using a high voltage power supply which, in most cases, generates voltages up to 30 kV. Detection of the separated analytes is often achieved on-column using various types of detectors, such as ultraviolet absorbance (UV), diode array (DAD), laser induced florescence (LIF) and conductivity. Detector response, recorded

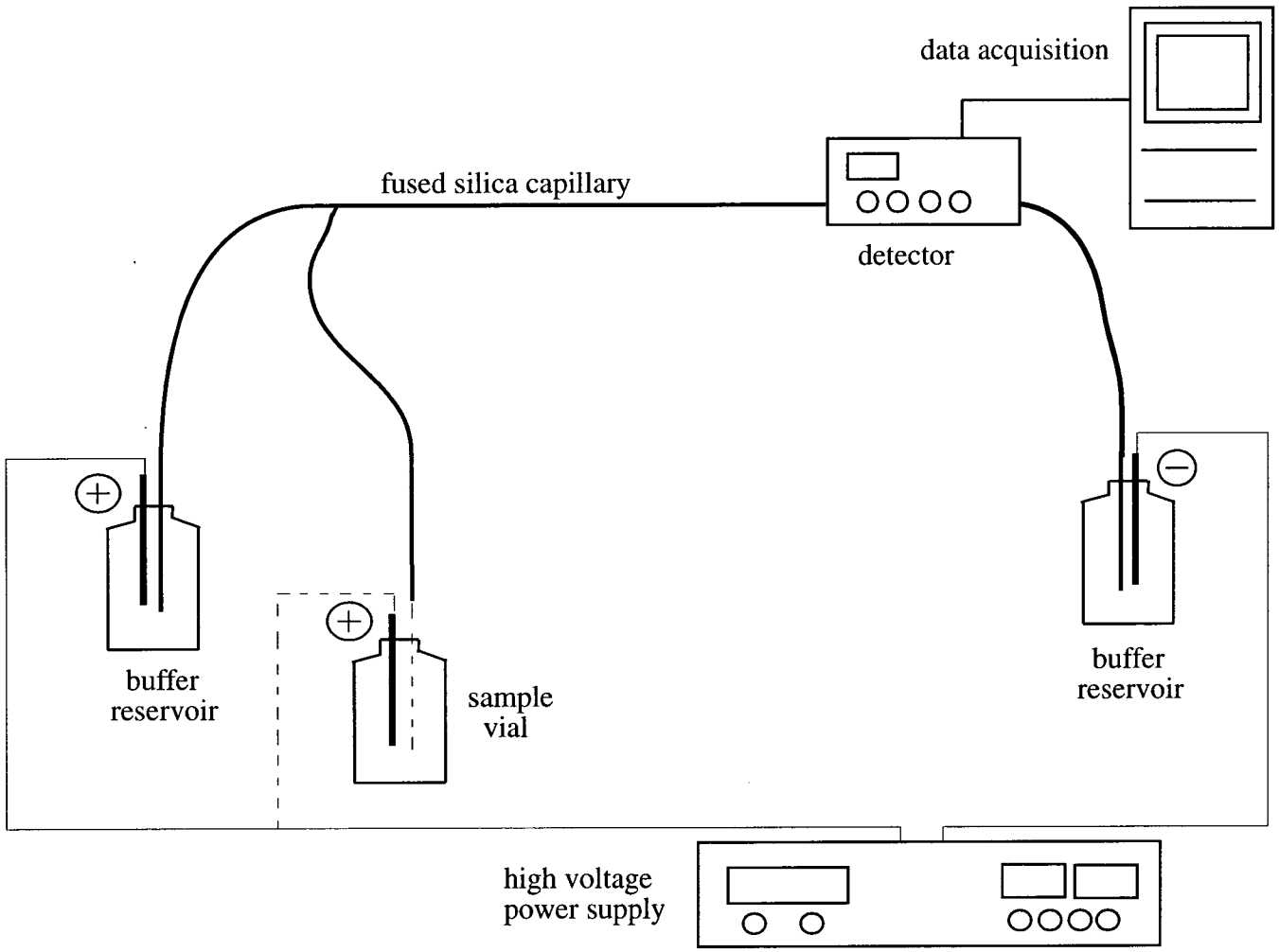

Figure 1.1 Instrumental set-up of a capillary electrophoresis system

versus the migration time, is called an electropherogram. The electropherogram is documented using a data acquisition device, such as a chart recorder or a computer. CE can also be coupled with other analytical methods in order to perform tandem experiments and achieve alternative methods of detection (e.g. CE/MS).

1.3 Theory

1.3.1 Electrophoretic Mobility, μ_{ep}

The electrophoretic mobility is an intrinsic characteristic of each individual ion. The electrophoretic mobility of sample components (ions or charged particles) is determined by the differences in analyte velocity in an electric field. The velocity of an analyte can be described by:

$$v = \mu_{ep} \cdot E \tag{1.1}$$

where v is the ion velocity ($cm \cdot s^{-1}$), μ_{ep} is the electrophoretic mobility ($cm^2 \cdot s^{-1} \cdot V^{-1}$) and E is the electric field strength ($V \cdot cm^{-1}$). This mobility depends on the electric force experienced by the molecule and the frictional drag of the molecule through the medium. That is:

$$\mu_{ep} \propto \frac{\text{electric force } (F_e)}{\text{frictional force } (F_f)} \tag{1.2}$$

In a homologous electric field, a charged component, A, is accelerated by the electric force:

$$F_e = z_A \cdot e_0 \cdot E \tag{1.3}$$

where z_A is the charge number of component A and e_0 is the elemental charge (1.602×10^{-19} A • s = Coulombs). This equation can be simplified by replacing ($z_A \cdot e_0$) with Q_{eff}, the effective charge of the ion (Coulombs). In a viscous hydrodynamic medium, the frictional force counteracts the electric force and is represented by:

$$F_f = -6 \cdot \pi \cdot r \cdot \eta \cdot v \tag{1.4}$$

where r is the radius of a spherical ion particle (cm) and η is the viscosity of the running buffer (Pa • s). During electrophoresis, an equilibrium between these two counteractive forces is obtained, at which point the forces are equal. Therefore:

$$Q_{eff} \bullet E = 6 \bullet \pi \bullet r \bullet \eta \bullet v \quad (1.5)$$

Solving for velocity and substituting equation 1.5 into equation 1.1 gives a more functional equation for the electrophoretic mobility:

$$\mu_{ep,A} = \frac{Q_{eff}}{6 \pi r \eta} \quad (1.6)$$

This equation implies that the electrophoretic mobility of each component in a sample mixture will depend only on its charge and size. Therefore, analytes that are small and highly charged will have larger mobilities than those that are large and less charged.

1.3.2 Electroosmotic Mobility, μ_{eo}

One of the most important controlling mechanisms in CE is the electroosmotic flow (EOF). This bulk flow of separation buffer through the capillary is created due to the ionizable nature of the capillary wall. The fused silica capillary used in CE is made up of bridged silicon dioxide compounds (Si-O-Si). The surface of the capillary wall is easily hydrolyzed by aqueous solutions, producing silanol groups (Si-OH). The silanol groups on the capillary wall act as weak polyprotic acids, which start to ionize above pH 2 [4]. Therefore, the silanol groups form $Si\text{-}O^-$ components on the wall of the capillary (Figure 1.2). This layer of negative charges attracts positively charged constituents in the separation buffer, creating a double layer at the capillary wall. This double layer, formed in order to maintain a charge balance on the wall surface, creates a difference in potential very close to the wall surface. The zeta potential is the potential drop across the diffuse layer (Figure 1.3). Once a high voltage is applied along the capillary, the cations in the diffuse layer begin to migrate towards the negative electrode. This cationic movement drags the bulk solution towards the cathode, generating the EOF. Therefore, the EOF can be described as the bulk flow of liquid through the capillary. The velocity of the EOF is dependent on the applied electric field and the relationship between the two can be denoted by:

$$v_{eo} = \mu_{eo} \bullet E \quad (1.7)$$

where μ_{eo} is the electroosmotic mobility ($cm^2 \bullet V^{-1} \bullet s^{-1}$). The electroosmotic mobility depends

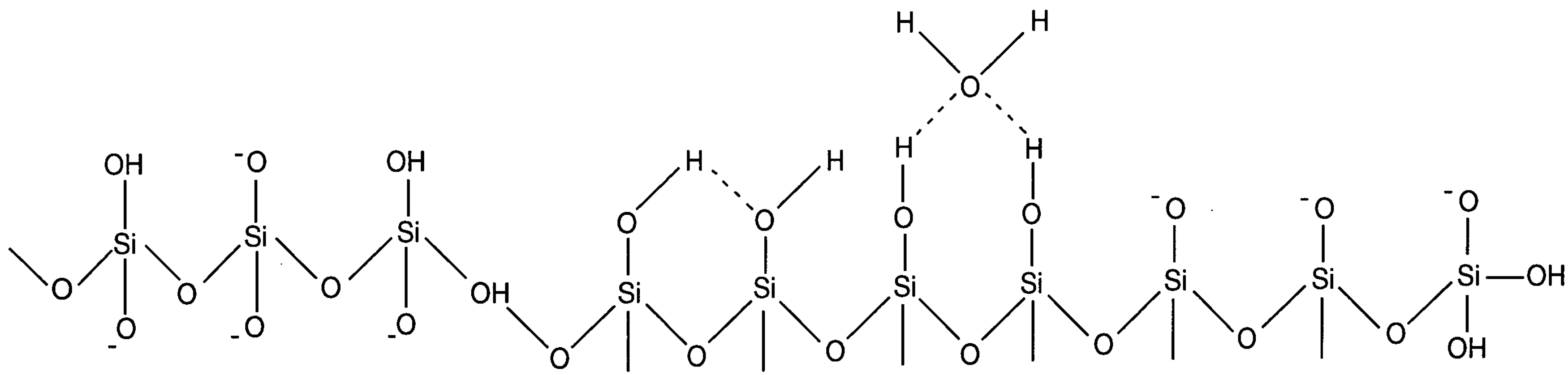

Figure 1.2 Silanol groups on the surface of a fused silica capillary

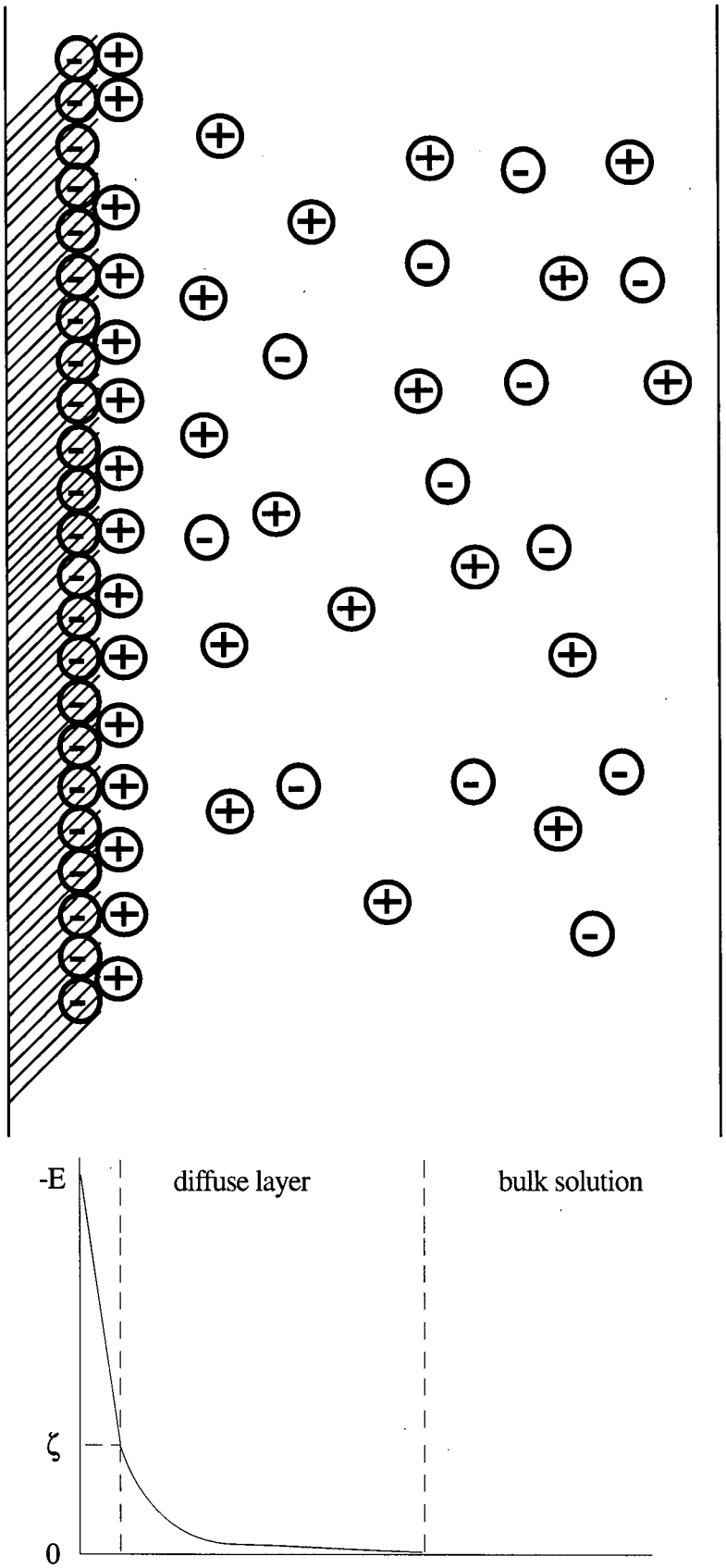

Figure 1.3 The double layer at the capillary wall between the separation buffer and the surrounding surface

on the zeta potential at the wall surface, as well as the viscosity of the separation buffer and the dielectric constant of the medium:

$$\mu_{eo} = \frac{\zeta \bullet \varepsilon}{4 \pi \eta} \tag{1.8}$$

where ζ is the zeta potential (V) and ε is the dielectric constant ($F \bullet m^{-1}$). Since the zeta potential at the wall surface depends on the pH and the ionic strength of the separation buffer, the electroosmotic mobility will also be dependent on these factors. At high pH, the silanol groups will be predominantly deprotonated, increasing the EOF significantly compared to at low pH. As the ionic strength of the separation buffer increases, the EOF is reduced.

A unique feature of the EOF is its flat flow profile (Figure 1.4). In CE, a plug flow profile is generated, instead of the parabolic flow profile in chromatographic techniques. In HPLC, frictional forces between the liquid-solid boundary lead to a parabolic flow profile. In CE however, the driving force behind the EOF is consistently applied along the entire capillary. Therefore, a uniform flow velocity is maintained across the entire capillary. This steady plug results in analyte separations that have sharper peaks and better resolution.

Another benefit the EOF provides is the movement of nearly all species, regardless of charge, in the same direction. This is due to the fact that the electroosmotic mobility is often larger than the electrophoretic mobility of most analytes in aqueous systems. Under normal conditions, the EOF flows from the positive electrode to the negative electrode. Therefore, cationic, anionic and neutral compounds can all be separated in the same direction (Figure 1.5). Small, positively charged analytes will migrate the fastest, followed by larger, positively charged analytes. All neutral analytes migrate together, following the positively charged analytes. Finally, large, negatively charged analytes followed by smaller, negatively charged analytes, will migrate out of the capillary.

The EOF is also beneficial as a controlling mechanism. By varying different parameters within the capillary, the EOF can be increased or decreased in order to better separate sample components. Electric field, buffer pH and ionic strength, temperature, buffer additives and

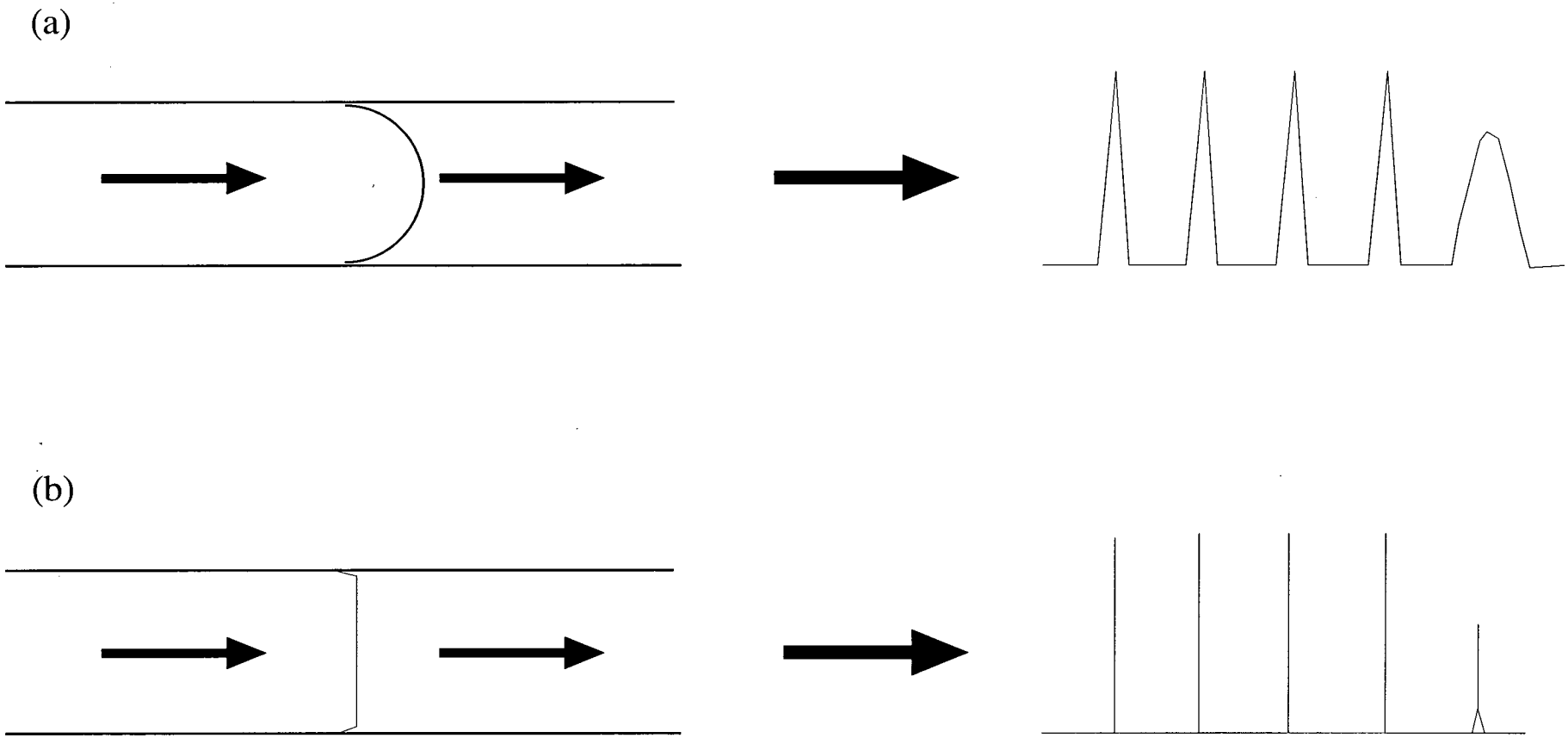

Figure 1.4 Flow profiles in (a) HPLC and (b) CE and their corresponding peak shape

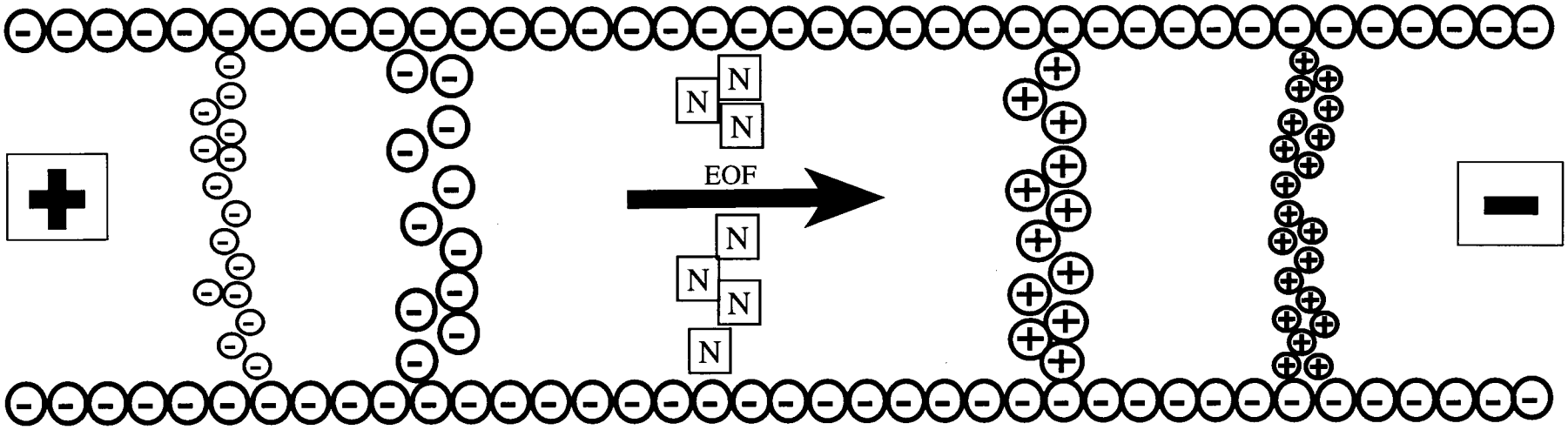

Figure 1.5 Migration of a mixture of analytes based on charge, size and EOF

covalent coatings are just a few variables through which the EOF can be modified to improve the separation.

1.3.3 Dynamic Complexation Capillary Electrophoresis (DCCE) Theory

Open tubular CE has a significant advantage over other types of separation techniques because various chemical equilibria can be easily introduced into the system. Chiral selectors, surfactants, zwitterionic substances, organic modifiers and linear hydrophilic polymers are a few examples of additives that can be introduced into the system to modify the mobility of the analytes in the separation buffer. The use of mixed additives has been increasing in the past few years and different models have been proposed to describe the separation processes [5-11].

In an effort to extend the separation power of CE to uncharged analytes, Terabe and co-workers introduced the use of ionic surfactants, in the form of micelles, to buffer solutions [12,13]. This mode of CE separation, now called micellar electrokinetic capillary chromatography (MECC), is a hybrid of electrophoresis and chromatography. Its main strength is that it is the only electrophoretic technique that can be used for the separation of neutral and charged analytes by simultaneously providing ionic and hydrophobic sites for analyte-additive interactions.

It has been demonstrated by our research group that a theory based on dynamic complexation of analytes with various additives can be used to accurately predict the analyte migration behavior not only for one additive CE systems but also for situations when more than one additive or higher order interactions are involved [11,14-17].

When an analyte migrates in a capillary, where an additive is used in the background electrolyte, the equilibrium can be expressed as:

$$A + C \rightleftharpoons AC \qquad (1.9)$$

where A is the analyte, C is the additive and AC is the analyte-additive complex. When the interactions between the analyte and the additive have a 1:1 stoichiometry, three parameters are required to describe the analyte migration behavior, the electrophoretic mobility of the free analyte

($\mu_{ep,A}$), the electrophoretic mobility of the analyte-additive complex ($\mu_{ep,AC}$) and the equilibrium constant (K).

The equilibrium constant (K) for equation 1.9 can be written as:

$$K = \frac{[AC]}{[A][C]} \tag{1.10}$$

where [AC] is the concentration of the analyte-additive complex, [A] is the concentration of the analyte and [C] is the concentration of the additive.

When the analyte stays in its free form, the electrophoretic mobility is represented by $\mu_{ep,A}$. When the analyte complexes with the additive in the buffer, the electrophoretic mobility of the analyte-additive complex is denoted by $\mu_{ep,AC}$. The capacity factor, k', can be described as the ratio of the amount of complex analyte to the amount of free analyte:

$$k' = \frac{n_{AC}}{n_C} = \frac{[AC]}{[A]} = K[C] \tag{1.11}$$

where n_{AC} is the amount of analyte-additive complex and n_C is the amount of free analyte.

If the fraction of free analyte, f, is defined as $[A]/[A]_0$ ($[A]_0$ is the original analyte concentration), when [C] is much greater than $[A]_0$, substituting $[A]_0$ by [A] + [AC] gives:

$$f = \frac{1}{1 + k'} \tag{1.12}$$

The net electrophoretic mobility of the analyte, expressed by μ_{ep}^{A}, can be written as:

$$\mu_{ep}^{A} = f\,\mu_{ep,A} + (1-f)\,\mu_{ep,AC} \tag{1.13}$$

$$= \frac{1}{1+k'}\mu_{ep,A} + \frac{k'}{1+k'}\mu_{ep,AC} \tag{1.14}$$

$$\mu_{ep}^{A} = \frac{1}{1+K[C]}\mu_{ep,A} + \frac{K[C]}{1+K[C]}\mu_{ep,AC} \tag{1.15}$$

In an ideal state, any additives used in the separation buffer will not affect the physicochemical properties of the buffer. However, the ideal state rarely applies. The electrophoretic mobility of an analyte is dependent on the viscosity of the separation buffer in the capillary, as shown in equation 1.6. When the concentration of the separation buffer is changed to shift the equilibrium,

the viscosity of the solution will also change. Hence, a correction factor is used to compensate for changes in viscosity. The electrophoretic mobility of the analyte can be rewritten as:

$$\nu\mu_{ep}^{A} = \frac{1}{1+K[C]}\mu_{ep,A} + \frac{K[C]}{1+K[C]}\mu_{ep,AC} \tag{1.16}$$

The correction factor, ν, is defined as η/η^0, where η is the viscosity of the running buffer at the various concentrations of additive and η^0 is the viscosity of the separation buffer when [C] approaches zero. The correction factor converts the net electrophoretic mobility to the ideal state where the change in viscosity is negligible.

Both the apparent (observed) mobility of the analyte (μ^A) and the electroosmotic mobility (μ_{eo}) can be calculated from the measured migration times using the following equations:

$$\mu^A = \frac{l\,L}{t_{mig}\,V} \tag{1.17}$$

$$\mu_{eo} = \frac{l\,L}{t_{eof}\,V} \tag{1.18}$$

where l is the length of the capillary from the injection end to the detector (cm), L is the total length of the capillary (cm), t_{mig} is the migration time of the analyte (s), t_{eof} is the migration time of the EOF marker (s) and V is the voltage applied along the capillary (V). The apparent mobility of the analyte (μ^A) is equal to the sum of the electroosmotic mobility and the net electrophoretic mobility:

$$\mu^A = \mu_{eo} + \mu_{ep}^{A} \tag{1.19}$$

1.3.4 Regression Methods

Once the values for the parameters μ^A, μ_{eo} and μ_{ep}^{A} are determined from the migration times, four different regression methods can be used to solve for the unknown parameters, $\mu_{ep,AC}$ and K. Three of the regression methods involve solving for the parameters graphically using linear regression. By rearranging equation 1.16, the following equations can be attained:

$$\frac{1}{(\nu\,\mu_{ep}^{A} - \mu_{ep,A})} = \frac{1}{(\mu_{ep,AC} - \mu_{ep,A})K}\,\frac{1}{[C]} + \frac{1}{(\mu_{ep,AC} - \mu_{ep,A})} \tag{1.20}$$

$$\frac{[C]}{(\nu\,\mu_{ep}^{A} - \mu_{ep,A})} = \frac{[C]}{(\mu_{ep,AC} - \mu_{ep,A})} + \frac{1}{(\mu_{ep,AC} - \mu_{ep,A})K} \tag{1.21}$$

$$\frac{(\nu\,\mu_{ep}^{A} - \mu_{ep,A})}{[C]} = -K\,(\nu\,\mu_{ep}^{A} - \mu_{ep,A}) + K\,(\mu_{ep,AC} - \mu_{ep,A}) \tag{1.22}$$

These three equations have been named the double reciprocal (equation 1.20), y-reciprocal (equation 1.21) and x-reciprocal plots (equation 1.22). Theoretically, all three of these methods should give the same values for the unknown parameters. In practice, errors associated with the variables often cause the methods to give different estimates of the parameters. When performing a linear regression, it is assumed that the error associated with each point is Gaussian and that all of the points have the same amount of error. However, because of the transformations in equations 1.20, 1.21 and 1.22, this is rarely the case. A study of these three linear relationships has been published recently [18].

The fourth method used to solve for $\mu_{ep,AC}$ and K is the nonlinear regression method [19]. Because the parameters in this regression method are never transformed (i.e. the reciprocal is not taken), all errors remain consistently Gaussian. This nonlinear regression method was used for all calculations presented in this thesis and thus, a detailed explanation of these calculations is included.

Nonlinear regression stems from the mathematical basis of least-squares analysis [20-22]. Using the DCCE theory to understand a CE system requires solving for two unknowns ($\mu_{ep,AC}$ and K). Therefore, a model function containing two unknowns can be represented by a rectangular hyperbola where:

$$y = \frac{x}{b + ax} \tag{1.23}$$

Equation 1.16 can be rearranged to take the form of this rectangular hyperbola giving:

$$(\nu\,\mu_{ep}^{A} - \mu_{ep,A}) = \frac{(\mu_{ep,AC} - \mu_{ep,A})\,K\,[C]}{1 + K\,[C]} \tag{1.24}$$

For any function containing two unknowns, a set of normal equations can be derived:

$$\sum w_i F_a^i F_a^i A + \sum w_i F_a^i F_b^i B = \sum w_i F_a^i F_0^i \quad (1.25)$$

$$\sum w_i F_b^i F_a^i A + \sum w_i F_b^i F_b^i B = \sum w_i F_b^i F_0^i \quad (1.26)$$

where w_i is the weight of the i^{th} observation. For the calculations presented in this thesis, it was assumed that the error in the data points was equal (i.e. $w_i = 1$ for all i). This, in reality, is a good estimate for the studies presented.

The parameters A and B in the normal equations are defined as:

$$A = a_0 - a \quad (1.27)$$

$$B = b_0 - b \quad (1.28)$$

where a_0 and b_0 are the initial estimates of the parameters to be solved and a and b are the refined estimates, determined by solving for A and B in equations 1.25 and 1.26. F_a^i and F_b^i in the normal equations are functions of x, a and b, where F^i is defined as:

$$F^i (a, b, x_i, y_i) = 0 \quad (1.29)$$

F_0^i in the normal equation is the initial estimate for the function and is defined as:

$$F_0^i = F^i (a_0, b_0, X_i, Y_i) \quad (1.30)$$

where X_i and Y_i are the experimental values of the variables in the i^{th} observation.

In a nonlinear regression calculation, preliminary estimates for the parameters a_0 and b_0 are chosen to solve for the resulting parameter values a and b. The values for a and b are then used as the values for a_0 and b_0 in a second iteration of the calculation. This process continues until the estimated values and the resulting parameters converge.

To develop the function of a rectangular hyperbola further, F can be defined as:

$$F = y - \frac{x}{b + ax} \quad (1.31)$$

and the partial derivatives of this equation are:

$$F_x = \frac{-b}{(b + ax)^2} \quad (1.32)$$

$$F_y = 1 \tag{1.33}$$

$$F_a = \frac{x^2}{(b + ax)^2} \tag{1.34}$$

$$F_b = \frac{x}{(b + ax)^2} \tag{1.35}$$

Also, F_0 is denoted by:

$$F_0 = y - \frac{x}{b_0 + a_0 x} \tag{1.36}$$

The substitution of these partial derivatives into equations 1.25 and 1.26 gives rise to the normal equations for this system where:

$$\sum \frac{x^4}{z^4} A + \sum \frac{x^3}{z^4} B = \sum \left(\frac{x^2 y}{z^2} - \frac{x^3}{z^3}\right) \tag{1.37}$$

$$\sum \frac{x^3}{z^4} A + \sum \frac{x^2}{z^4} B = \sum \left(\frac{x y}{z^2} - \frac{x^2}{z^3}\right) \tag{1.38}$$

where:

$$z = b_0 + a_0 x \tag{1.39}$$

Using matrix mathematics, an equation can be set up to solve these two normal equations. The two normal equations above can be written in matrix form as:

$$\begin{bmatrix} \frac{x^4}{z^4} & \frac{x^3}{z^4} \\ \frac{x^3}{z^4} & \frac{x^2}{z^4} \end{bmatrix} \begin{bmatrix} A \\ B \end{bmatrix} = \begin{bmatrix} \frac{x^2 y}{z^2} & \frac{-x^3}{z^3} \\ \frac{xy}{z^2} & \frac{x^2}{z^3} \end{bmatrix} \tag{1.40}$$

A and B can be solved by:

$$\begin{bmatrix} A \\ B \end{bmatrix} = \begin{bmatrix} \frac{x^4}{z^4} & \frac{x^3}{z^4} \\ \frac{x^3}{z^4} & \frac{x^2}{z^4} \end{bmatrix}^{-1} \begin{bmatrix} \frac{x^2 y}{z^2} & \frac{-x^3}{z^3} \\ \frac{xy}{z^2} & \frac{x^2}{z^3} \end{bmatrix} \tag{1.41}$$

As previously stated, from the definition of A and B (equations 1.25 and 1.26) and the initial estimates of a_0 and b_0, values for a and b can be calculated. These values are then designated as a_0 and b_0 in the next iteration and the process continues until the parameters converge.

The constants and variables in equation 1.23 can be replaced by the parameters used in the DCCE theory where:

$$y = \nu \mu_{ep}^{A} - \mu_{ep,A} \tag{1.42}$$

$$x = [C] \tag{1.43}$$

$$b = \frac{1}{(\mu_{ep,AC} - \mu_{ep,A})\, K} \tag{1.44}$$

$$a = \frac{1}{(\mu_{ep,AC} - \mu_{ep,A})} \tag{1.45}$$

For the calculations presented in this thesis, the initial estimates (a_0 and b_0) were set to 0.1 and 0.1 or -0.1 and -0.1, depending on the sign of the difference between $\mu_{ep,AC}$ and $\mu_{ep,A}$. Then, using a spreadsheet program, the values for a and b were determined. After several iterations the values of a and a_0 and b and b_0 converged and the values for the parameters $\mu_{ep,AC}$ and K were then determined using equations 1.44 and 1.45. The values of mobility and concentration were then plotted to give a nonlinear graphical representation of the binding isotherm.

1.4 Aims of Research

The aim of this work was to gain more understanding about how additives affect the analyte migration behavior in CE. Regardless of the type or number of additives chosen for a particular experiment, the DCCE theory can always be used to describe the migration behavior of the analytes.

The first part of this project was to investigate the relationship between the species observed in the gas phase and the species observed in liquid solutions. β-CD and several nitrophenols were employed in this study to compare the trends of the complex to free ion ratios in the gas and liquid phase. Information on the relative amount of each species provided some insight into the behavior of the analyte interactions in both phases, as well as effect of the electrospray process on chemical equilibria.

The second part of this thesis was a quantitative study of ion-pairing interactions in CE. In the past, ion-pairing agents have been predominantly used to enhance the resolution of analytes. Both aqueous and nonaqueous CE were employed in this part of the thesis to thoroughly examine all aspects of ion-pairing effects in the separation process.

The objective in the third part of this thesis was to study multicomponent additives, in the form of derivatized cyclodextrins with various degrees of substitution. SBE-β-CD and HP-β-CD were used as differently charged additives in this study. Once the relationship between each analyte-additive pair was understood, the effects of a mixture of the two differently charged additives were examined.

Chapter II Relating the Species Observed in the Gas Phase to the Process of Dynamic Complexation in Capillary Electrophoresis

2.1 Introduction

The concept of equilibrium was proposed very early in the history of chemistry. Quantitative work involving equilibria was first presented in 1862 by the French chemists P.E.M. Berthollet and Péan de St. Gilles, who introduced the idea of an equilibrium constant. Other scientists followed with their interpretations of equilibrium expressions, including the first thermodynamic treatment of the equilibrium equation by Willard Gibbs in 1874 [23]. Since the late nineteenth century, the experimental determination and theoretical treatment of equilibrium constants have been important aspects in the understanding of chemical systems.

The investigation of analyte-additive interactions in the liquid phase has been of great interest in CE research because equilibrium is one of the controlling factors in CE and, in the presence of additives, the measured analyte mobilities can be used to determine the equilibrium constant. In many previous studies, cyclodextrins (CDs) have been used as additives in CE and the equilibrium constants for analyte-additive interactions have been examined [8,14,16,24-41]. Equilibrium constants can also be determined by other analytical methods. Many additives have also been used as complexing agents in these methods and, like in CE, CDs have proven to be efficient additives. The analytical techniques used to study analyte-additive complexation of CDs with analytes include calorimetry [19,42-48], fluorescence spectroscopy [19,49-64], nuclear magnetic resonance (NMR) [19,45,65], potentiometry [19,66], UV [63], spectrophotometry [67] and liquid chromatography (LC) [37,40,68-75]. There are essentially two approaches for applying CDs in LC. The first involves the use of CDs bonded to silica gel [68], while the second uses CDs as a mobile phase additive [37,40,69-75]. Considering the attention given to the importance of equilibrium, it is often necessary to compare results between an emerging technique and established analytical methods. One recent study addressed the examination of enantiomeric separations in CE and LC [37,40]. The equilibrium constants of analyte-additive complexes are often compared using two methods. Under the same conditions, the equilibrium constants determined by different techniques should be identical. Discrepancies in results are

often an indication that either one of the techniques is not suitable for the measurement or there may be other interactions introduced during the measurement which would require further exploration of these processes.

The calculation of an equilibrium constant using MS and the comparison of the parameter values to those calculated using CE has only been elaborated by one other research group to date [76]. In this study, Penn *et al.* used electrospray ionization-mass spectrometry (ESI-MS) to study analyte-additive complexes of various forms of CDs in the gas phase. The average binding constant of the complex was determined from the data points and compared to CE derived binding constants.

In this chapter, CE is used to examine the interaction between *ortho-*, *meta-* and *para-* nitrophenol and β- CD in ammonium acetate buffer (pH ≈ 9). The net electrophoretic mobility (μ_{ep}^{A}) of each analyte was measured at various β-CD concentrations. The measured electrophoretic mobilities were corrected for the viscosity change when the additive was used and the equilibrium constant (K) was obtained by using the ideal state (where the additive concentration approaches zero) electrophoretic mobilities.

In a separate experiment, each analyte-additive pair dissolved in an aqueous solution (e.g. *p*-nitrophenol-β-CD dissolved in ammonium acetate buffer) was introduced into an electrospray mass spectrometer, with identical initial concentrations of the analyte and the additive. The ratio of the number of ions, $n_{AC}/(n_A n_C)$, was calculated for each analyte, assuming that ionization efficiencies are comparable. This experiment provided information about the behavior of the analyte-additive pair in the gas phase. It was observed that the trend of the complex to free ion ratios in the gas phase was consistent with the trend of equilibrium constants obtained by CE. The MS study provided additional information concerning the dynamic equilibria in CE. It was found, using the positive ion mass spectra, that ammonium ions are always bound to β-CD in the gas phase. In order to determine if this is also the case in the liquid phase, further CE studies were performed using 10 mM and 30 mM phosphate buffer with identical analyte-additive pairs.

2.2 Experimental

2.2.1 Apparatus

A Beckman P/ACE 5500 automated CE system (Beckman Instruments (Canada) Inc., Mississauga, Ontario, Canada) was used for the experiments. The uncoated fused silica capillary (Polymicro Technologies, Phoenix, AZ) had a 50 μm inner diameter, a 362 μm outer diameter and was 57 cm in length (50 cm to the detector).

An electrospray API 300 mass spectrometer (PE Sciex, Concord, ON) was used for the mass spectrometry studies. The analyses were carried out by Dr. Shouming He in Dr. Steven Withers laboratory at the University of British Columbia.

For the CE and MS studies, ammonium acetate was used as the separation buffer and the capillary was conditioned by rinsing with 0.1 M NaOH for 15 minutes, deionized water for 5 minutes and 10 mM ammonium acetate buffer (pH 9.0) for 15 minutes followed by overnight equilibration in 10 mM ammonium acetate.

For the further CE studies involving various concentrations of phosphate buffer, the capillary was conditioned as above except for the final wash, where the capillary was rinsed with 30 mM phosphate buffer (pH 9.01) instead of ammonium acetate and was then followed by overnight equilibration in 30 mM phosphate buffer.

To measure the electroosmotic flow (EOF), methanol was added to each sample (5% v/v) and the UV absorption signal was monitored at 214 nm. Samples were introduced into the capillary by pressure injection for 5 seconds at 0.5 psi and separated at 16 kV. Data was collected using System Gold software (Beckman).

Prior to injection, the instrument was programmed to rinse the capillary with the separation buffer at high pressure (20 psi) for 2 minutes and then with the running buffer containing appropriate concentrations of additive(s) for 2 minutes. The capillary temperature was kept at 27°C. The viscosity of the running buffer was measured by injecting a plug of benzene solution (dissolved in the running buffer, 2.5% v/v) into the capillary and measuring the time required for

the plug to reach the detector when 20 psi of pressure was applied to the inlet of the capillary [14].

2.2.2 Chemicals

The 10 mM ammonium acetate separation buffer was made by dissolving solid ammonium acetate (CH_3COONH_4) (BDH Chemicals, Toronto, ON) in deionized water, adding 80% of the total volume and then adding concentrated aqueous ammonium hydroxide (NH_4OH) (Fisher Scientific, Nepean, ON) until a pH above 9.0 was reached. The volumetric flask was then topped up with deionized water, giving a final pH of 9.0. The 30 mM phosphate buffer was made by dissolving solid sodium phosphate dibasic (Na_2HPO_4) (Fisher Scientific, Nepean, ON) in deionized water to give a pH of 9.01. The 10 mM phosphate buffer was made by diluting the 30 mM phosphate buffer with deionized water. Solutions of various concentrations of β-CD (Sigma Chemical Co., St. Louis, MO) were prepared using the separation buffers. The concentrations of β-CD ranged from 0 to 20.0 mM. Individual stock solutions (1.0×10^{-3} M) of *ortho-*, *meta-* (Aldrich Chemical Co. Inc., Milwaukee, NJ) and *para*-nitrophenol (Fisher Scientific, Nepean, Ontario) were prepared in the various separation buffers. A mixture of the three analytes was then prepared by combining equal amounts of the three stock solutions and diluting 1:10 with the appropriate electrophoresis buffer giving a concentration of 3.3×10^{-5} M for each analyte.

2.3 Discussion

2.3.1 Gas Phase Species from Analytes Dissolved in Ammonium Acetate Buffer

In the first part of this study, identical concentrations (5 mM) of analyte (*p*-nitrophenol) and additive (β-CD) in ammonium acetate buffer were introduced into an electrospray mass spectrometer. Two significant peaks were observed, including one with a mass to charge ratio (m/z) of 1152.5 and the other with a m/z of 1292.2 (Figure 2.1). The peak at 1152.5 was assigned as β-CD : NH_4^+, while the 1292.2 peak was assigned as β-CD-*p*-nitrophenol : NH_4^+.

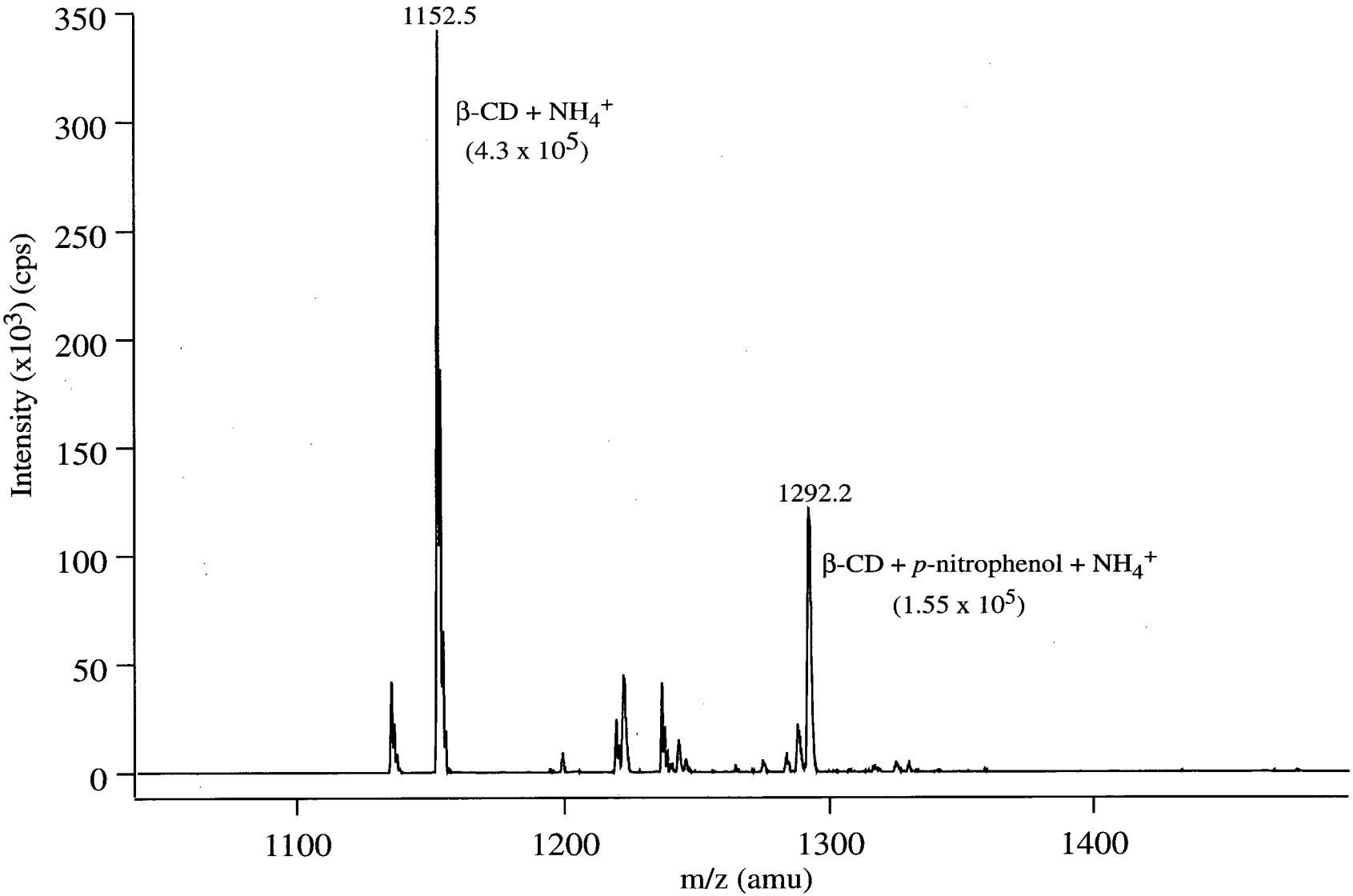

Figure 2.1 Electrospray mass spectrum of 5 mM *p*-nitrophenol and 5 mM β-CD in 10 mM ammonium acetate buffer (aqueous sample : methanol : acetic acid - 50 : 50 : 1)

An ammonium ion (NH_4^+) appeared to be attached to the β-CD, due to the presence of the ammonium acetate buffer. Using an analogous procedure, the other two analytes, *m*- and *o*-nitrophenol, were sprayed into the mass spectrometer and their spectra showed similar results (Figure 2.2 and Figure 2.3). The initial additive concentration can be expressed by:

$$[C]_0 = [C] + [AC] \quad (2.1)$$

By assigning h_C as the peak height of β-CD : NH_4^+ (4.3×10^5), h_{AC} as the peak height of β-CD-*p*-nitrophenol : NH_4^+ (1.55×10^5) and h_{C_o} as the total additive peak height (5.85×10^5) in Figure 2.1, and considering the total concentration of additive in the sample (in this case, 5 mM), the equivalent concentrations of the additive and the analyte-additive complex can be calculated by cross multiplication giving, [C] = 3.675 mM and [AC] = 1.32 mM. Because the equilibrium constant is:

$$K = \frac{[AC]}{[A]\,[C]} \quad (2.2)$$

where [A] = [C] due to experimental design, K(*p*-nitrophenol) was calculated to be 98.1 M^{-1}. Similarly, the equilibrium constant for *m*-nitrophenol was determined to be 76.6 M^{-1} and the value of K for *o*-nitrophenol was too small to be detected.

2.3.2 Gas Phase Species from Analytes Dissolved in Deionized Water

The next part in this study was to introduce identical initial concentrations of analyte (*p*-nitrophenol) and additive (β-CD) in deionized water into the electrospray mass spectrometer. The purpose of this part of the study was to verify that the m/z of 18 attached to the β-CD peak in Figures 2.1, 2.2 and 2.3 was indeed NH_4^+ and not simply a water molecule. Therefore, β-CD, dissolved in deionized water only, was first introduced into the mass spectrometer. Only one peak was found, with a m/z of 1135.5 (Figure 2.4). From this spectrum, it can be determined that the extra 18 mass units on β-CD in the first three spectra was not water, but NH_4^+. To ensure that this was also the case when analytes were added to the sample, identical initial

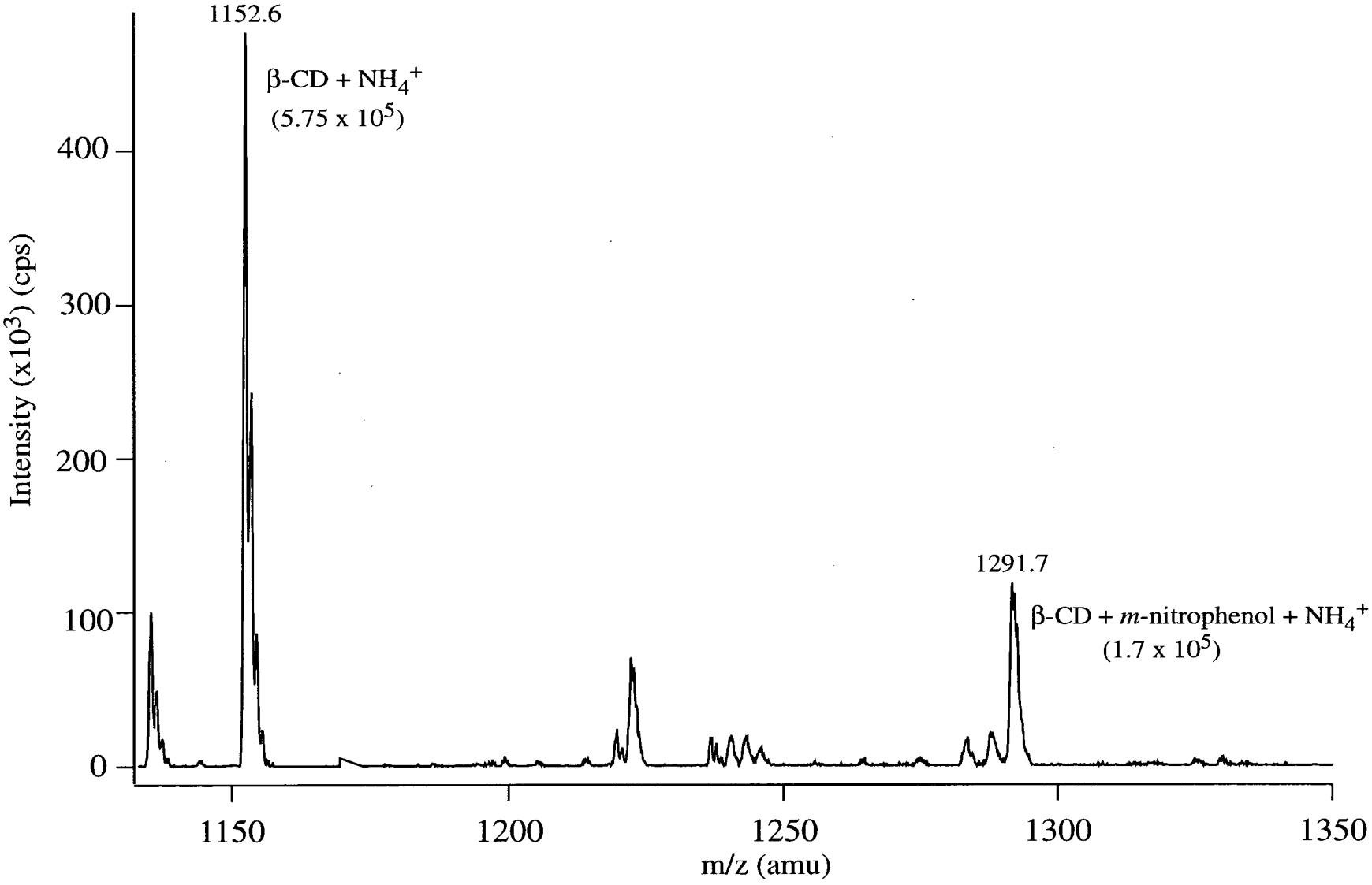

Figure 2.2 Electrospray mass spectrum of 5 mM *m*-nitrophenol and 5 mM β-CD in 10 mM ammonium acetate buffer (aqueous sample : methanol: acetic acid - 50 : 50 :1)

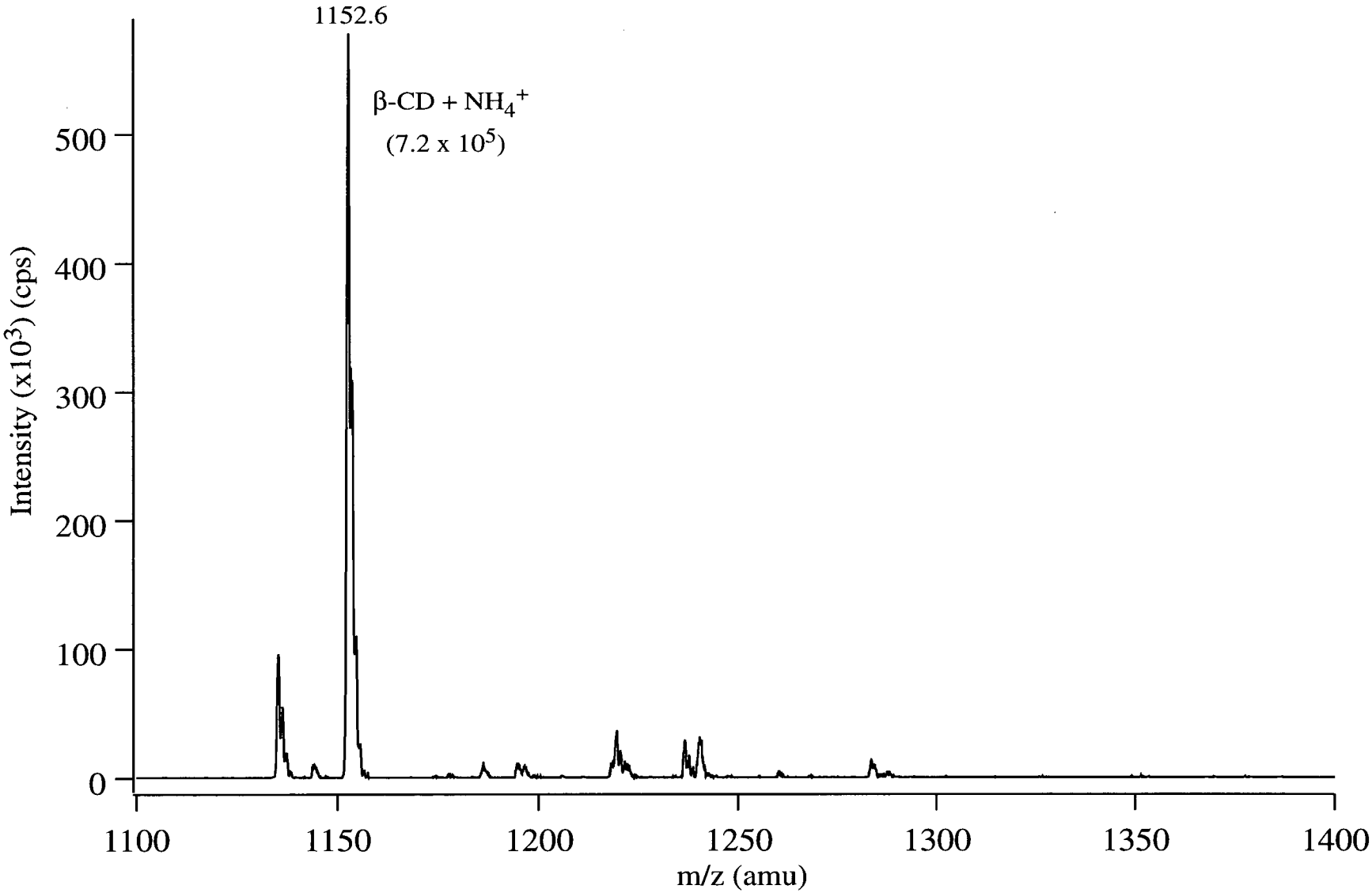

Figure 2.3 Electrospray mass spectrum of 5 mM *o*-nitrophenol and 5 mM β-CD in 10 mM ammonium acetate buffer (aqueous sample : methanol : acetic acid - 50 : 50 : 1)

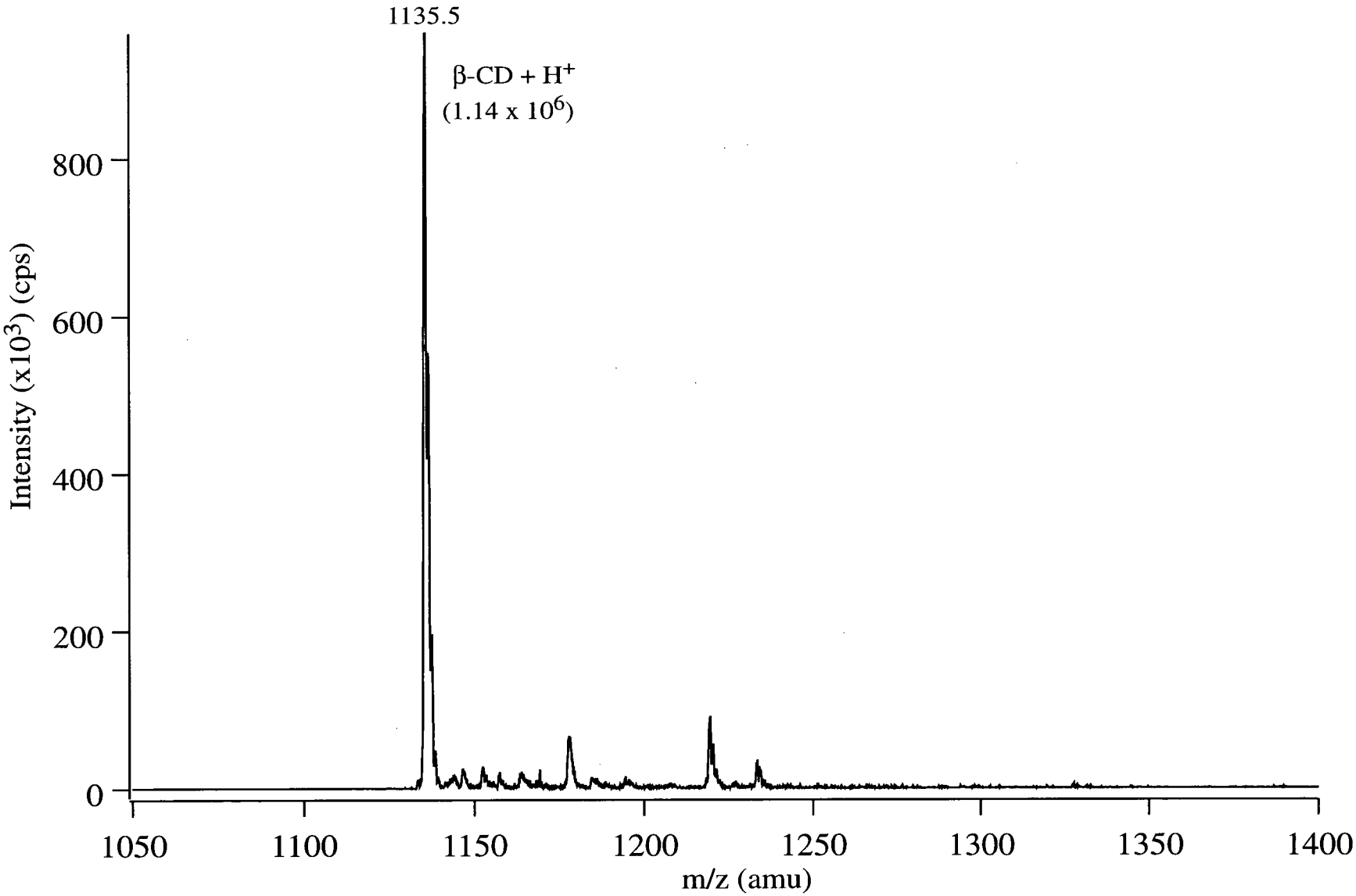

Figure 2.4 Electrospray mass spectrum of 10 mM β-CD in deionized H_2O

concentrations of analyte (*p*-nitrophenol) and additive (β-CD) dissolved in water were introduced into the mass spectrometer. Two peaks were again found in the spectra with m/z ratios of 1135.5 (β-CD : H^+) and 1274.5 (β-CD-*p*-nitrophenol : H^+) (Figure 2.5). The equilibrium constants for this interaction, as well as for β-CD with *m*- and *o*-nitrophenol (Figure 2.6 and Figure 2.7) were determined using the same calculation procedure as the previous experiment. The K values were determined to be 90.8 M^{-1}, 74.8 M^{-1} and 24.0 M^{-1} for β-CD with *p*-, *m*- and *o*-nitrophenol, respectively. When the MS determination of the equilibrium constants in ammonium acetate buffer and in water were compared, it was concluded that there was agreement between the parameters. The small difference in the values was attributed to the ammonium ion bound to the β-CD.

2.3.3 Analyte-Additive Interactions in Ammonium Acetate Buffer Using CE

The third part in this study was to study the relationship between analyte and additive in the liquid phase by CE. Using a sample mixture containing *p*-, *m*- and *o*-nitrophenol, the concentration of β-CD in the separation buffer was varied and several separations were performed. A composite of several of the electropherograms from this experiment shows the changes in migration times of the analytes with the increase in the concentration of β-CD (Figure 2.8). Initially, as the concentration of additive was increased, the negative mobility of the three analytes decreased. As increasing amounts of additive were used, the mobility showed less change. The equilibrium constant was determined for each analyte-additive pair using nonlinear regression as previously described (Section 1.3.4). The equilibrium constants for the binding of *p*-, *m*- and *o*-nitrophenol to β-CD were determined to be 694 ± 2 M^{-1}, 101 ± 1 M^{-1} and 47.2 ± 0.2 M^{-1}, respectively.

After the equilibrium constants were determined by both CE and MS for each analyte-additive complex, the trend in the data was compared (Table 2.1). It was observed that the trend of the

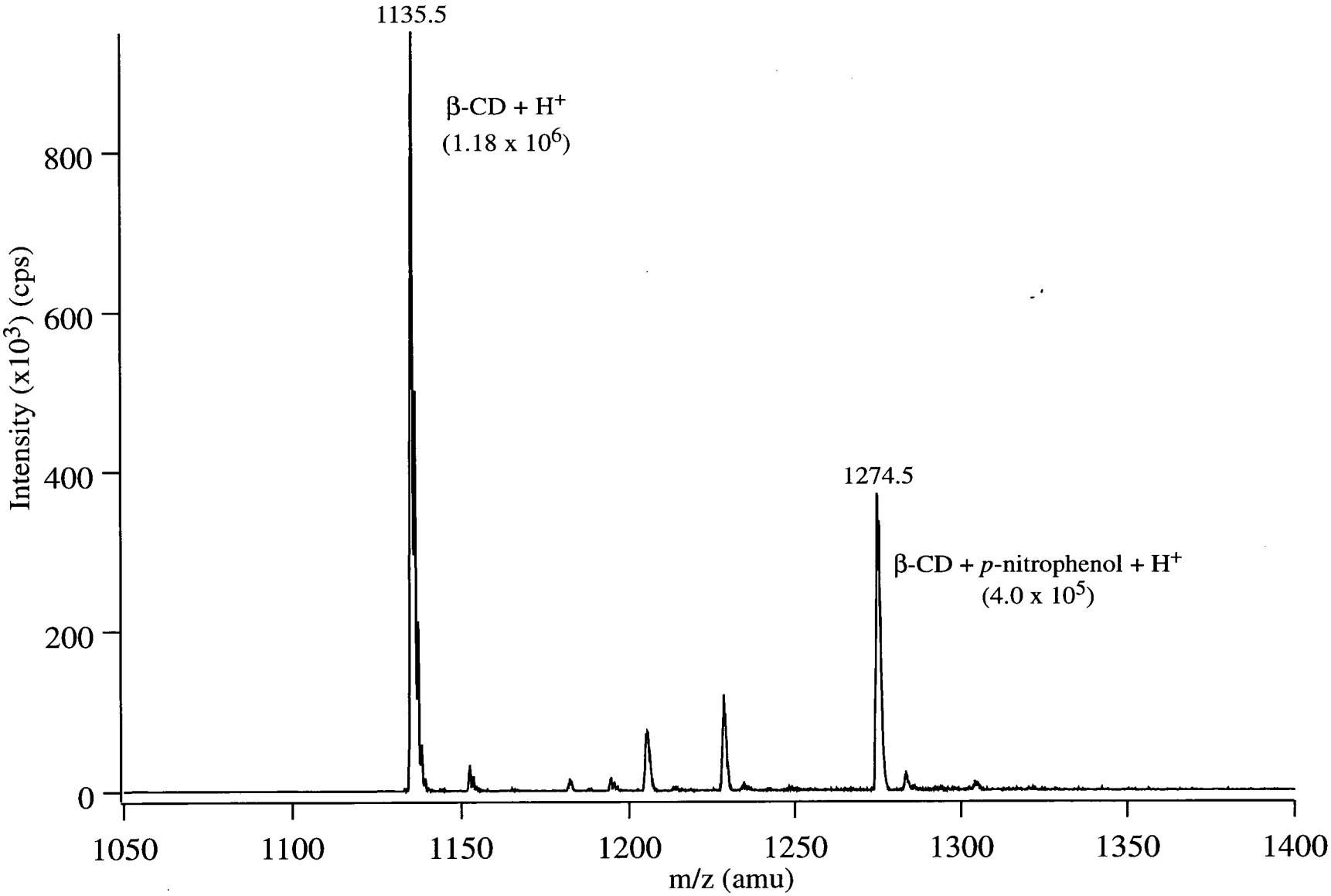

Figure 2.5 Electrospray mass spectrum of 5 mM *p*-nitrophenol and 5 mM β-CD in deionized H_2O (aqueous sample : methanol : acetic acid - 50 : 50 : 1)

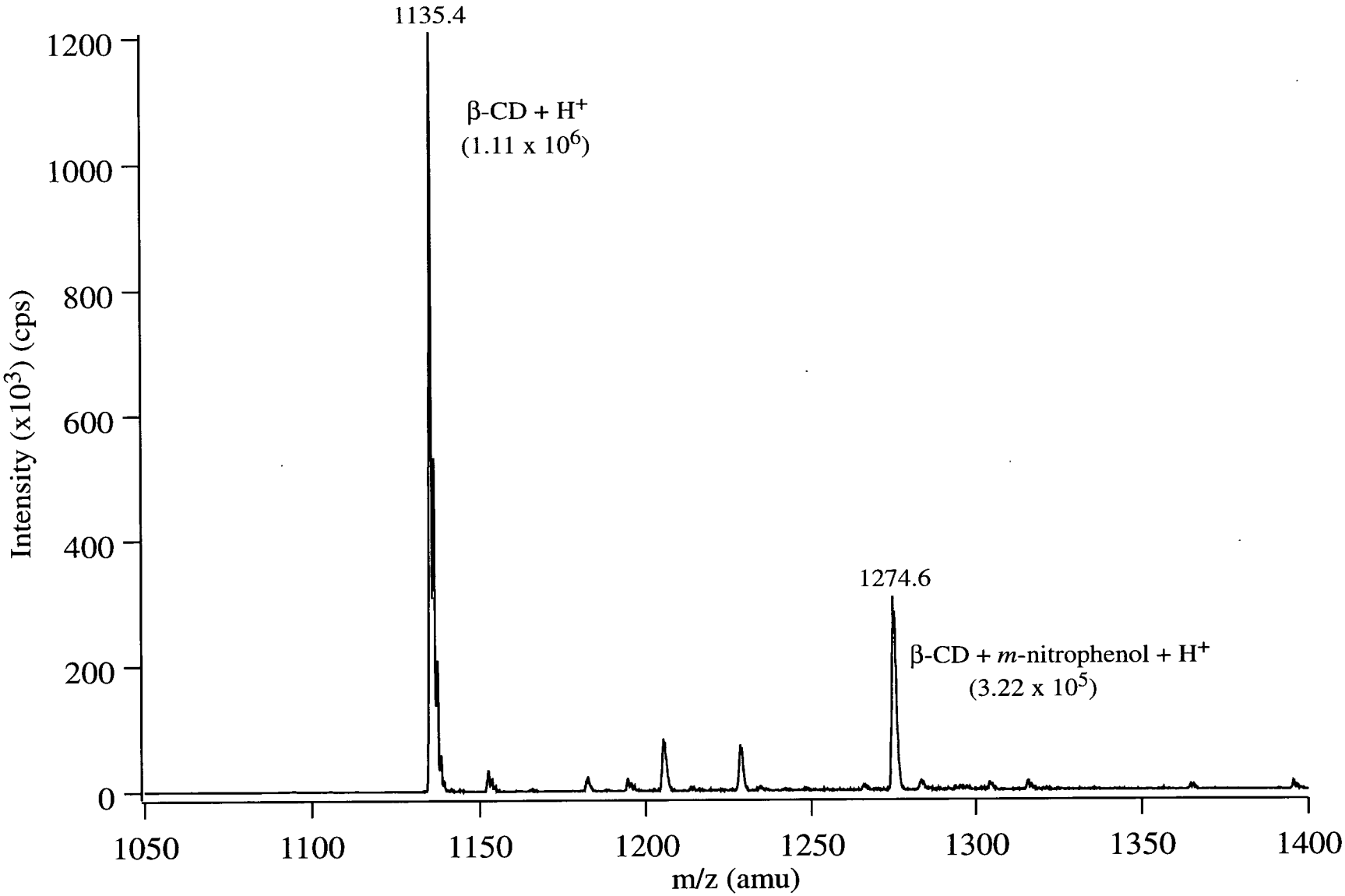

Figure 2.6 Electrospray mass spectrum of 5 mM *m*-nitrophenol and 5 mM β-CD in deionized H_2O (aqueous sample : methanol : acetic acid - 50 : 50 :1)

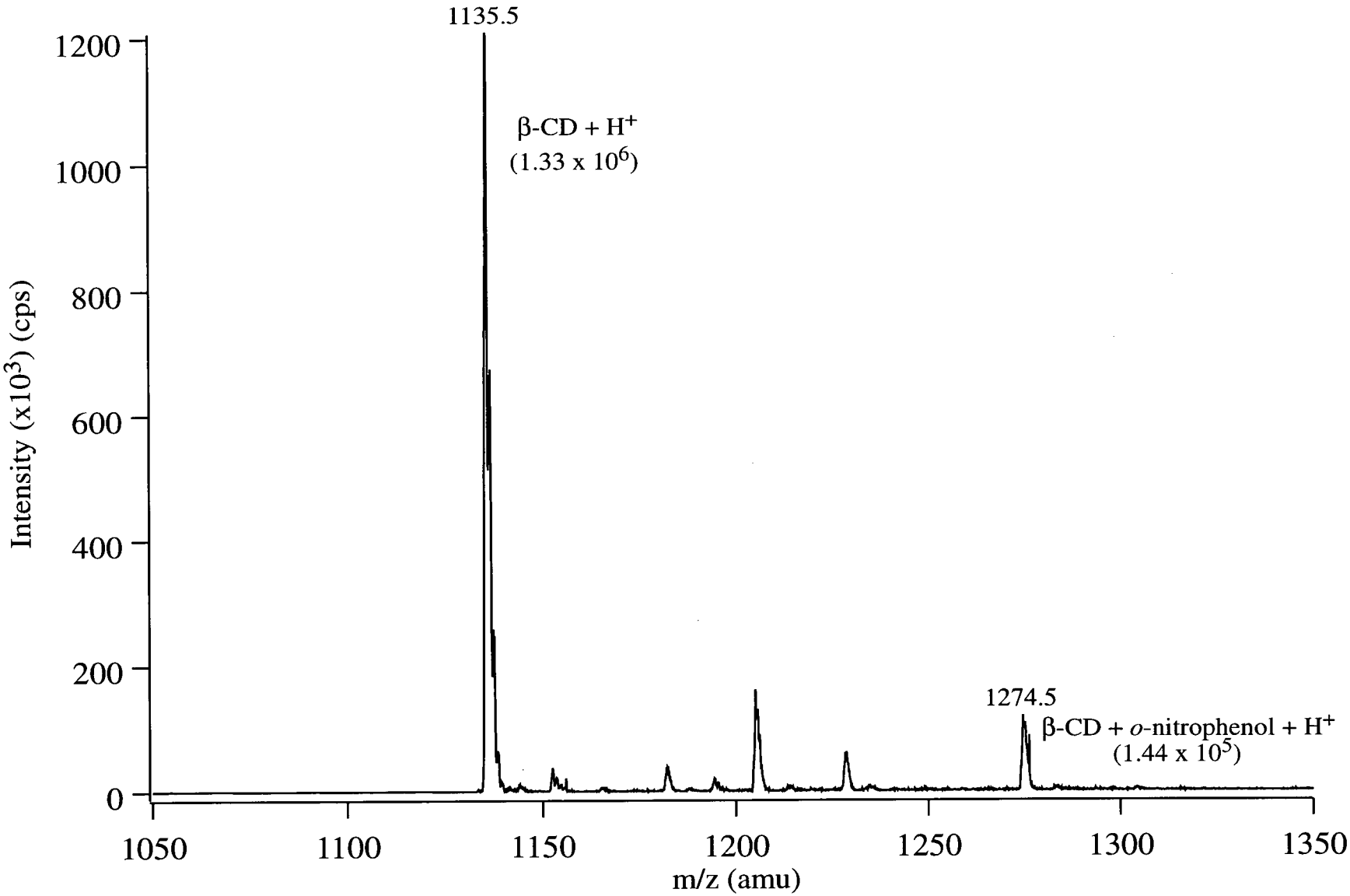

Figure 2.7 Electrospray mass spectrum of 5 mM *o*-nitrophenol and 5 mM β-CD in deionized H_2O (aqueous sample : methanol : acetic acid - 50 : 50 :1)

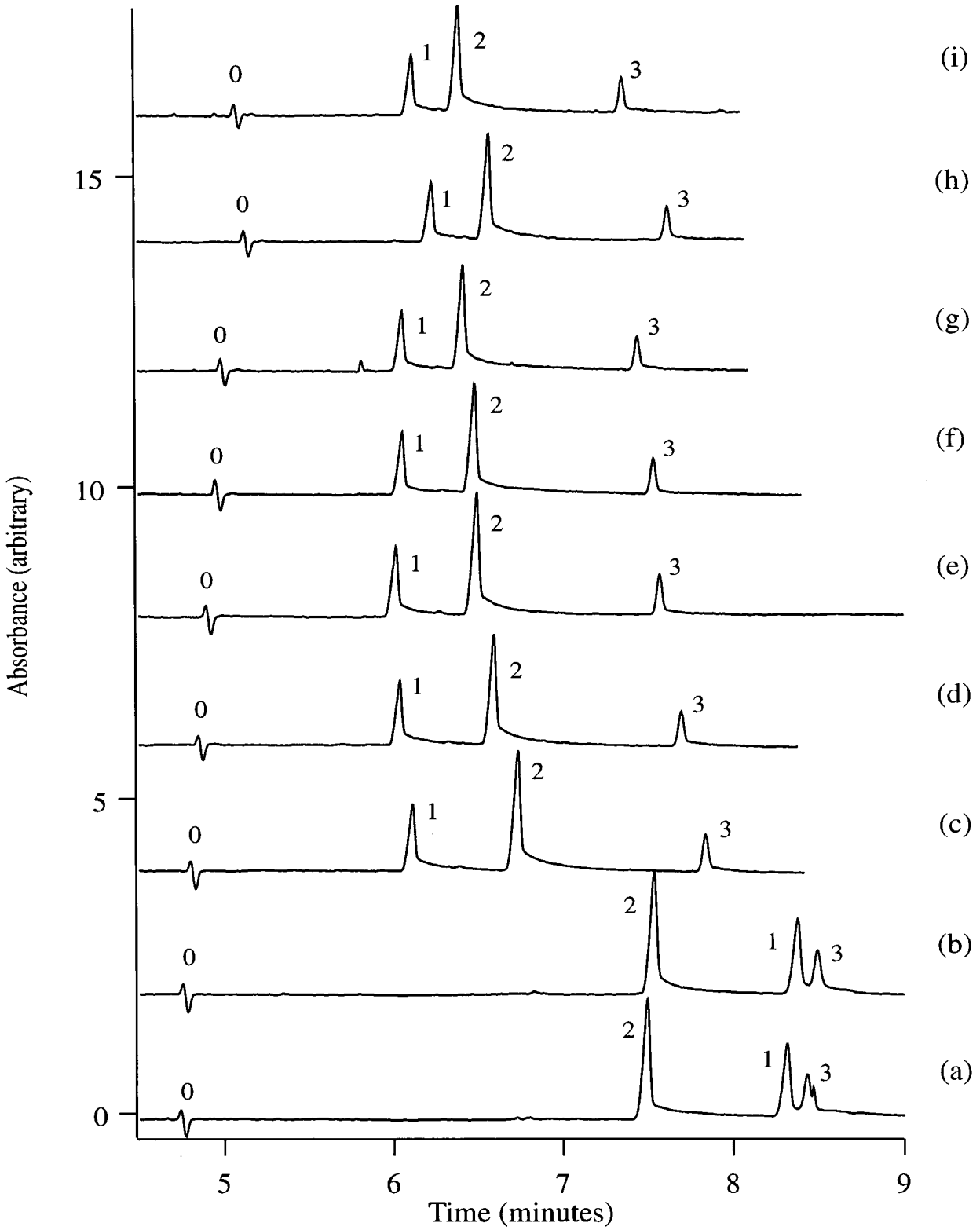

Figure 2.8 Electropherograms obtained using 0 to 20.0 mM β-CD in 10 mM ammonium acetate buffer. The peak numbers correspond to 0 (EOF), 1 (*p*-nitrophenol), 2 (*m*-nitrophenol) and 3 (*o*-nitrophenol). The concentrations of β-CD shown are: (a) and (b) 0 mM, (c) 5.0 mM, (d) 7.5 mM, (e) 10.0 mM, (f) 12.5 mM, (g) 15.0 mM, (h) 17.5 mM and (i) 20.0 mM.

Table 2.1 Equilibrium constants obtained by MS and CE

METHOD	SAMPLE	K (M^{-1})
Electrospray Mass Spectrometry		
50 : 50 : 1 sample : methanol : acetic acid (ammonium acetate buffer)	β-CD + *para*	98.1
	β-CD + *meta*	76.6
	β-CD + *ortho*	too small to detect
50 : 50 : 1 sample : methanol : acetic acid (water)	β-CD + *para*	90.8
	β-CD + *meta*	74.8
	β-CD + *ortho*	24.0
METHOD	SAMPLE	K (M^{-1}) ± SD
Capillary Electrophoresis		
10 mM ammonium acetate pH = 8.93	β-CD + *para*	694.0 ± 2.2
	β-CD + *meta*	101.0 ± 0.3
	β-CD + *ortho*	47.2 ± 0.2

complex to free ion ratios in the gas phase was similar to the trend of equilibrium constants obtained by CE, that is, $K_{para} > K_{meta} > K_{ortho}$. The complexation between *p*-nitrophenol and β-CD is the strongest suggesting that, of the three analytes, *p*-nitrophenol has the best fit inside the CD cavity. *m*-Nitrophenol fits less well into the cavity than *p*-nitrophenol and the structure of *o*-nitrophenol makes it difficult for it to fit into the cavity of the CD. The suggested configurations of the complexes are illustrated in Figure 2.9.

2.3.4 Analyte-Additive Interactions in Phosphate Buffer Using CE

As previously described, ammonium ions (NH_4^+) were found to interact with the β-CD additive in the gas phase. In order to determine if ammonium ions are bound to β-CD in the liquid phase, further CE studies were performed using 10 mM and 30 mM phosphate buffer and the analyte-additive pairs as in Section 2.3.3. If the ammonium ions were attached to the β-CD additive in the liquid phase, then the mobilities found in the ammonium acetate buffer would have been different than those in the phosphate buffers. However, if the mobilities in the phosphate buffers were similar to those in the ammonium acetate buffer, it could be concluded that the ammonium ion was only attached to the β-CD in the gas phase. This could be the case if the ammonium cation (NH_4^+) was only an adduct in the gas phase during the ionization process. An adduct, in the field of mass spectrometry, can be described as a weak ionic bond formed in the gas phase between the cation of the buffer and the analyte of interest. For example, when sodium phosphate buffer is used as the background electrolyte in mass spectrometry studies, it is common to see sodium ion adducts attached to the various peaks in the spectra. Therefore, in these experiments, the ammonium ion could have either been an adduct in the gas phase or may have truly been interacting with the β-CD in both the gas and liquid phases.

Figures 2.10 and 2.11 show the electropherograms from this experiment with increasing concentrations of β-CD in 10 mM and 30 mM phosphate buffer, respectively. When comparing the two figures, the separation of the analytes appears to be quite different. When using 10 mM

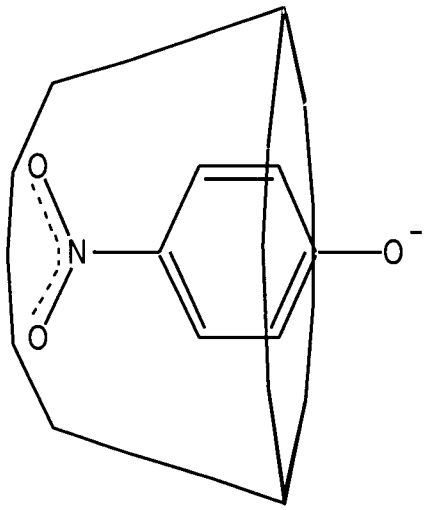

para-nitrophenol + β-CD

-fits best in cavity

-highest K value

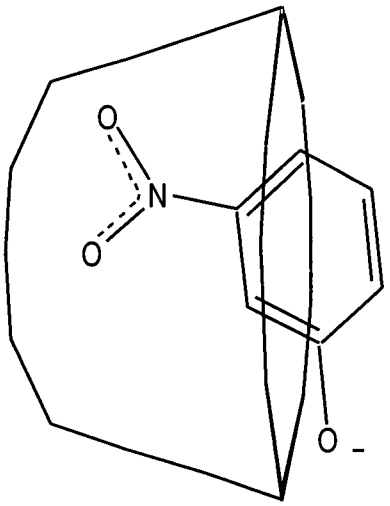

meta-nitrophenol + β-CD

-fits less well in cavity than *para*

-lower K value

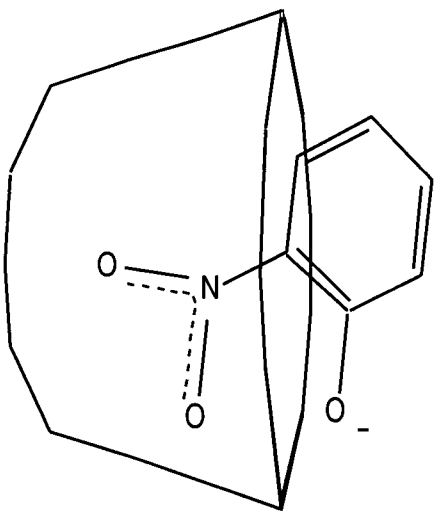

ortho-nitrophenol + β-CD

-fits even less well in cavity
than either *para* or *meta*

-lowest K value

Figure 2.9 Proposed configurations of the various complexes formed by β-CD and the analytes

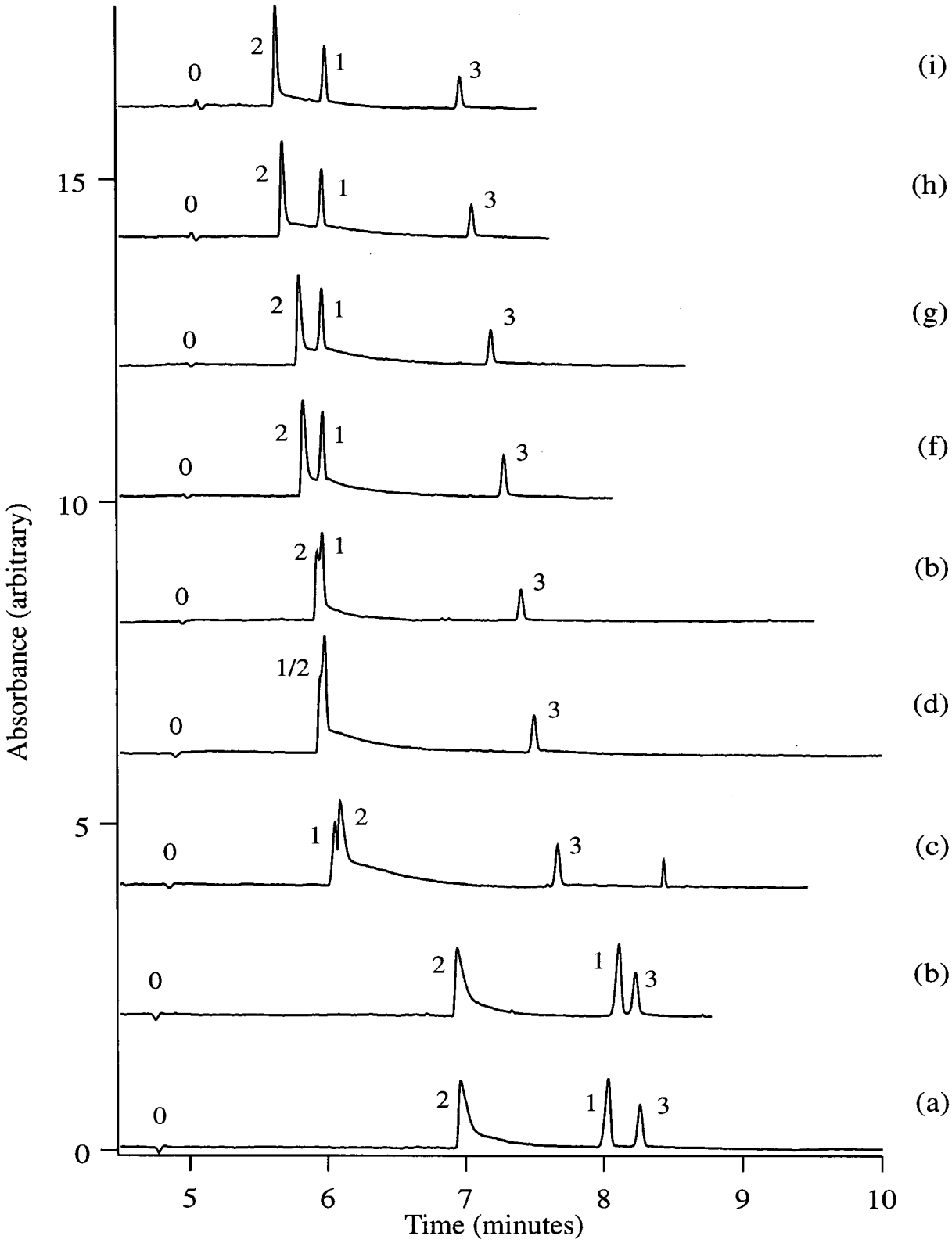

Figure 2.10 Electropherograms obtained using 0 to 20.0 mM β-CD in 10 mM phosphate buffer. The peak numbers correspond to 0 (EOF), 1 (*p*-nitrophenol), 2 (*m*-nitrophenol) and 3 (*o*-nitrophenol). The concentrations of β-CD shown are: (a) and (b) 0 mM, (c) 5.0 mM, (d) 7.5 mM, (e) 10.0 mM, (f) 12.5 mM, (g) 15.0 mM, (h) 17.5 mM and (i) 20.0 mM.

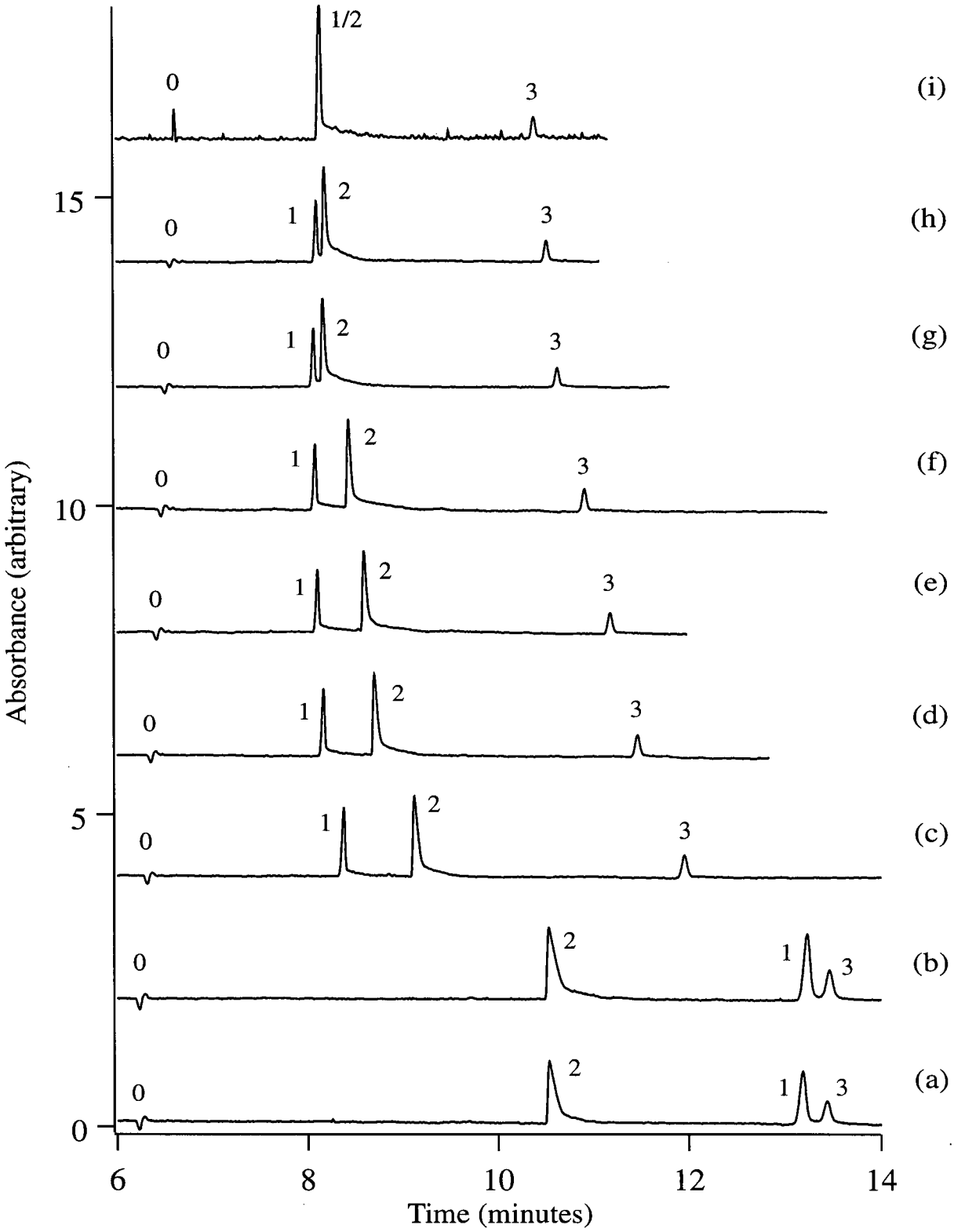

Figure 2.11 Electropherograms obtained using 0 to 20.0 mM β-CD in 30 mM phosphate buffer. The peak numbers correspond to 0 (EOF), 1 (*p*-nitrophenol), 2 (*m*-nitrophenol) and 3 (*o*-nitrophenol). The concentrations of β-CD shown are: (a) and (b) 0 mM, (c) 5.0 mM, (d) 7.5 mM, (e) 10.0 mM, (f) 12.5 mM, (g) 15.0 mM, (h) 17.5 mM and (i) 20.0 mM.

phosphate as the separation buffer, *p*- and *m*-nitrophenol converge and then completely separate from one another with the addition of 12.5 mM β-CD. However, when using 30 mM phosphate buffer, *p*- and *m*-nitrophenol do not converge until 20.0 mM β-CD is added. If concentrations of β-CD above 20.0 mM could have been added (which was not possible because of the limited solubility), the peaks should have eventually been separated again. Using the migration times from these electropherograms, the free mobility ($\mu_{ep,A}$), the complex mobility ($\mu_{ep,AC}$) and the equilibrium constants (K) were determined (Table 2.2). The standard deviations and corresponding 95% confidence intervals (SD x t_{stat}) were also calculated. Since the 95% confidence interval ranges determined were very close, the differences between the obtained parameters using the two buffer solutions were not significant. For example, if the complex mobilities of *p*-nitrophenol using 10 mM phosphate and 10 mM ammonium acetate are compared, taking into consideration the 95% confidence intervals, the complex mobility, $\mu_{ep,AC}$, in 10 mM phosphate is equal to -7.449 x 10^{-5} to -8.831 x 10^{-5} cm^2 V^{-1} sec^{-1} and the $\mu_{ep,AC}$ in 10 mM ammonium acetate is equal to -9.136 x 10^{-5} to -9.484 x 10^{-5} cm^2 V^{-1} sec^{-1}. If the ammonium ions were to interact with the complex in the solution, the negative complex mobility would have been reduced in ammonium acetate solution. The results, however, seem to suggest that this is not the case. Changes in the experimental conditions, such as variations in temperature and the properties of the capillary surface, may lead to such uncertainties. Further study is needed to understand the exact cause of such variations.

2.4 Conclusion

Comparison of binding constants of *p*-, *m*- and *o*-nitrophenol with β-CD in the gas phase and in the liquid phase indicates that binding is stronger in the liquid phase. The trend of the equilibrium constant (K) in the aqueous phase using CE was found to be the same as in the gaseous phase using electrospray MS, that is, $K_{para} > K_{meta} > K_{ortho}$. It was also determined that

Table 2.2 Fundamental parameters obtained by MS and CE

METHOD	SAMPLE	K (M^{-1})	$\mu_{ep,AC}$ ± 95% (cm^2/V sec) confidence interval	$\mu_{ep,A}$ ± 95% (cm^2/V sec) confidence interval
Electrospray Mass Spectrometry				
50 : 50 : 1 sample : methanol : acetic acid (ammonium acetate buffer)	β-CD + *para*	98.1		
	β-CD + *meta*	76.6		
	β-CD + *ortho*	too small to detect		
(water)	β-CD + *para*	90.8		
	β-CD + *meta*	74.8		
	β-CD + *ortho*	24.0		
Capillary Electrophoresis	SAMPLE	K (M^{-1}) ± SD		
10 mM phosphate pH = 8.72	*para*	640 ± 31	-8.14E-05 ± 6.91E-06	-2.56E-04 ± 6.59E-06
	meta	127 ± 3	-1.03E-05 ± 1.57E-05	-2.00E-04 ± 1.03E-05
	ortho	39.2 ± 1.1	-5.22E-05 ± 2.60E-05	-2.62E-04 ± 2.57E-06
30 mM phosphate pH = 8.85	*para*	681 ± 10	-7.52E-05 ± 2.24E-06	-2.51E-04 ± 2.14E-06
	meta	101 ± 2	-2.85E-05 ± 2.11E-05	-2.04E-04 ± 1.82E-05
	ortho	41.5 ± 0.5	-7.11E-05 ± 9.96E-06	-2.55E-04 ± 2.34E-06
10 mM ammonium acetate pH = 8.93	*para*	694 ± 2	-9.31E-05 ± 1.74E-06	-2.67E-04 ± 1.73E-06
	meta	101 ± 1	-7.75E-05 ± 2.45E-06	-2.28E-04 ± 1.55E-06
	ortho	47.2 ± 0.2	-1.06E-04 ± 4.08E-06	-2.72E-04 ± 1.81E-06

ammonium ions are bound to β-CD in the gas phase. By comparing the mobilities of the analytes in ammonium acetate buffer and in phosphate buffer using CE, it was established that the 95% confidence interval ranges of the mobilities were very close and that the differences between the obtained parameters using the two buffer solutions were not significant.

2.5 Future Experiments

The preliminary results presented in this chapter provide more questions than answers. This project could be explored in several directions:

(1) Measure the mobilities of the analytes at an elevated pH (i.e. pH 11). The pKa's of *p*-, *m*- and *o*-nitrophenol are 7.14, 8.35 and 7.23, respectively. The separation buffer used in these experiments had a pH of approximately 9.0. Since this pH is quite close to the pKa of the analytes, the analytes may not have been fully negatively charged. By increasing the pH of the separation buffer to 11.0, this factor would no longer need to be considered.

(2) Carry out further CE studies using larger, bulkier, positive counter-ions (i.e. ion-pairing agents). The experiments presented in this chapter had to take into consideration the counter-ions associated with the buffer ions. Sodium and ammonium are both small counter-ions which may have played a role in the interaction between analyte-additive. By using larger counter-ions, such as ion-pairing agents, the effect of these ions on the analyte-additive complexation may be different.

(3) Carry out further MS studies using different experimental parameters. These studies would include the process of collision induced dissociation (CID). The voltage difference between the orifice and the skimmer can be varied to control the CID process. If the signal of the complex : NH_4^+ decreases with the increase in voltage difference, it would be an indication that the ammonium cations were merely weakly bonded to the outside of the CD (as an adduct) and were not involved in the complexation process in the solution.

Chapter III Complexation Interactions of Tetraalkylammonium Ion-Pairing Agents With Various Analytes in Aqueous and Nonaqueous Media

3.1 Introduction

Ion-pairing, first described by Niels Bjerrum in 1926 [23], occurs when two ions of opposite charge interact with each other in solution. Complexing agents based on ion-pairing have been used to improve the separation of analytes in micellar electrokinetic capillary chromatography (MECC) [77-81] and in other types of CE [82-95].

In MECC, the use of ion-pairing agents as additives causes a notable change in the analyte migration behavior. For example, when a cationic tetraalkylammonium ion-pairing agent is added to a solution, the reagent will form an ion-pair with any anionic analytes present. In solutions containing an anionic micellar agent like SDS, this ion-pairing agent reduces the electrostatic repulsion between the anionic analyte and the anionic micelle and allows hydrophobic interactions between the analyte and the micelles. Conversely, the binding of cationic analytes to the anionic micelle is reduced in the presence of the tetraalkylammonium ion-pairing agent. In both cases, the separation is modified with the addition of increasing amounts of ion-pairing agent. Bjergegaard *et al.* applied the principle of ion-pairing in MECC to the separation of several anions in biological samples [81]. Nishi *et al.* have used similar MECC protocols to study the effect of ion-pairing agents on the micelle for the separation of β-lactam antibiotics and water-soluble vitamins [77,78]. Kaneta *et al.* studied ion association equilibria of analytes with a surfactant both below and above the critical micelle concentration (CMC) and related their findings to MECC theory [79]. The use of ion-pairing agents in MECC has recently been reviewed by Terabe [80].

Ion-pairing agents have also been used to improve the separation of analytes in other types of CE. The application of ion-pairing agents has significantly enhanced the separation of sugars [92] and organic and inorganic anionic components [85,86,88,90]. In previous studies, Greve *et al.* used phytic acid as an ion-pairing agent to increase the resolution of oligosaccharides in complex mixtures [92]. Haddad *et al.* demonstrated indirect detection of electrolytes using

mixtures of the surfactants tetradecyltrimethylammonium bromide (TTAB) and dodecyltrimethylammonium bromide (DTAB) [90]. Similarly, Harakuwe *et al.* optimized the separation of inorganic anions using a cationic additive mixture [88]. Although the separation was improved, the mechanisms for these improvements were not specified in these studies.

There are several examples of enhanced resolution attributed to the ion-pairing mechanism in the separation of peptides and proteins [89,91,94]. Okafo *et al.* effectively suppressed Coulombic interactions between positively charged proteins and the negatively charged silanol groups on the inner wall of the capillary using phytic acid as an ion-pairing agent. Phytic acid, a polyacidic species, when added in small amounts to the separation buffer, enhanced the resolution due to an ion-pairing mechanism between the additive and several standard basic peptides and proteins [89,91]. In another study using ion-pairing agents as complexing additives, Weldon *et al.* addressed several different factors responsible for improvements in resolution, including ionic interactions and hydrophobic associations between analytes and additives. Furthermore, resolution could be optimized by varying the size and concentration of the ion-pairing agents in the buffer system [94]. In a study by Nashabeh and Rassi, capillary zone electrophoresis was employed to analyze the α_1-acid glycoprotein fragments from trypsin and endoglycosidase digestions. Once again, an ion-pairing agent, tetrabutylammonium bromide, was used to achieve better separation of the analytes. However, the increased separation was attributed to the ion-pair formation between the quaternary ammonium salt and the carbohydrate chains of the sialic acid "and/or" by hydrophobic interactions between the alkyl chains of the organic cation and the pyridylamino-oligosaccharides [84]. Although ion-pairing agents have been studied in numerous chemical systems, the effect of such additives is not completely understood. The potential role of hydrophobic interactions in the effect of these ion-pairing agents, in addition to the ion-pairing mechanism, requires further examination.

Ion-pairing agents have also been used to manipulate the electroosmotic flow (EOF) of a system [85,86,95]. Added into the running buffer, ion-pairing agents can be used to reduce the EOF or reverse the direction of the EOF, resulting in alterations in the net mobility of the analytes being studied. These alterations usually result in shorter analysis times and increased resolution.

Jones and Jandik studied the selectivity changes in the separation of ions by incorporating an alkylammonium additive into the running buffer which reversed the direction of the EOF and increased the net mobility of the analytes [85]. Romano *et al.* examined the optimization of inorganic CE (ICE) for the analysis of anionic solutes such as inorganic anions, organic acids and alkylsulphonates. The addition of an EOF modifier was studied as one in a number of parameters that influence ICE separations on electrolyte analytes [86]. Similarly, the effect of some cationic amines, including spermine (N,N′-bis(3-aminopropyl)-1,4-butanediamine), hexamethonium bromide and tetramethylammonium bromide, on the EOF in open fused-silica capillaries was studied by Govindaraju *et al.* In their study, it was determined that spermine caused a significant reduction in the EOF while other additives were less effective [95].

Nonaqueous CE, first introduced by Walbroehl and Jorgenson [96], can be used for the separation of analytes that have small solubilities or form aggregates in aqueous solution. Studies involving analyte-additive interactions in nonaqueous CE were not quantitatively measured until 1995 by Okada [97]. Okada investigated the separation of nonionic polyethers and determined their complexation constants with an electrolyte cation. Since then, nonaqueous CE has become an important component in the examination of additive mixtures. The developments in nonaqueous CE have been compiled in a recent review and the effects of solvent on analyte-additive interactions have been discussed [98].

The use of ion-pairing agents to increase the resolution of various analytes in nonaqueous CE has been previously demonstrated [82,93]. Walbroehl and Jorgenson separated neutral organic molecules by solvophobic association with tetraalkylammonium ions. A mixture of water and acetonitrile was used to enhance the solvophobic relationship between the analyte and the tetraalkylammonium additive and to place a charge on a normally neutral analyte molecule [82]. In another study, chiral separations based on diastereomeric ion-pair formation in nonaqueous media were achieved. The enantiomeric pure (+)- and (-)-camphorsulphonates were used as additives to separate fifteen basic chiral drug analytes. It was demonstrated that substances with

low water solubilities such as cisapride and other enantiomeric analytes containing a β-amino alcohol, could be separated with the aid of ion-pairing agents [93].

In this chapter, the theory of DCCE (previously described in Section 1.3.3) is used to investigate both aqueous and nonaqueous ion-pair formation. This study examined the properties of two tetraalkylammonium ion-pairing agents, dodecyltrimethylammonium bromide (DTAB) and tetramethylammonium bromide (TMAB) and evaluated their suitability as additives in CE separations. The nucleoside adenosine (A) and its monophosphate (AMP), diphosphate (ADP) and triphosphate (ATP), as well as *para*-, *ortho*- and *meta*-nitrophenol were used as model analytes. Both neutrally coated (hydrophobic bonded phase coupled with an external polyacrylamide layer) and uncoated (bare silica) capillaries were used in the experiments and their effects on the separation process were examined. Three parameters, the equilibrium constant (K), the free analyte mobility ($\mu_{ep,A}$) and the mobility of the analyte-additive complex ($\mu_{ep,AC}$), were used to describe the analyte mobility. The increased resolution due to ion-pairing mechanisms and hydrophobic interactions were considered in this study. Both the equilibrium constant and the mobility values for DTAB and TMAB yielded comparable results suggesting that hydrophobic interactions did not play a part in the complexation and that both compounds are suitable additives for CE.

3.2 Experimental

3.2.1 Apparatus

The apparatus used in these experiments was identical to that used in Section 2.2.1 with the following exceptions. Experiments were performed using eCAP neutral coated (hydrophobic bonded phase coupled with an external polyacrylamide layer) fused silica capillaries (Beckman) in addition to uncoated fused silica capillaries.

The rinsing procedures for each part of these experiments vary depending on the type of capillary and media used. The measurement of the EOF is also dependent on these factors. Therefore, these procedures are described in the beginning of each relevant section.

The UV absorption was monitored at 214 nm and 254 nm, depending on the analytes being studied. The maximum absorption (λ_{max}) of nucleoside and nucleotides is 254 nm while the λ_{max} of nitrophenols is 214 nm.

Within the range of the concentrations of the additives used, the viscosity did not change significantly and therefore, the viscosity correction factor was set to one.

3.3.2 Chemicals

In these experiments, two different electrophoresis buffers were used. The first buffer, 30 mM phosphate (pH 8.9), was made using deionized water and was used for the aqueous studies in this chapter. The second buffer, 20 mM Borax ($Na_2B_4O_7 \bullet 10\ H_2O$) (Sigma Chemical Co., St. Louis, MO), when dissolved in HPLC-grade methanol (Fisher Scientific, Nepean, Ontario) yielded 80 mM borate and had an apparent pH of 8.7 when measured with a pH meter. This buffer was used for the nonaqueous studies. Solutions of various concentrations of dodecyltrimethylammonium bromide (DTAB) and tetramethylammonium bromide (TMAB) (Aldrich Chemical Co. Inc., Milwaukee, NJ) were prepared using the two separation buffers. The concentrations of the ion-pairing agents ranged from 0 mM to 20.0 mM DTAB for the nucleoside and nucleotide studies and 0 mM to 60.0 mM DTAB and TMAB for the nitrophenol studies.

Individual stock solutions of A (1.1×10^{-2} M), AMP (5.8×10^{-3} M), ADP (1.0×10^{-2} M) and ATP (3.7×10^{-3} M) (Sigma Chemical Co., St. Louis, MO) were prepared in deionized water. A mixture of the four analytes was then prepared by combining varying amounts of the four stock solutions, depending on the initial stock solution concentration and diluting with deionized water to give final concentrations of 2.5×10^{-4} M for each analyte. Individual stock solutions (1.0×10^{-2} M) of *para*-, *ortho*- and *meta*-nitrophenol were prepared in methanol. Two mixtures of the three analytes were then prepared by combining equal amounts of the three stock solutions and diluting (i) 0.2:10 and (ii) 2:10 with methanol giving final concentrations of (a) 2.5×10^{-4} M and (b) 2.5×10^{-3} M for each analyte. Mixture (a) was used as the analyte mixture for running buffers having

additive concentrations less than 10 mM and mixture (b) was used for running buffers having additive concentrations of 10 mM and higher.

3.3 Discussion

3.3.1 The Effect of DTAB in Aqueous Media in an Uncoated Capillary

A 57 cm uncoated fused silica capillary was used to separate the mixture of A, AMP, ADP and ATP. The capillary was conditioned by rinsing with 0.1 M NaOH for 10 minutes, deionized water for 5 minutes and 30 mM phosphate buffer (pH 8.9) for 15 minutes followed by overnight equilibration in the same buffer. The EOF was measured by adding acetonitrile (Sigma Chemical Co., St. Louis, MO) to each sample (5% v/v) and the UV absorption signal was measured at 254 nm. Samples were injected via pressure injection for 5 seconds at 0.5 psi and separated at 20 kV or -20 kV, depending on the direction of the analyte mobility.

One of the most important steps in this set of experiments was to determine the critical micelle concentration (CMC). The CMC can be described as the concentration of surfactant at which micelles form. The literature value for DTAB in water at 25 °C is 15 mM [1]. However, the actual CMC is often much lower in solutions with higher ionic strength [99]. Therefore, the current was measured at different concentrations of additive. A graph of conductivity versus concentration of DTAB is shown in Figure 3.1.

The following equation was used to calculate the conductivity:

$$\sigma = \frac{L\,I}{V\,A} = \frac{L\,I}{V\,\pi\,r^2} \qquad (3.1)$$

where σ is the conductivity (A/Vm), L is the length of the capillary (m), I is the current (A), V is the voltage (V) and A is the cross sectional area of the capillary (m^2). A sudden change in the slope of the conductivity versus DTAB concentration was observed, indicating that the CMC for DTAB under these conditions was approximately 6 mM. This becomes an important factor when studying the mobility values of various analytes. Whether the additive forms micelles in solution or remains a single component affects the net electrophoretic mobility of the analytes significantly.

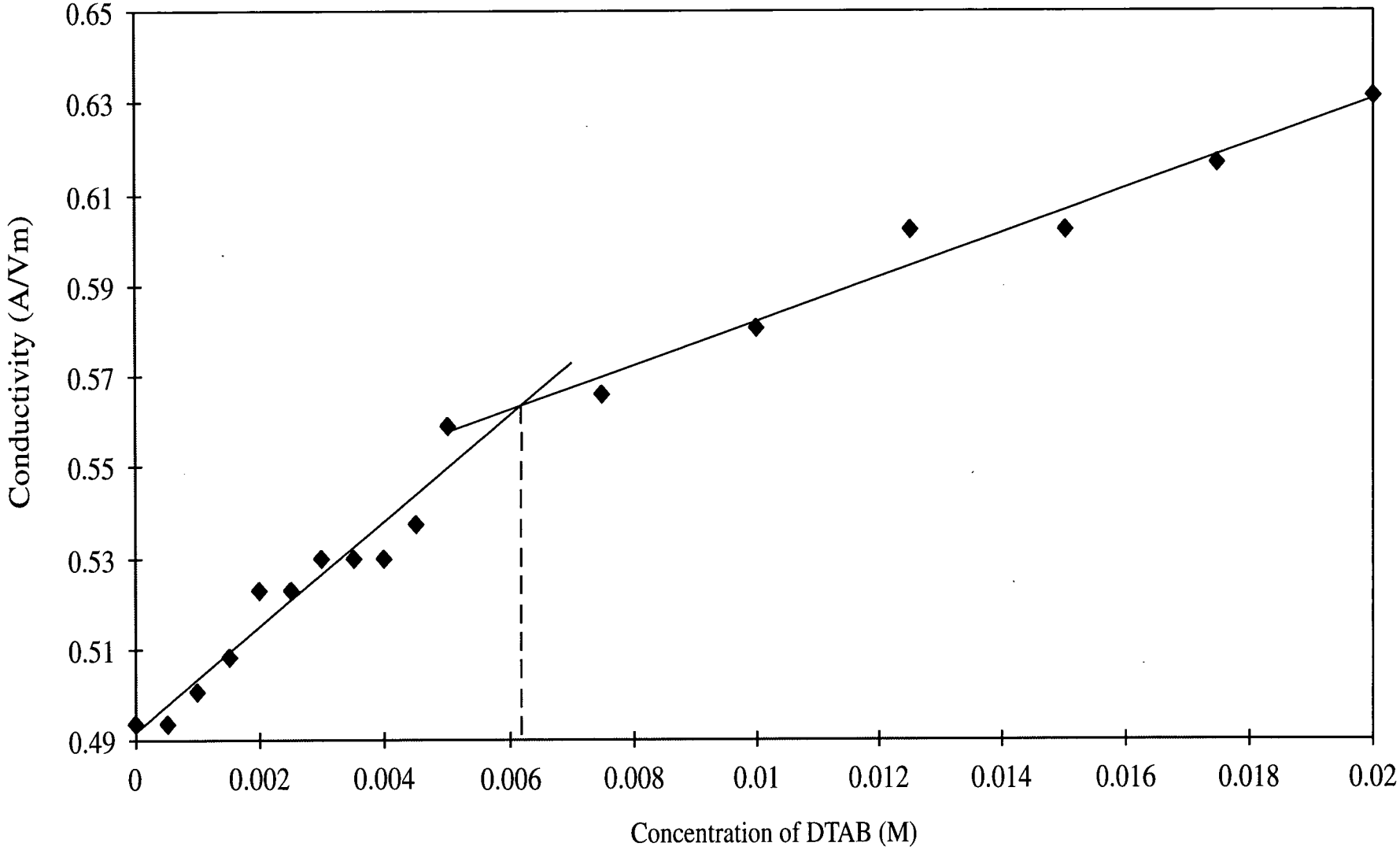

Figure 3.1 Conductivity versus additive concentration in 30 mM phosphate buffer, pH 8.9. The actual critical micelle concentration was determined to be approximately 6 mM.

Figure 3.2 and Figure 3.3 show the electropherograms under the above conditions. It is important to note that at 0 mM DTAB (Figure 3.2a), all of the analytes migrated in the same direction when a normal polarity mode was used. However, with the addition of increasing amounts of additive (1.0 mM DTAB - Figure 3.2c), some analytes began to take longer to migrate. At 1.5 mM DTAB (Figure 3.2d and e) both a normal polarity mode separation and a reversed polarity mode separation needed to be carried out in order for all of the analyte peaks to reach the detector. At concentrations of 2.0 mM DTAB and above (Figure 3.2f and Figure 3.3), all separations were carried out using the reversed polarity mode.

The tabulated order in which the nucleoside/nucleotides were detected helped to explain how the various conditions affected the separation process (Table 3.1). The elution order from 0 to 2.0 mM DTAB was relatively straight forward. ATP was the most negative of all of the analytes and thus, remained in the capillary the longest. With the increasing concentration of ion-pairing agent, ATP remained the most negatively charged analyte (it needed to acquire more positively charged ion-pairing agent to become neutral) and had the longest migration time. Eventually at 1.5 mM DTAB, the nucleotides migrated so slowly and the EOF was so small that the electrophoretic mobility of some of the analytes (ATP, ADP and AMP) was greater than the EOF (Figure 3.2d). This required the polarity on the system to be reversed (Figure 3.2e). At 2.0 mM DTAB, all of the analytes required a reversed polarity in order to be detected (Figure 3.2f). When the polarity was reversed, ATP became the fastest migrating analyte, due to the fact that it was the most negatively charged of all of the analytes. Meanwhile, AMP had less negative constituents than ADP and therefore, it migrated slower (Figure 3.3a to h). When the DTAB concentration was greater than the CMC, the negative ADP interacted more with the positively charged micelles and the migration order of ADP and AMP was switched (Figure 3.3i to l). Before the CMC is reached, with increasing concentrations of ion-pairing agent, the EOF marker remained the slowest migrating peak (Figure 3.3a to h). However, once the concentration of DTAB was greater than the CMC, the migration order of A and EOF began to switch because of the interaction between A and the micelles (Figure 3.3i to l).

Above 6 mM DTAB, the ion-pairing agent no longer acted through a pairing mechanism but as

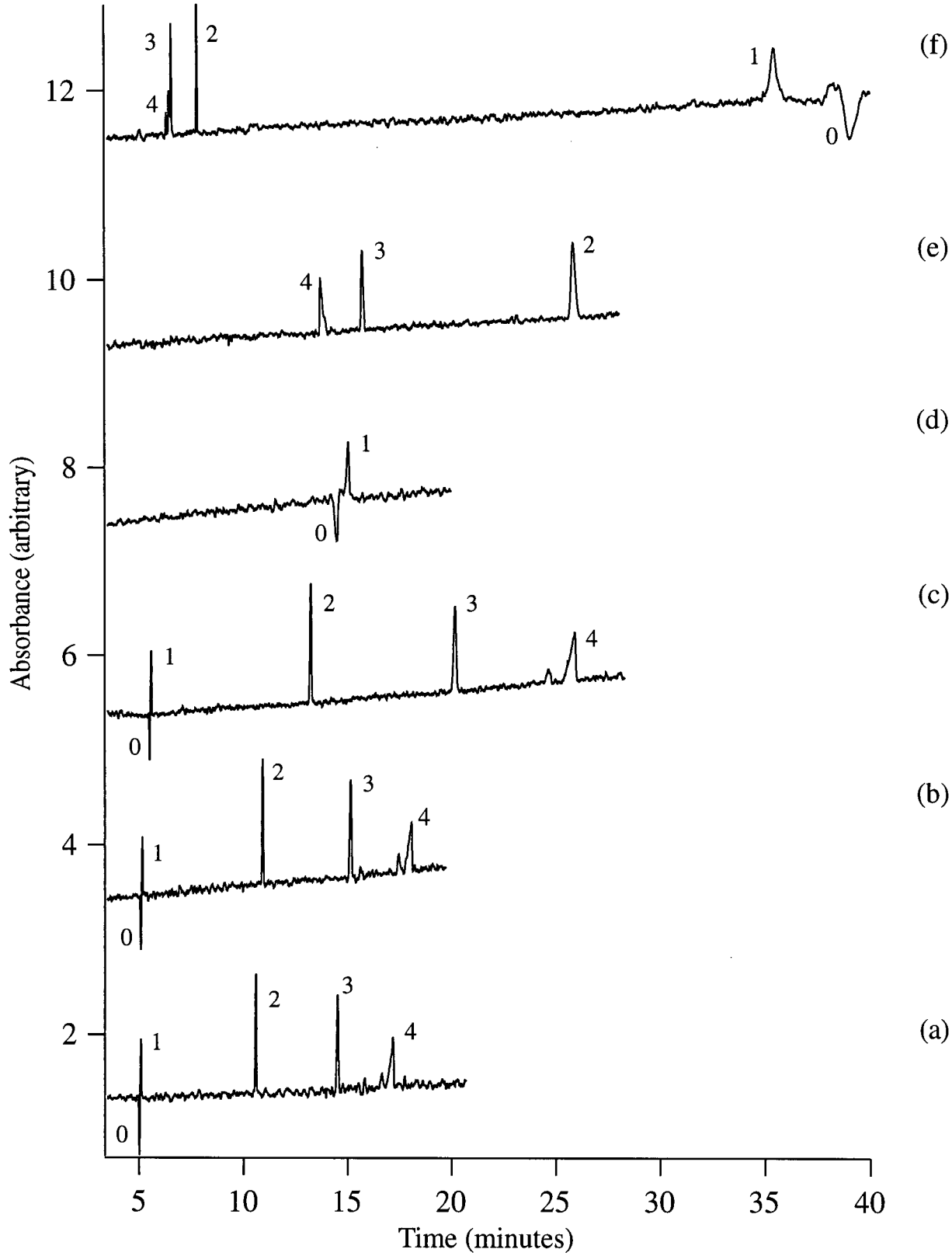

Figure 3.2 Electropherograms obtained using 0 to 2.0 mM DTAB in 30 mM phosphate buffer. The peak numbers correspond to 0 (EOF - acetonitrile), 1 (A), 2 (AMP), 3 (ADP) and 4 (ATP). The concentrations of DTAB shown are: (a) 0 mM, (b) 0.5 mM, (c) 1.0 mM, (d) 1.5 mM, (e) 1.5 mM - reversed polarity, (f) 2.0 mM - reversed polarity.

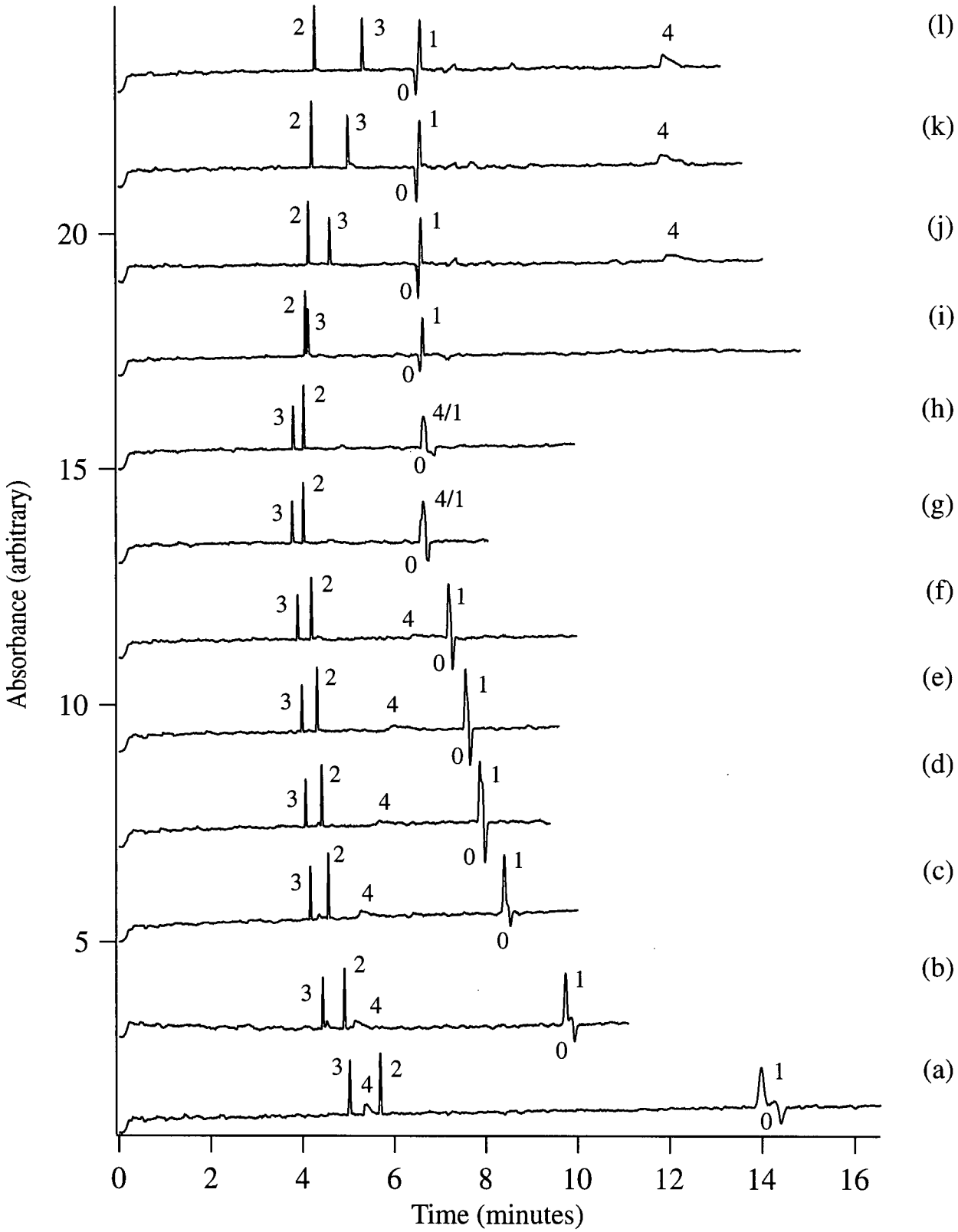

Figure 3.3 Electropherograms obtained using reversed polarity mode and 2.5 to 20.0 mM DTAB in 30 mM phosphate buffer. The peak numbers correspond to 0 (EOF - acetonitrile), 1 (A), 2 (AMP), 3 (ADP) and 4 (ATP). The concentrations of DTAB shown are: (a) 2.5 mM, (b) 3.0 mM, (c) 3.5 mM, (d) 4.0 mM, (e) 4.5 mM, (f) 5.0 mM, (g) 7.5 mM, (h) 10.0 mM, (i) 12.5 mM, (j) 15.0 mM, (k) 17.5 mM and (l) 20.0 mM.

Table 3.1 Nuceloside/nucelotide migration order with increasing concentrations of DTAB additive

Polarity	DTAB Concentration	Analyte Trend
Normal	0 mM	EOF A AMP ADP ATP
Normal	0.5 mM	EOF A AMP ADP ATP
Normal	1.0 mM	EOF A AMP ADP ATP
Normal	1.5 mM	EOF A
Reversed	1.5 mM	ATP ADP AMP
Reversed	2.0 mM	ATP ADP AMP A EOF
Reversed	2.5 mM	ADP ATP AMP A EOF
Reversed	3.0 mM	ADP AMP ATP A EOF
Reversed	3.5 mM	ADP AMP ATP A EOF
Reversed	4.0 mM	ADP AMP ATP A EOF
Reversed	4.5 mM	ADP AMP ATP A EOF
Reversed	5.0 mM	ADP AMP ATP A EOF
Reversed	7.5 mM (> CMC)	ADP AMP ATP/A EOF
Reversed	10.0 mM	ADP AMP ATP/A EOF
Reversed	12.5 mM	AMP ADP EOF A ATP
Reversed	15.0 mM	AMP ADP EOF A ATP
Reversed	17.5 mM	AMP ADP EOF A ATP
Reversed	20.0 mM	AMP ADP EOF A ATP

micelles. Micelle formation should be considered in the analyte-additive interaction. The binding isotherm for this type of analyte-additive interaction should have two distinct sections: the interaction prior to the micelle formation and the multiple equilibria between DTAB monomers, micelles and the analyte when the concentration of additive is higher than the CMC. To study the effect of pure ion-pairing interactions, the formation of micelles should be avoided. This was achieved by performing the experiment in nonaqueous media. Micelles are unlikely to be formed in nonaqueous solutions [98] and therefore, these conditions allowed the analyte-DTAB interaction to be studied at various concentrations without this interference.

3.3.2 The Effect of DTAB in Nonaqueous Media in an Uncoated Capillary

A 27 cm uncoated fused silica capillary was used to separate the mixture of *p*-, *o*- and *m*-nitrophenol. Nucleosides and nucleotides are insoluble in nonaqueous media and therefore, nitrophenols were chosen as alternative analytes for these experiments. The capillary was conditioned by rinsing with saturated nonaqueous NaOH (BDH Inc., Toronto, Ontario) for 20 minutes, methanol for 5 minutes and 80 mM borate separation buffer for 15 minutes followed by overnight equilibration in the same buffer. In order to measure the EOF, benzene (Caledon Laboratories Ltd., Georgetown, Ontario) was added to each sample (0.02% v/v) as described in the discussion. Samples were injected electrokinetically for 20 seconds at -10 kV (reversed polarity) and separated at -15 kV.

Before presenting the results of this part of the ion-pairing agent study, it is necessary to understand how the migration times were measured. At all concentrations of additive, it was necessary for at least one analyte to be injected electrokinetically at the outlet of the capillary. Table 3.2 depicts an overall schematic of how each analyte was injected at different concentrations of additive. Figure 3.4 shows the electropherograms for the three nitrophenols when the DTAB concentration is changed from 0 to 60.0 mM in 80 mM borate buffer. When no DTAB was added and the analyte mixture was injected at the inlet, only the *p*-nitrophenol peak migrated past the detector (Figure 3.4a). Since the EOF marker and *o*- and *m*-nitrophenol migrated towards the cathode (-), another injection was performed at the outlet. These two

Table 3.2 Experimental conditions for the separation of *p*-, *o*-, and *m*-nitrophenol in 0 mM and 5.0 to 60.0 mM DTAB

[DTAB]		Inlet (-)	Outlet (+)
0 mM	Run 1	injection of analyte mix (only *p*-nitrophenol elutes)	injection of EOF marker (travels only 7 cm before reaching detection window)
	Run 2		injection of analyte mix and EOF marker (*m*- and *o*-nitrophenol elute)
5.0 to 60.0 mM	Run 1	injection of analyte mix (*p*- and *o*-nitrophenol elute)	injection of EOF marker
	Run 2		injection of analyte mix and EOF marker (*m*-nitrophenol elutes)

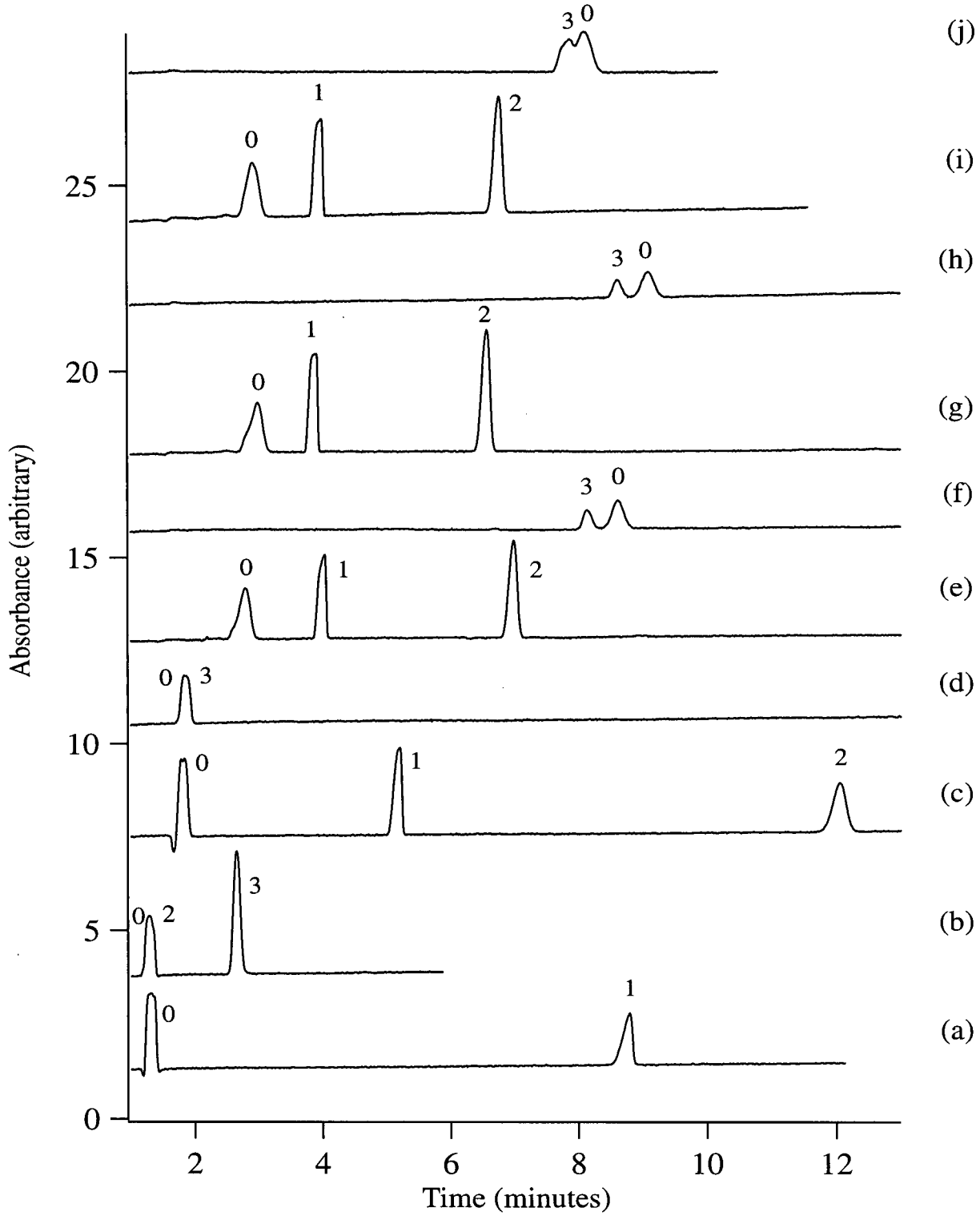

Figure 3.4 Electropherograms obtained using 0 to 60 mM DTAB in 80 mM borate buffer. The peak numbers correspond to 0 (EOF - benzene), 1 (*p*-nitrophenol), 2 (*o*-nitrophenol) and 3 (*m*-nitrophenol). The concentrations of DTAB shown are: (a) 0 mM - inlet injection, (b) 0 mM - outlet injection, (c) 5.0 mM - inlet injection, (d) 5.0 mM - outlet injection, (e) 12.5 mM - inlet injection, (f) 12.5 mM - outlet injection, (g) 15.0 mM - inlet injection, (h) 15.0 mM - outlet injection, (i) 20.0 mM - inlet injection, (j) 20.0 mM - outlet injection. Runs (a) through (e) and (g) and (i) were carried out using reversed polarity while runs (f), (h) and (j) were obtained using normal polarity.

analytes and the EOF marker traveled only 7 cm through the capillary before reaching the detection window (Figure 3.4b). With the addition of DTAB in the running buffer, *p*- and *o*-nitrophenol were detected when injected at the cathode end of the capillary (Figure 3.4c, e, g and i), while the EOF marker and the *m*-nitrophenol peaks eluted only when injected at the anode (Figure 3.4d). To confirm that peak 3 was migrating out of the capillary after the EOF in reversed polarity mode, the polarity was switched to normal mode in order for peaks 0 and 3 to migrate through a longer piece of capillary which increased the separation (Figure 3.4f, h and j). Injecting samples from both ends required the EOF to be measured in each run, compensating for any deviation in migration time between runs of the same buffer.

Assuming a 1:1 interaction between the analytes and the additive, nonlinear regression was used to calculate the parameters in these experiments. Table 3.3 lists the values of the equilibrium constants (K) and of the free and complex mobilities ($\mu_{ep,A}$ and $\mu_{ep,AC}$) for the separation of *p*-, *o*- and *m*-nitrophenol with DTAB as an additive. It was evident from the data listed in Table 3.3 that the constants obtained could not accurately describe the migration behavior of the three nitrophenols. The DTAB-nitrophenolate interactions appeared to be too small to measure accurately, giving rise to large deviations in the K values. There was a possibility that the method for measuring the EOF in the system (i.e. benzene as the EOF marker) was an inaccurate reflection of the EOF. Perhaps benzene was interacting with the additive, resulting in a false reading of the EOF.

Because benzene may have been interfering with the analyte-additive interactions, the next step in this study was to determine if benzene could be replaced with other neutral EOF markers in an attempt to more accurately measure the EOF. Figure 3.5 illustrates the electropherograms of two alternative EOF markers, N, N-dimethyl formamide (DMF) (Fisher Scientific, Nepean, Ontario) and dimethyl sulfoxide (DMSO) (Fisher Scientific, Nepean, Ontario) in addition to benzene. Using Figure 3.5, it was observed that of the three chemicals studied, benzene interacted the least with DTAB. Both DMF and DMSO migrated out of the capillary at similar times, 6.056 and 6.274 minutes respectively, while benzene eluted from the capillary much later, at 9.093 minutes. Since the polarity of the system was reversed in this study and the EOF markers were

Table 3.3 Equilibrium constants and electrophoretic mobilities of the free and complexed species for the separation of *p*-, *o*- and *m*-nitrophenol with DTAB additive obtained from nonlinear regression

analyte	DTAB K (M^{-1})	free mobility $\mu_{ep,A}$ (x 10^{-4} cm^2 $V^{-1}s^{-1}$)	complex mobility $\mu_{ep,AC}$ (x 10^{-4} cm^2 $V^{-1}s^{-1}$)	R^2
p-nitrophenol	3 ± 5	-2.28 ± 0.01	-1.16 ± 1.22	0.805
o-nitrophenol	-5629 ± 3516	-0.073 ± 0.003	-1.61 ± 0.02	0.128
m-nitrophenol	7876 ± 9240	-0.840 ± 0.003	0.033 ± 0.013	0.0517

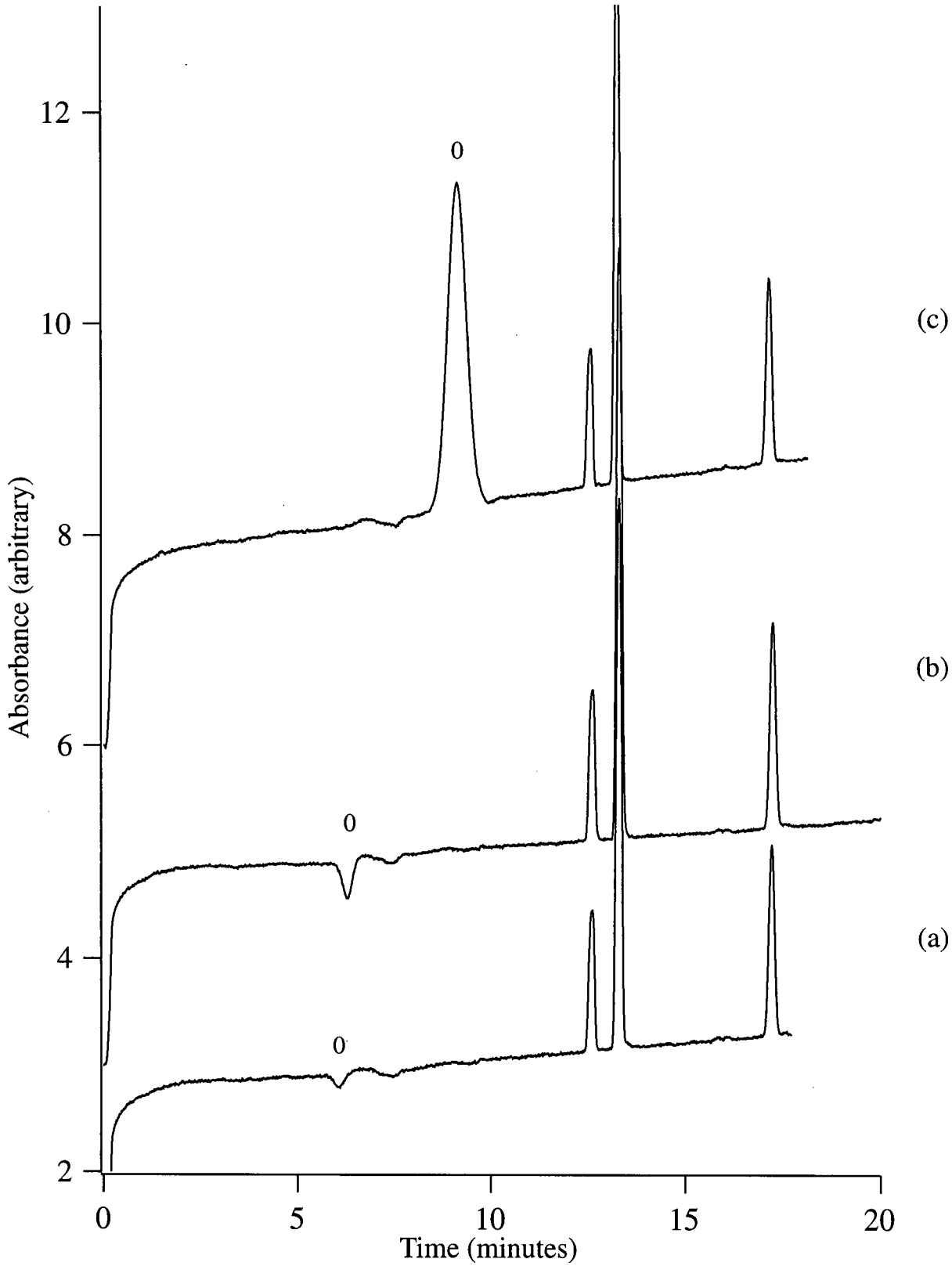

Figure 3.5 Electropherograms obtained using three different EOF markers: (a) 0 = EOF = DMF, (b) 0 = EOF = DMSO and (c) 0 = EOF = benzene. All runs were completed in 20 mM DTAB additive buffer using reversed polarity with the EOF marker injected at the outlet.

electrokinetically injected via the outlet, analytes having faster migration times reached the detection window sooner. Since DTAB, having a positive charge, also traveled toward the cathode, EOF markers that interacted with the additive would have traveled in the same direction. Therefore, in this study, the longer it took for the EOF marker to be detected, the less likely that the EOF marker was interacting with the additive. Of the three EOF markers, benzene seemed to interact the least. Although using benzene seemed to be the most accurate way to measure the EOF, it was still possible that minor interactions were affecting the migration. To solve this problem, the capillary needed to be coated with a neutral coating. With a neutral coated capillary, there is no EOF to be measured and the problem of the interaction of an EOF marker with the additive is eliminated.

3.3.3 The Effect of DTAB in Nonaqueous Media in an eCAP Neutral Capillary

Neutral eCAP capillaries, designed by Beckman Instruments Inc. for "electrophoresis chemistries applied for P/ACE", are capillaries covered with different types of coatings including polyvinylalcohol (Nacho capillary), polyacrylamide (SDS and DNA capillaries) and hydrophobic bonded/polyacrylamide (neutral capillary). Each coated surface allows for the separation of different analytes under specific conditions. In this part of the study, an eCAP neutral capillary was rinsed with the 20 mM borax (80 mM borate) separation buffer for 15 minutes followed by overnight equilibration in the same buffer. No nonaqueous NaOH was used to rinse this capillary in order to preserve the neutral coating. No EOF marker was required with this capillary because the neutral coating eliminates or greatly reduces the EOF. Samples were injected into the coated capillary by pressure injection for 5 seconds at 0.5 psi and separated at -15 kV.

Figure 3.6 shows the electropherograms of 0 to 20.0 mM DTAB in 80 mM borate buffer, using the eCAP neutral capillary. From the migration times collected in this set of experiments, the values for the equilibrium constants (K) and the free and complex mobilities ($\mu_{ep,A}$ and $\mu_{ep,AC}$) were calculated and are presented (Table 3.4). With the use of a neutral coated capillary, DTAB-nitrophenolate interactions appeared to be more accurately represented compared to the measurement made in the uncoated capillaries.

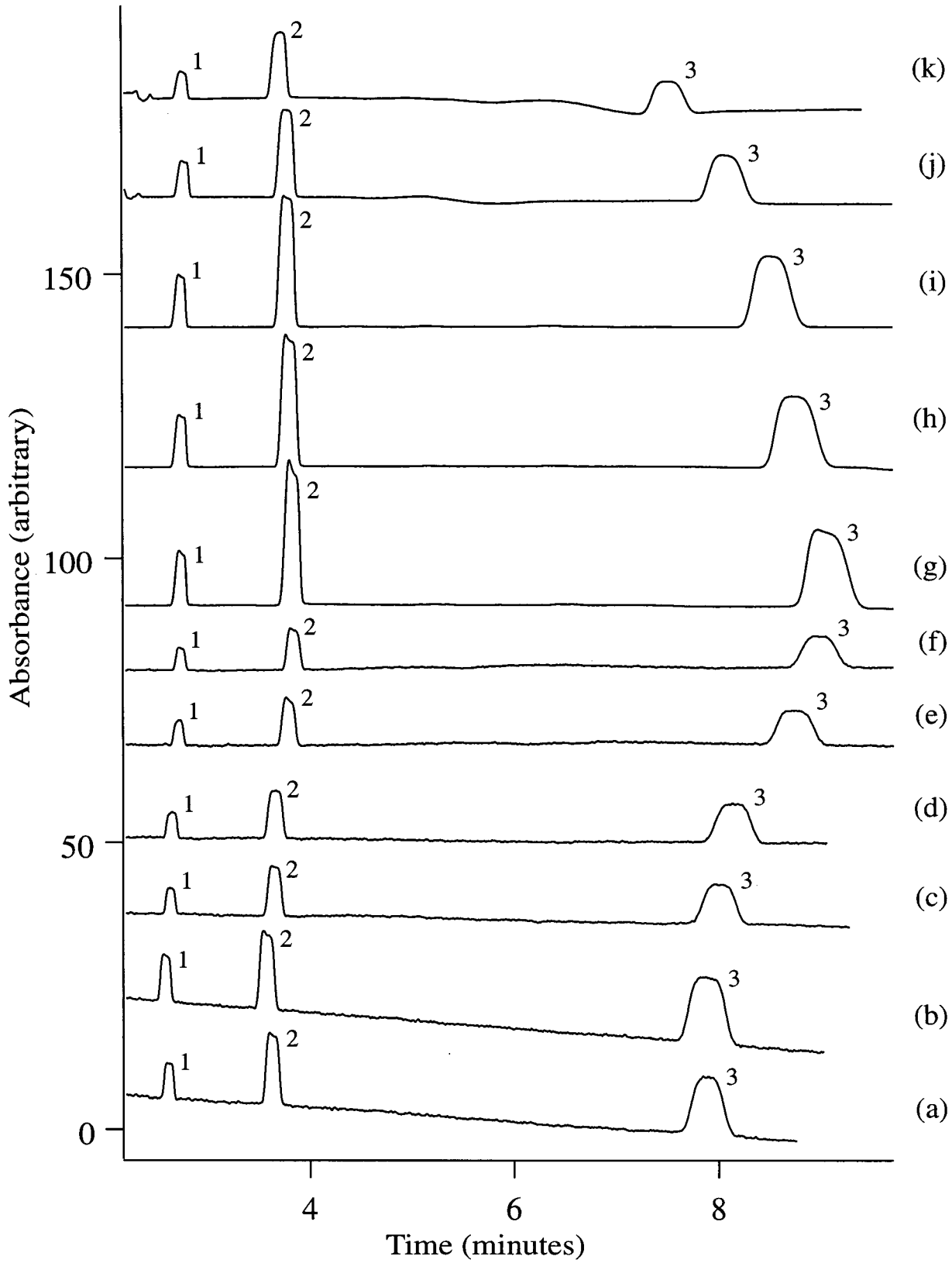

Figure 3.6 Electropherograms obtained using 0 to 20.0 mM DTAB in 80 mM borate buffer and an eCAP capillary. The peak numbers correspond to 1 (*p*-nitrophenol), 2 (*o*-nitrophenol), 3 (*m*-nitrophenol). The concentrations of DTAB shown are: (a) 0 mM, (b) 1.0 mM, (c) 2.0 mM, (d) 3.0 mM, (e) 4.0 mM, (f) 5.0 mM, (g) 10.0 mM, (h) 12.5 mM, (i) 15.0 mM, (j) 17.5 mM and (k) 20.0 mM.

Table 3.4 Equilibrium constants and electrophoretic mobilities of the free analytes and their DTAB complexes for each analyte obtained from nonlinear regression

analyte	DTAB K (M^{-1})	free mobility $\mu_{ep,A}$ (x 10^{-4} cm^2 $V^{-1}s^{-1}$)	complex mobility $\mu_{ep,AC}$ (x 10^{-4} cm^2 $V^{-1}s^{-1}$)	R^2
p-nitrophenol	158 ± 11	-2.32 ± 0.02	-2.11 ± 0.03	0.812
o-nitrophenol	220 ± 21	-1.67 ± 0.02	-1.52 ± 0.03	0.716
m-nitrophenol	444 ± 61	-0.78 ± 0.02	-0.66 ± 0.02	0.584

Upon studying the trends in the data listed in Table 3.4, several conclusions were drawn. In terms of K values, the trend in the data was *para* < *ortho* < *meta*. Therefore, *p*-nitrophenol interacted the least with the DTAB additive, while *m*-nitrophenol interacted the most. This trend was explained using the pKa values of the analytes. The pKa values of the model analytes in this study are *p*-nitrophenol (7.14), *o*-nitrophenol (7.23) and *m*-nitrophenol (8.35). When separating these analytes using borate buffer at an apparent pH of 8.7, it was concluded that the hydroxyl group on *p*-nitrophenol spent much more time as a negatively charged constituent compared to *m*-nitrophenol which had much less of a negatively charged component. Therefore, the negatively charged group in the *p*-nitrophenol form was very open to sodium ions from the borate buffer, allowing sodium ions to surround the negatively charged hydroxyl group. This charge screening, due to the development of a double layer around the analyte by the sodium ions, decreased the affinity for the positively charged DTAB additive to attach to the constituent and form an ion-pair. Conversely, *m*-nitrophenol's pKa is much closer to that of the buffer's pH, so the hydroxyl group was constantly changing between being negative and neutral. This situation gave the sodium ions less chance to surround the negatively charged hydroxyl group. Therefore, DTAB was able to form an ion-pair with the negative component. This relationship between the analyte/sodium complex and the analyte/DTAB complex can be described using the following equations:

$$\text{fraction of analyte/Na}^{+}\text{ complex} = \frac{k'_{Na}}{1 + k'_{Na} + k'_{DTAB}} \tag{3.2}$$

$$\text{fraction of analyte/DTAB complex} = \frac{k'_{DTAB}}{1 + k'_{Na} + k'_{DTAB}} \tag{3.3}$$

In terms of negative mobility, the $\mu_{ep,AC}$ values are smaller than the $\mu_{ep,A}$ values. Therefore, when the nitrophenol species are in the free form, they have a larger negative mobility than when they are in the complexed form. A graph of electrophoretic mobility versus DTAB concentration shows how the data accurately fits the binding isotherm (Figure 3.7).

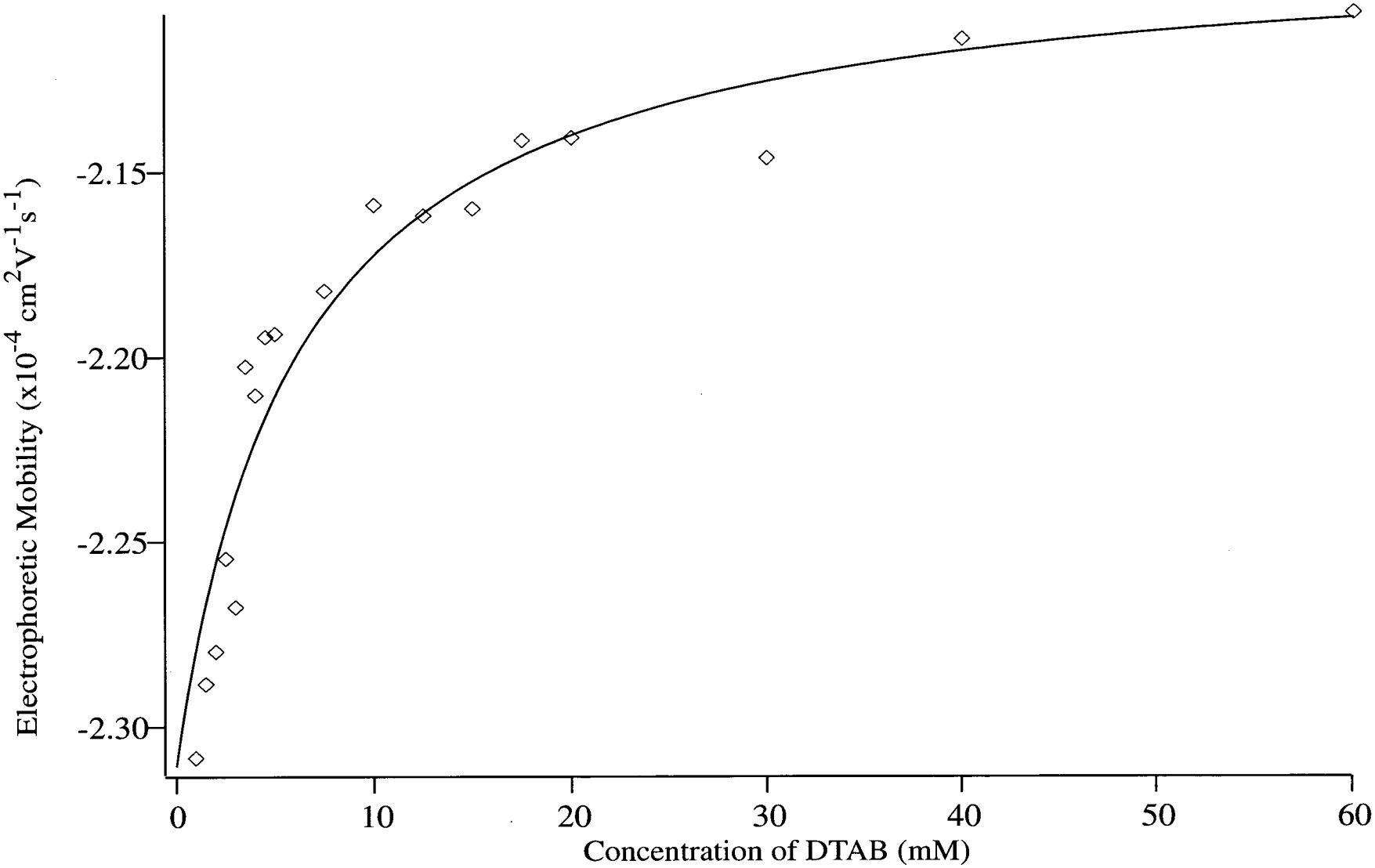

Figure 3.7 Electrophoretic mobility of *p*-nitrophenol versus DTAB concentration. The solid line represents the binding isotherm determined by the free and complex mobility and the equilibrium constant, and the points represent the experimental data.

3.3.4 The Effect of TMAB in Nonaqueous Media in an eCAP Neutral Capillary

Because DTAB has an extended hydrophobic tail, there was some uncertainty as to whether the complexation of DTAB was truly due to ion-pairing or whether hydrophobic interactions played a part in the complexation. To confirm the ion-pairing interaction, a similar investigation was performed, using an ion-pairing agent that had minimal hydrophobic constituents. Tetramethylammonium bromide (TMAB), having very short alkyl groups, does not form micelles in water and should have contributed very little to hydrophobic interactions in nonaqueous media. Therefore, if the ammonium-nitrophenolate complexation of TMAB and the analytes in question could be accurately measured and the parameter values were determined to be similar to those previously calculated using DTAB, it could be inferred that the DTAB complexation was truly due to the phenomenon of ion-pairing. Figure 3.8 depicts the electrophoretic separations of the analytes using TMAB as the additive. The migration times seemed to resemble those in Figure 3.6. The migration times from Figure 3.8 were measured and their corresponding equilibrium constants (K) and the free and complex mobilities ($\mu_{ep,A}$ and $\mu_{ep,AC}$) were calculated and tabulated (Table 3.5). After close examination of the data, it appeared that using TMAB as the additive and carrying out the separations in an eCAP neutral capillary using nonaqueous media allowed the ammonium-nitrophenolate interaction to be accurately measured. When the values of K, $\mu_{ep,A}$ and $\mu_{ep,AC}$ from Table 3.4 and Table 3.6 were compared, the values of the three parameters were found to be similar in magnitude. Thus, the interaction between analyte and additive was concluded to be mainly due to ion-pairing.

In the DTAB and TMAB studies in this chapter, there were indications that the surface of the coated capillary was changing. For example, when repeating a trial of nonaqueous additive experiments on the second day using the same coated capillary, the migration times of the analytes were significantly different from those measured the previous day. To investigate this, the mobility versus the concentration of TMAB with *p*-nitrophenol as the analyte was plotted (Figure 3.9). At higher concentrations of TMAB, the mobility curve descended, which meant the

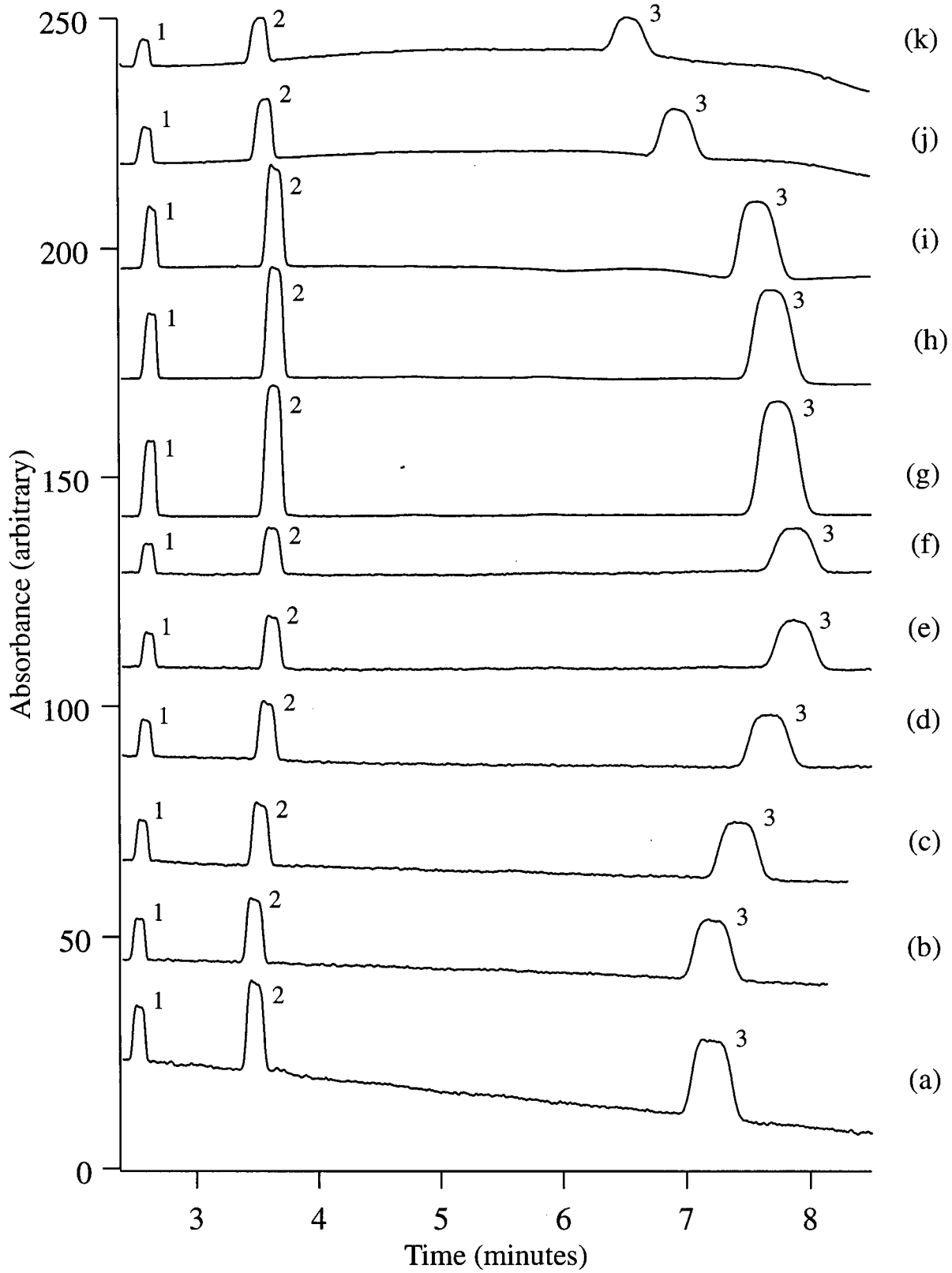

Figure 3.8 Electropherograms obtained using 0 to 20.0 mM TMAB in 80 mM borate buffer and an eCAP capillary. The peak numbers correspond to 1 (*p*-nitrophenol), 2 (*o*-nitrophenol), 3 (*m*-nitrophenol). The concentrations of TMAB shown are: (a) 0 mM, (b) 1.0 mM, (c) 2.0 mM, (d) 3.0 mM, (e) 4.0 mM, (f) 5.0 mM, (g) 10.0 mM, (h) 12.5 mM, (i) 15.0 mM, (j) 17.5 mM and (k) 20.0 mM.

Table 3.5 Equilibrium constants and electrophoretic mobilities of the free analytes and their TMAB complexes for each analyte obtained from nonlinear regression

analyte	TMAB K (M^{-1})	free mobility $\mu_{ep,A}$ (x 10^{-4} cm^2 $V^{-1}s^{-1}$)	complex mobility $\mu_{ep,AC}$ (x 10^{-4} cm^2 $V^{-1}s^{-1}$)	R^2
p-nitrophenol	203 ± 20	-2.36 ± 0.01	-2.24 ± 0.02	0.842
o-nitrophenol	239 ± 32	-1.72 ± 0.01	-1.62 ± 0.02	0.760
m-nitrophenol	659 ± 238	-0.830 ± 0.009	-0.77 ± 0.01	0.359

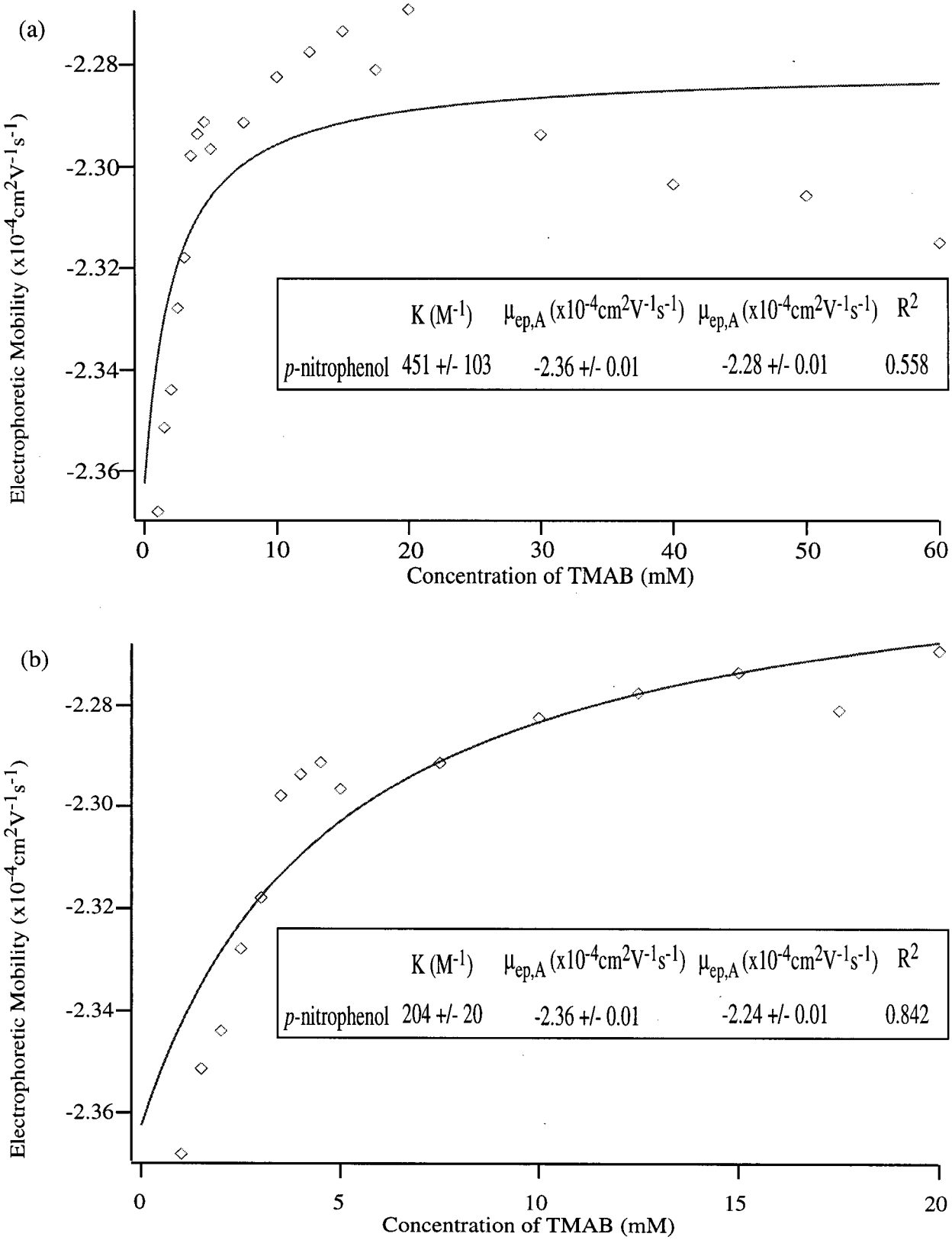

Figure 3.9 Two graphs of the electrophoretic mobility versus concentration of TMAB additive using *p*-nitrophenol as the analyte. The solid line represents the binding isotherm determined by the free and complex mobility and the equilibrium constant, and the points are the experimental data. Figure (a) depicts additive concentrations from 0 to 60.0 mM. Figure (b) shows additive concentrations from 0 to 20.0 mM only.

negative mobility increased significantly (Figure 3.9a). When the points above 20 mM TMAB were removed, the graph appeared to be a normal binding isotherm (Figure 3.9b). For both graphs, the equilibrium constant and mobility values were calculated and compared. The parameter values appeared to be quite different when the points above 20.0 mM were removed.

The neutral, bi-layer coated capillaries used in these experiments have been rigorously tested by Beckman Instruments and are designed to tolerate a range of pH values (pH 3 to pH 8). The apparent pH in these experiments was 8.7, which is higher than the working pH for which the capillary was designed. Furthermore, the capillary has not been tested in 100% nonaqueous media, which was the media used in these experiments. It is possible that, as the experiment proceeded, the coating began to degrade. Finally, there was a possibility that when the concentration of the positively charged additive increased, absorption of the additive molecules on the capillary wall led to the formation of a double layer with the negatively charged species in the buffer. This negative diffuse layer may have resulted in an EOF which was added to the negative analyte electrophoretic mobility. This is consistent with the observation that the analytes with smaller electrophoretic mobilities were affected more than the analytes with larger electrophoretic mobilities. For the purpose of this study, all of the parameters were calculated using 0 to 20.0 mM additive only. It should be noted that *m*-nitrophenol had the largest mobility and remained in the capillary the longest. The R^2 value of this analyte's curve is quite low, compared to that of *p*- and *o*-nitrophenol. Therefore, the data associated with this analyte is less reliable. Further investigation into this situation is needed.

3.4 Conclusion

By comparing DTAB and TMAB in nonaqueous buffer using a neutral eCAP capillary, the interactions between *p*-, *m*- and *o*-nitrophenol and the two additives were found to be mainly due to ion-pairing. A quantitative examination of these two ion-pairing agents suggests their suitability as additives in CE.

3.5 Future Experiments

Now that the quantitative CE separation of tetraalkylammonium ion-pairing agents is better understood, this study opens up many new avenues to be explored in the realm of ion-pairing in CE. The ion-pairing interaction in aqueous buffer solution may be too small to be accurately measured. Several variations on the above experimental condition could be implemented:

(a) The addition of an organic solvent (5% DMF/DMSO for nitrophenolates and 5% acetonitrile/methanol for nucleosides and nucleotides) could be added to the separation buffer to reduce hydrophobic capillary wall interactions between the additive and the wall. This may also increase the analyte-additive interaction especially at low concentrations of additive.

(b) Using a lower ionic strength buffer may decrease the various ions in the separation buffer, minimizing the buffer's interference with the analyte-additive complex. However, this will increase the EOF which may affect the resolution of the analytes.

The neutral capillary studies may also be improved by changing the following experimental conditions:

(a) Lowering the pH of the separation buffer into the range previously tested by Beckman (pH 3 to pH 8). However, more acidic analytes compared to nitrophenols would have to be used for these studies.

(b) Using less than 100% organic solvents may allow for measurable equilibrium constants and mobilities without the degradation of the capillary and at the same time, avoid the formation of micelles.

Chapter IV The Effects of a Mixture of Charged and Neutral Additives on Analyte Migration Behavior in Capillary Electrophoresis

4.1 Introduction

Equilibrium and the effect of field are the two determining factors in separation science [100]. Early separation techniques, such as chromatography [101,102], centrifugation [103] and carrier free electrophoresis [2,104,105] were developed based on a single physical or chemical interaction that had differential effects on the chemicals of interest during the separation process. However, the separation power of these individual techniques alone is often inadequate for more difficult separations such as chiral compounds or other isomers in complex matrices. The introduction of a pseudophase, in addition to the original stationary and mobile phases, has improved the separation power of chromatography due to the presence of more than one equilibrium for each analyte [106-108]. With the use of additives in the background electrolyte, Terabe and co-workers dramatically increased the separation power of CE by employing both (electric) field and equilibrium in one separation process [12,13,109].

As previously stated, open tubular CE has a significant advantage over other types of separation techniques in terms of the ease with which more than one equilibrium can be introduced into the system while the electric field affects the mobility of both the ions of the free analytes and the complexes formed with the different additives. The use of mixed additives has been increasing in the past few years and different models have been proposed to describe the separation processes [5-11]. It has been demonstrated that a theory based on dynamic complexation of analytes with various additives can be used to accurately predict the analyte migration behavior not only for one additive CE systems but also for situations when more than one additive or higher order interactions are involved [11,14-17].

Cyclodextrins (CDs) have previously been used as pseudophases or stationary phases in chromatography [110-112] and as additives in CE [7,8,11,14,16,26-32,34,35,109,113-118]. To maximize the effect of the electric field, CDs derivatized with charged functional groups are of particular interest in the CE separation of complex mixtures [109]. Sulfobutylether-β-

cyclodextrin (SBE-β-CD, commercially named Advasep) is a sodium salt with the degree of substitution (DS) ranging between 1 and 9 (average negative charge of 4) [119]. SBE-β-CD is one of the most potent additives because most of its components have multiple charges. The mobility of the analyte can be changed dramatically even when the interactions between the analyte and SBE-β-CD are weak. Although this additive has been used successfully for the separation of chiral isomers [120], cationic drugs of forensic interest [8] and environmental contaminants such as polyaromatic hydrocarbons [121], more quantitative studies of its properties are needed to fully understand the potential and limitations of this additive.

The properties of SBE-β-CD as an additive in CE separations, as well as when it is used in conjunction with another additive, hydroxypropyl-β-CD (HP-β-CD), were studied using phenol, 1-naphthol and 2-naphthol as model analytes. Neutral HP-β-CD was chosen as the second additive because its effect on most anionic analytes is opposite to that of SBE-β-CD. While the addition of SBE-β-CD increased the mobility of an anionic analyte towards the positive electrode (negative mobility), HP-β-CD reduced the negative electrophoretic mobility of anions.

Three parameters, the free analyte mobility ($\mu_{ep,A}$), the mobility of the analyte-additive complex ($\mu_{ep,AC}$) and the equilibrium constant (K), are used to describe analyte mobility with each individual additive as well as with the combined additives. Both SBE-β-CD and HP-β-CD are mixtures with various degrees of molar substitution. Multicomponent additives, such as derivatized cyclodextrins with various degrees of substitution, can be considered single component additives as long as the fraction of each component remains constant. There has been no previous theoretical treatment of the effect these multicomponent additives have on analyte migration behavior in CE. This section describes the fundamental theory and the practical implications for use of these multicomponent additives.

4.2 Theory

In all separation techniques, the average migration rate of an analyte can be described by the following equation [100]:

$$\nu\overline{U}_A = \sum_{i=1}^{m} f_i \overline{U}_i \qquad (4.1)$$

where $\overline{U}_A$ is the average linear velocity of the analyte (A), f_i is the fraction of the analyte present as a certain species, i, $\overline{U}_i$ is the average linear velocity of that species, m is the number of species and ν is the correction factor that converts the velocity of the analyte to an ideal state where the additive concentration approaches zero. Depending on the additive and experimental conditions, corrections for viscosity or other factors may or may not need to be addressed. Care must be taken to ensure that changes in the mobilities caused by changing the concentration of the additive (or the amount of stationary phase) are only due to the interaction between the analyte and additive (or stationary phase) and not to other factors [14,35]. In the context of CE, equation 4.1 can be modified by replacing the velocity term with the electrophoretic mobility.

The fraction of each species present in a separation system can be obtained by:

$$f_i = k'_i / (\sum_{i=1}^{m} k'_i) \qquad (4.2)$$

where k'_i is defined as:

$$k'_i = \frac{\text{the amount of analyte present as species i}}{\text{the amount of free analyte}} \qquad (4.3)$$

Additives such as SBE-β-CD and HP-β-CD have been treated as single components in the very limited number of theoretical studies to date [14,121]. In reality, there are 9 detectable components in the commercially available SBE-β-CD with the degree of substitution (DS) ranging from 1 to 9 and 8 detectable components in HP-β-CD with the DS ranging from 3 to 10. When an analyte migrates in a capillary where SBE-β-CD is used as the additive in the

background electrolyte and is considered a single component, the equilibrium can be expressed as:

$$A + C \rightleftharpoons AC \tag{4.4}$$

where A is the analyte, C is SBE-β-CD and AC is the analyte-SBE-β-CD complex.

Because each additive is a mixture itself, [C] is composed of:

$$[C] = [C_1] + [C_2] + ... + [C_m] \tag{4.5}$$

where C_1, C_2, ... and C_m are the components of SBE-β-CD with various DS (i.e. 1 to 9 in this case). In order to account for interactions between the analyte and the individual components of C, the equation used to calculate the net electrophoretic mobility of the analyte (μ_{ep}^{A}) (equation 1.16 of Section 1.3.3) must be written as:

$$\nu\mu_{ep}^{A} = \frac{\mu_{ep,A} + k_{AC1}[C_1]\mu_{ep,AC1} + k_{AC2}[C_2]\mu_{ep,AC2} + ... + k_{ACm}[C_m]\mu_{ep,ACm}}{1 + k_{AC1}[C_1] + k_{AC2}[C_2] + ... + k_{ACm}[C_m]} \tag{4.6}$$

where k_{AC1}, k_{AC2}, ... and k_{ACm} are the equilibrium constants of the analyte interacting with C_1, C_2, ... and C_m, respectively and $\mu_{ep,AC1}$, $\mu_{ep,AC2}$, ..., $\mu_{ep,ACm}$ are the mobilities of each complex formed between the analyte and the additives. If the relative amounts of the additive components remain constant, the concentration of each additive will be proportional to the total additive concentration, allowing equation 4.6 to be simplified to:

$$\nu\mu_{ep}^{A} = \frac{\mu_{ep,A} + [C](k_{AC1}f_{AC1}\mu_{ep,AC1} + k_{AC2}f_{AC2}\mu_{ep,AC2} + ... + k_{ACm}f_{ACm}\mu_{ep,ACm})}{1 + [C](k_{AC1}f_{AC1} + k_{AC2}f_{AC2} + ... + k_{ACm}f_{ACm})} \tag{4.7}$$

where f_{AC1}, f_{AC2}, ... and f_{ACm} are the fractions of additive present as each component. When equation 4.7 is compared with equation 1.16, it is clear that equation 4.7 can be further simplified to give equation 1.16, where:

$$K_{AC} = k_{AC1}f_{AC1} + k_{AC2}f_{AC2} + ... + k_{ACm}f_{ACm} \tag{4.8}$$

and

$$\mu_{ep,AC} = \frac{k_{AC1}f_{AC1}\mu_{ep,AC1} + k_{AC2}f_{AC2}\mu_{ep,AC2} + ... + k_{ACm}f_{ACm}\mu_{ep,ACm}}{k_{AC1}f_{AC1} + k_{AC2}f_{AC2} + ... + k_{ACm}f_{ACm}} \tag{4.9}$$

The observed equilibrium constant and complex mobility are weighted averages, reflecting the fraction of each additive component. As long as the composition of the additive remains constant, equation 1.16 can be used to quantitatively describe the analyte mobility. In other words, the analyte migration behavior is independent of the DS of the additive.

The same logic can be applied to other additives including polyethers, surfactants and most of the derivatized CDs, including HP-β-CD. The electrophoretic mobility of the analyte, when HP-β-CD is used as the additive, can be calculated in the same way:

$$\nu\mu_{ep}^{A} = \frac{1}{1+K_{AD}[D]}\mu_{ep,A} + \frac{K_{AD}[D]}{1+K_{AD}[D]}\mu_{ep,AD} \tag{4.10}$$

where D is used to denote HP-β-CD, the second additive, in these experiments. When a mixture of SBE-β-CD and HP-β-CD is used, the analyte mobility is described by [14]:

$$\nu\mu_{ep}^{A} = \frac{1}{1+K_{AC}[C]+K_{AD}[D]}\mu_{ep,A} + \frac{K_{AC}[C]}{1+K_{AC}[C]+K_{AD}[D]}\mu_{ep,AC} + \frac{K_{AD}[D]}{1+K_{AC}[C]+K_{AD}[D]}\mu_{ep,AD} \tag{4.11}$$

4.3 Experimental

4.3.1 Apparatus

The apparatus used in these experiments was identical to that used in Section 2.2.1 of this thesis, with the following exceptions. The capillary was conditioned by rinsing with 0.1 M NaOH for 15 minutes, deionized water for 5 minutes and 160 mM borate buffer (pH 9.0) for 15 minutes followed by overnight equilibration in the same buffer. Samples were introduced into the capillary by pressure injection for 5 seconds at 0.5 psi and separated at 10 kV.

4.3.2 Chemicals

The electrophoresis buffer was made with 40 mM Borax (pH 9.01) in deionized water. The 40 mM Borax yields a 160 mM borate concentration. Solutions of various concentrations of SBE-β-CD (CyDex, Inc., Overland Park, KS) , HP-β-CD (Aldrich, Milwaukee, WI) and

mixtures of SBE-β-CD and HP-β-CD were prepared using this 160 mM borate electrophoresis buffer. The concentrations ranged from 0 to 20 mM for the SBE-β-CD and from 0 to 80 mM for the HP-β-CD. The concentrations of SBE-β-CD were calculated without considering moisture and therefore, the actual concentrations could be slightly lower. Individual stock solutions (1.0×10^{-3} M) of phenol (BDH Inc., Toronto, ON), 2-naphthol and 1-naphthol (Aldrich, Milwaukee, WI) were prepared in 160 mM borate buffer. Due to limited solubility, it was necessary to dissolve both 2- and 1-naphthol in 20% methanol prior to dissolving them in the electrophoresis buffer. A mixture of the three analytes was then prepared by combining equal amounts of the three stock solutions and diluting 1:10 with the appropriate electrophoresis buffer giving a concentration of 3.3×10^{-5} M for each analyte.

4.4 Discussion

4.4.1 The Effect of a Single Additive on Analyte Migration Behavior

As discussed by many recent papers, the analyte electrophoretic mobility is determined by the free analyte mobility ($\mu_{ep,A}$), the complex mobility ($\mu_{ep,AC}$) and the capacity factor (k'_{AC}) provided that corrections are made for the factors that obscure any effects other than those due to equilibrium [14,15,35]. The capacity factor is the product of the equilibrium constant (K) and the additive concentration for 1:1 interactions [14].

The parameters are calculated by the least square variance covariance nonlinear regression method [15] (Section 1.3.4) and the values are listed (Table 4.1). The differences in the effects of the two additives on the analyte migration behavior is apparent when Figure 4.1 and Figure 4.2 are compared. When the SBE-β-CD concentration is increased, as shown in Figure 4.1, the values of the negative mobility of the analytes are also increased due to the negative charges on the additive molecules and the increase in viscosity. Contrary to the effect of SBE-β-CD, Figure 4.2 shows that an increase in the HP-β-CD concentration decreases the negative mobilities of the

Table 4.1 Equilibrium constants and electrophoretic mobilities of the free and complexed species for each analyte obtained from nonlinear regression

analyte	SBE-β-CD K_{AC} (M^{-1})	HP-β-CD K_{AD} (M^{-1})	free mobility $\mu_{ep,A}$ ($\times 10^{-5}$ $cm^2 V^{-1}s^{-1}$)	complex mobility (with SBE-β-CD) $\mu_{ep,AC}$ ($\times 10^{-5}$ $cm^2 V^{-1}s^{-1}$)	complex mobility (with HP-β-CD) $\mu_{ep,AD}$ ($\times 10^{-5}$ $cm^2 V^{-1}s^{-1}$)
phenol	129 ± 0.3	96 ± 2	-4.69 ± 0.04	-26.0 ± 0.1	-1.23 ± 0.05
2-naphthol	1304 ± 12	729 ± 7	-7.99 ± 0.18	-26.2 ± 0.1	-1.86 ± 0.18
1-naphthol	1720 ± 23	795 ± 6	-10.80 ± 0.29	-26.1 ± 0.1	-0.96 ± 0.29

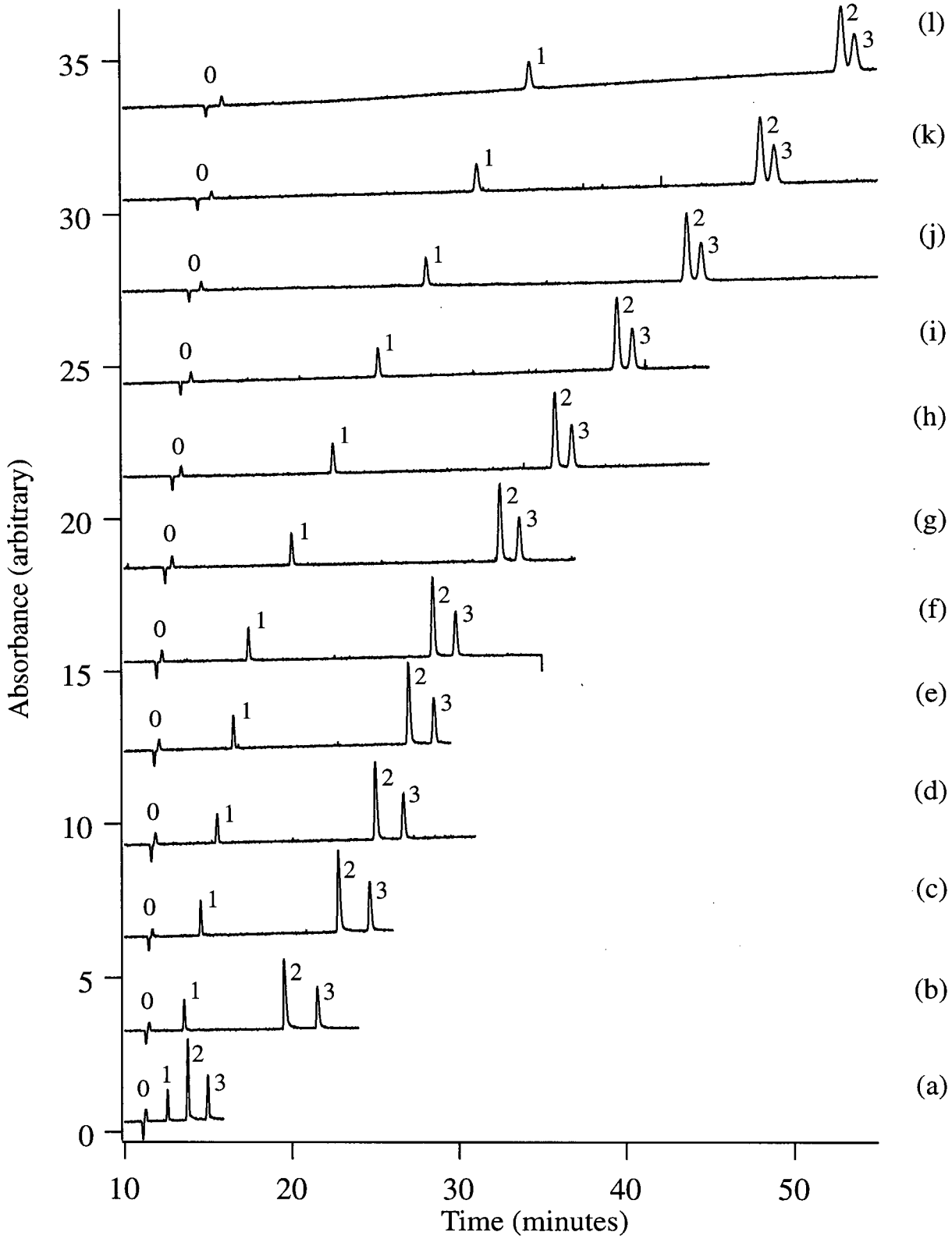

Figure 4.1 Electropherograms obtained using 0 to 20.0 mM SBE-β-CD in 160 mM borate buffer. The peak numbers correspond to 0 (EOF - methanol), 1 (phenol), 2 (2-naphthol) and 3 (1-naphthol). The concentrations of SBE-β-CD shown are: (a) 0 mM, (b) 1.0 mM, (c) 2.0 mM, (d) 3.0 mM, (e) 4.0 mM, (f) 5.0 mM, (g) 7.5 mM, (h) 10.0 mM, (i) 12.5 mM, (j) 15.0 mM, (k) 17.5 mM and (l) 20.0 mM.

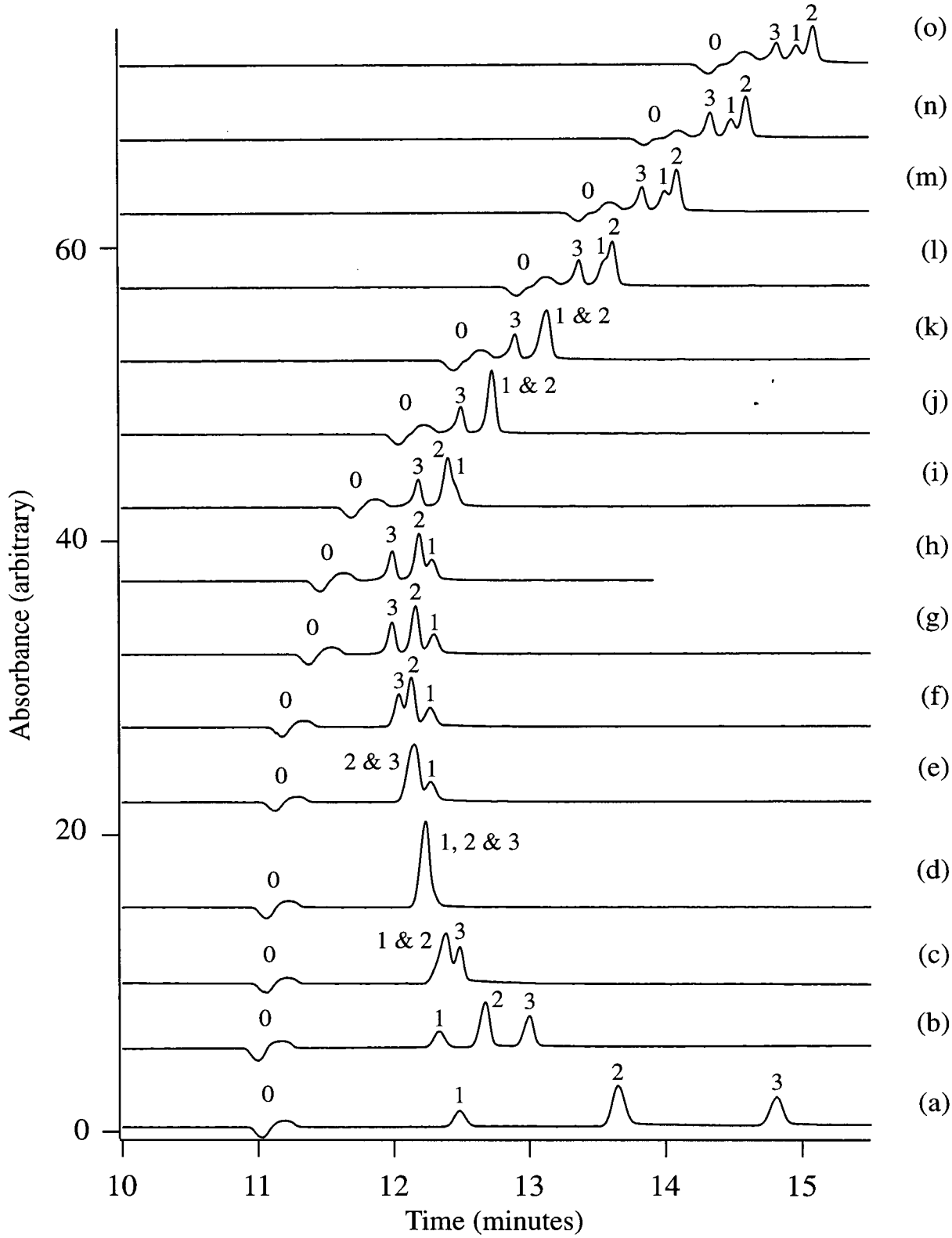

Figure 4.2 Electropherograms obtained using 0 to 80.0 mM HP-β-CD in 160 mM borate buffer. The peak numbers correspond to 0 (EOF - methanol), 1 (phenol), 2 (2-naphthol) and 3 (1-naphthol). The concentrations of HP-β-CD shown are: (a) 0 mM, (b) 1.0 mM, (c) 2.0 mM, (d) 3.0 mM, (e) 4.0 mM, (f) 5.0 mM, (g) 10.0 mM, (h) 15.0 mM, (i) 20.0 mM, (j) 30.0 mM, (k) 40.0 mM, (l) 50.0 mM, (m) 60.0 mM, (n) 70.0 mM and (o) 80.0 mM.

analytes at first because the additive is neutral and the analytes (phenol, 2-naphthol and 1-naphthol) are weakly acidic. At higher HP-β-CD concentrations, the migration times become longer mainly due to the effect of the increased viscosity.

An interesting phenomena was observed in Figure 4.2. Peaks 1 and 2 (phenol and 2-naphthol) were separated when the HP-β-CD concentration is zero. As the additive concentration increased, the two peaks converged at 3 mM HP-β-CD. They are separated again and then reconverge with increased HP-β-CD concentration before being separated a third time when the HP-β-CD concentration is above 40 mM. This phenomenon can be explained by plotting the electrophoretic mobility of the analyte versus the additive concentration, as shown in Figure 4.3. There are two situations that can give rise to this type of phenomena. In the present case, where $|\mu_{ep,A}|$ is greater than $|\mu_{ep,AD}|$, one analyte has a larger free ion mobility, $\mu_{ep,A}$, a larger complex mobility, $\mu_{ep,AD}$ and a larger equilibrium constant, K_{AD}, than the other analyte (B). The large K_{AD} value of the 2-naphthol : HP-β-CD interaction made the fraction of the analyte in the complexed form increase drastically when the concentration of the additive is increased and the net mobility of 2-naphthol crosses that of phenol. However, at higher additive concentrations, the absolute change in the mobility of 2-naphthol is small because the analyte is almost fully complexed with the additive. With a smaller K_{BD} value and a smaller negative complex mobility ($\mu_{ep,BD}$), phenol slowly catches up with 2-naphthol and finally passes it when the concentration of HP-β-CD in the buffer is higher than 40 mM. The other case in which two analyte peaks cross twice occurs when $|\mu_{ep,A}|$ is less than $|\mu_{ep,AD}|$ and one analyte has a larger free ion mobility, $\mu_{ep,B}$, a larger complex mobility, $\mu_{ep,BD}$ and a smaller equilibrium constant, K_{BD}, than the other analyte. The additive concentrations where the two analytes converge in the electropherograms can be predicted.

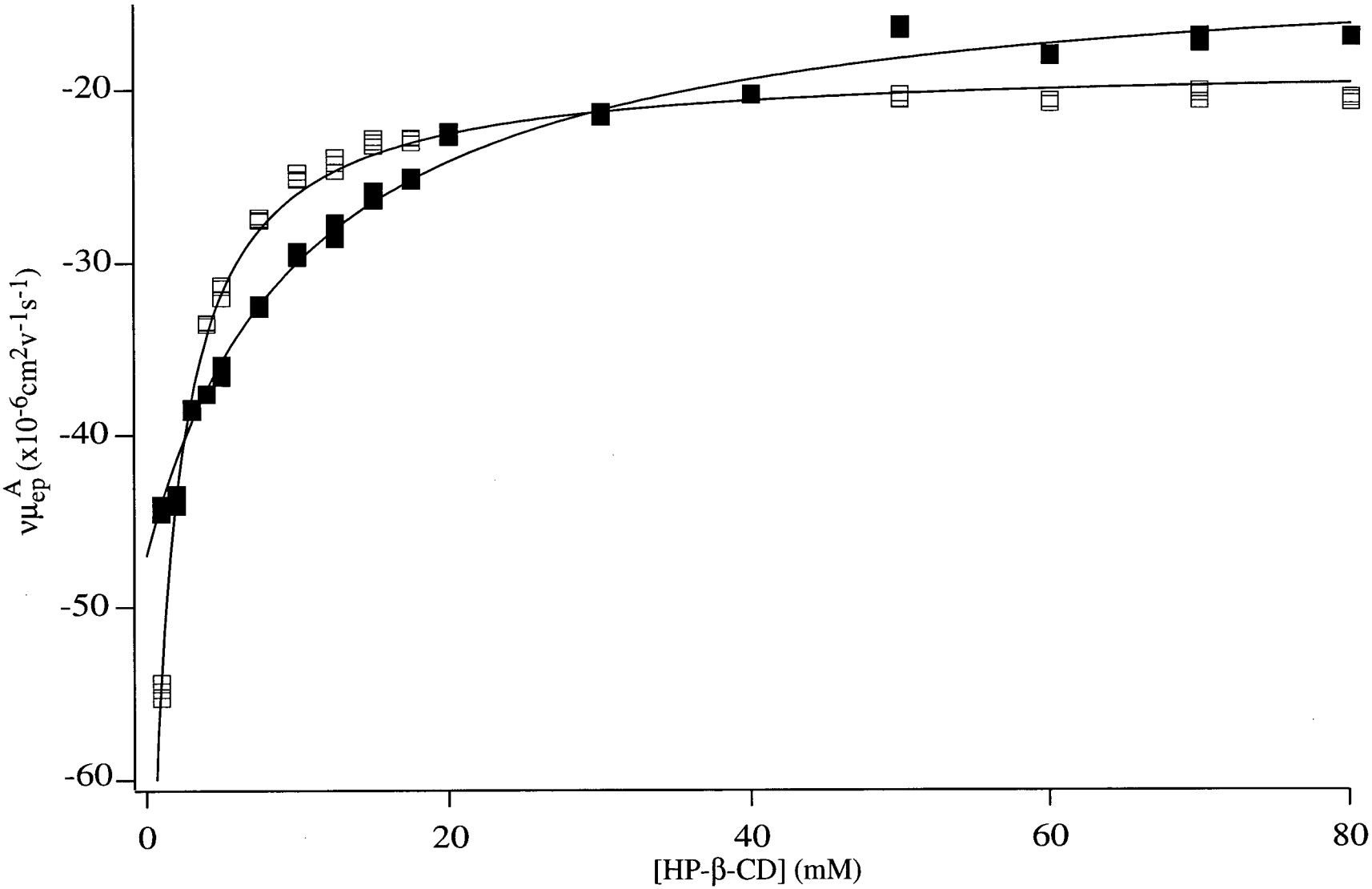

Figure 4.3 Plot of $\nu\mu_{ep}^{A}$ versus [HP-β-CD] for phenol (■) and 2-naphthol (□). The solid line represents the binding isotherm determined by the free and complex mobility and the equilibrium constant.

4.4.2 The Effect of a Mixture of Charged and Neutral Additives on Analyte Migration Behavior

Once the relationship between each additive and individual analyte is understood, the effect of a mixture of the two differently charged additives can be examined. Equation 4.11 can be used to predict the analyte migration behavior at all possible concentrations of the individual additives and that of any combination of the two additives. Figure 4.4 shows the three dimensional (3D) plots of the mobility values of the three analytes versus the two additive concentrations. The experimental verification of these predicted mobilities in the 3D plots poses a challenge to the accuracy of the estimated individual equilibrium constants, K_{AC} and K_{AD} and the complex mobility values, $\mu_{ep,AC}$ and $\mu_{ep,AD}$. If these values are not accurate, the fractions of the analytes in the free or complexed forms can introduce significant errors because the effect of the two additives oppose each other. This contrasting effect can be observed more clearly when Figure 4.4 is rotated so that the origin of the two additive concentrations is at the center, as shown in Figure 4.5. The concentration of SBE-β-CD increases to the left of the origin and the concentration of HP-β-CD increases to the right. Therefore, Figures 4.5a, 4.5b and 4.5c are projections of the 3D plots whose concentration axes of the additives are perpendicular to each other and the origin is pointing towards the reader. The darker colored edge shows the mobility values when there is only one additive present in the system. The edges away from the reader, with the lighter colors, are the mobilities when 80 mM of one additive is used in the system and various concentrations of the second additive is used. For illustration, when 0 to 80 mM of SBE-β-CD is used and 80 mM HP-β-CD is used, the light colored edge on the left hand side of Figure 4.5(a) results. It can also be observed that while the formation of SBE-β-CD complexes increase the negative mobilities of the analytes, the formation of HP-β-CD complexes force the net electrophoretic mobilities of the analytes towards zero. The mobilities of the analytes at different mixtures of additives were measured and compared with the calculated values and the results are listed in Table 4.2. At nearly all tested conditions the relative error of the measured values is less

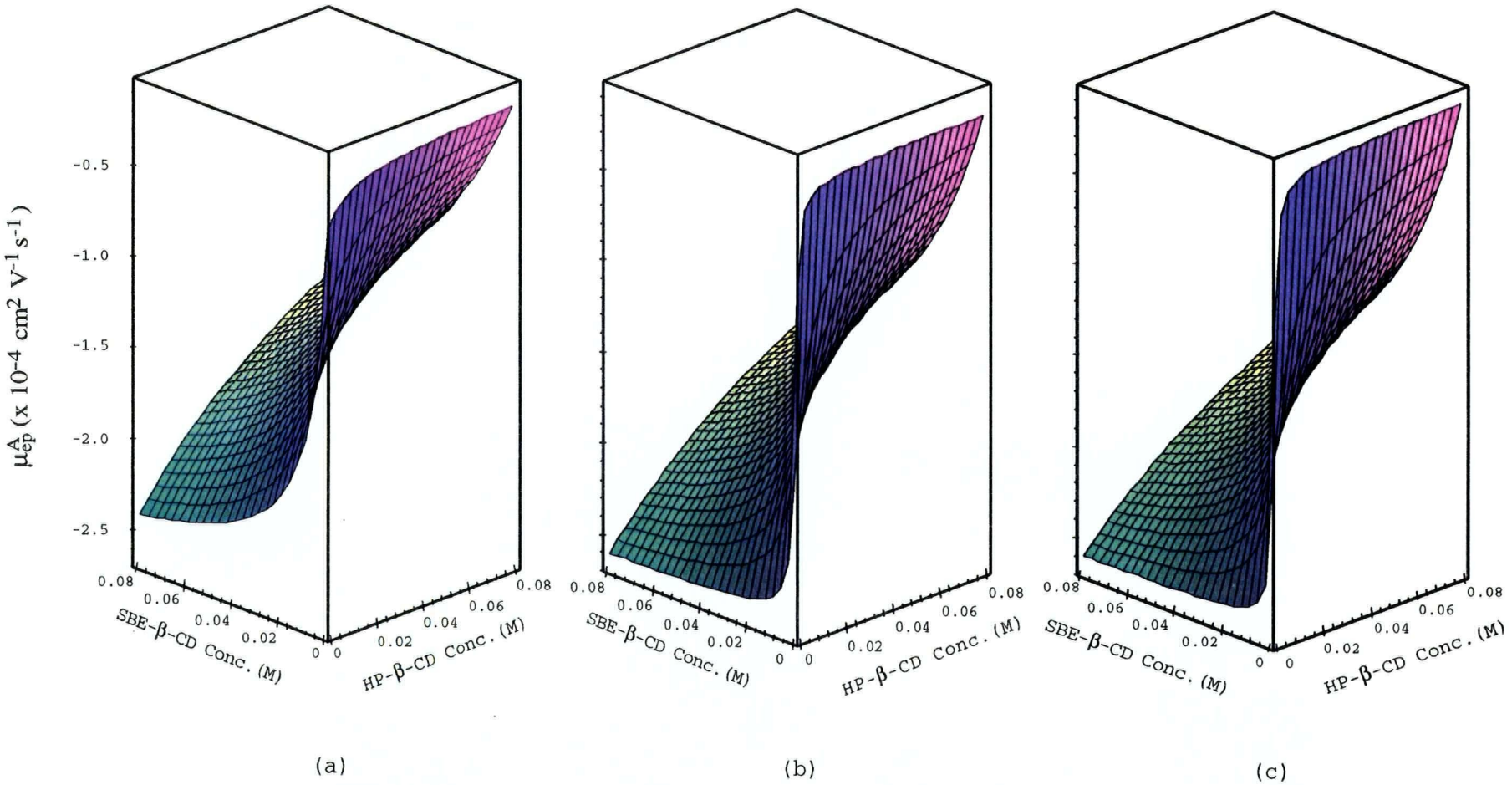

Figure 4.4 The effect of two additives on the electrophoretic mobility depicted by a 3-dimensional plot with the x-axis as the concentration of HP-β-CD, the y-axis as the concentration of SBE-β-CD, and the z-axis as $\nu\mu_{ep}^{A}$ (a) phenol, (b) 2-naphthol and (c) 1-naphthol.

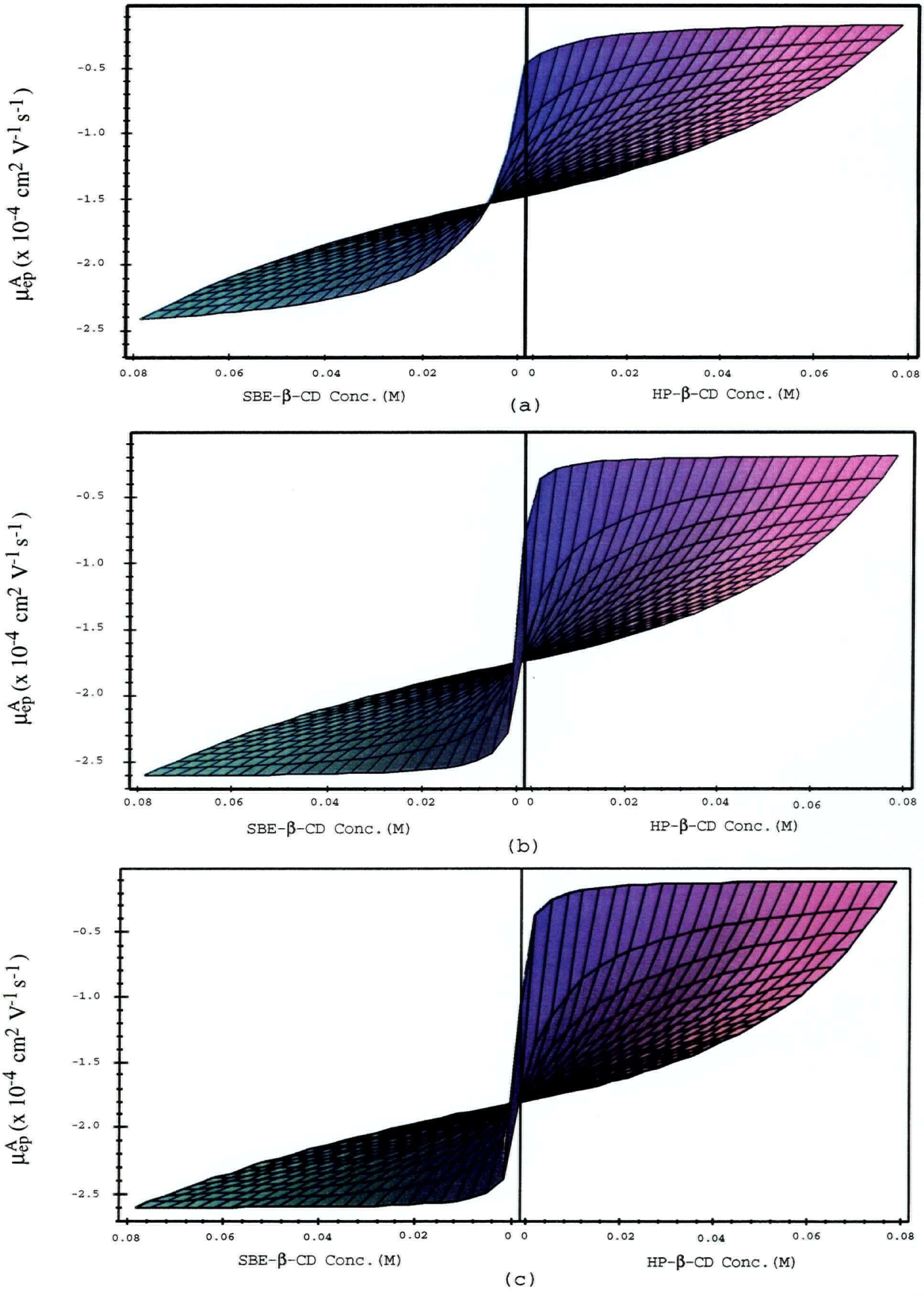

Figure 4.5 Projections of the surfaces in Figure 4.4, rotated so the origin is centered (a) phenol, (b) 2-naphthol and (c) 1-naphthol.

Table 4.2 Net electrophoretic mobilities of the analytes in the presence of SBE-β-CD and HP-β-CD

additives (mM)		phenol μ_{ep}^{A} ($\times 10^{-5} cm^2 V^{-1} s^{-1}$)			2-naphthol μ_{ep}^{A} ($\times 10^{-5} cm^2 V^{-1} s^{-1}$)			1-naphthol μ_{ep}^{A} ($\times 10^{-5} cm^2 V^{-1} s^{-1}$)		
SBE-β-CD	HP-β-CD	calculated	measured*	% difference	calculated	measured*	% difference	calculated	measured*	% difference
5	20	-5.78	-5.81	0.4	-8.08	-7.89	2.4	-8.49	-8.22	3.4
5	60	-2.78	-2.90	4.3	-3.66	-3.65	0.2	-3.50	-3.48	0.5
15	20	-9.55	-9.72	1.9	-12.73	-12.67	0.5	-13.40	-13.23	1.2
15	60	-4.72	-4.28	10.3	-6.23	-5.58	11.7	-6.50	-5.79	12.4
25	20	-11.23	-11.47	2.1	-14.18	-14.27	0.6	-14.76	-14.73	0.2
25	60	-5.94	-6.45	8.7	-7.63	-7.91	3.7	-8.04	-8.26	2.7
35	20	-12.03	-12.20	1.4	-14.61	-14.60	0.08	-15.08	-15.00	0.6
35	60	-6.62	-7.35	11.0	-8.29	-8.82	6.4	-8.73	-9.19	5.3

* Averaged from three separate runs

than 5%. Considering that some of these values are very small, these results reflect reasonable accuracy for the K_{AC}, K_{AD}, $\mu_{ep,AC}$ and $\mu_{ep,AD}$ values determined in the previous section.

Another phenomenon is the existence of contour lines in the binding isotherm surfaces shown in Figure 4.4. Binding isotherms are plots of $\nu\mu_{ep}^{A}$ at various additive concentrations while the equilibrium constants are kept constant. In this case, because there are two independent variables (i.e. [C] and [D]), the isotherm is a 3D surface. In a two additive system at a distinct concentration of one additive, the mobility of the analyte stays the same regardless of the concentration of the other additive. This point has been defined as the dengsu point, which means "equal speed" [14]. When two additives have the opposite effect on the analyte mobility, as occurs in this study, the net effect is quite different and the dengsu point does not exist [122]. Theoretically, for every concentration of one additive, the effect on the analyte mobility can be counterbalanced by the other additive at a corresponding concentration if there is no limit to the solubility of the additives. The net analyte mobility in this situation (where the change in the mobility is only caused by equilibria shift) can be kept constant at any concentration of one additive by adjusting the concentration of the other additive. Therefore, contour lines exist throughout the binding isotherm surfaces. The waists of the projected surfaces in Figure 4.5 are the locations where the contour lines cross the two concentration axes at a 45° angle. Because Figure 4.5 is rotated so that the two concentration axes are 45° away from the reader, the three contour lines have slopes of unity (shown as the waists of the projected surfaces). Figure 4.6a shows the top view of the binding isotherm surface of phenol with the two additives (rotated from Figure 4.5a) and Figure 4.6b is when the isotherm surface is rotated to another angle. The waists of the projected surfaces are marked with dashed lines. The contour lines in Figure 4.6 are spaced at a constant difference of the mobility value, which means the mobility changes slower where the contour lines are sparse and faster where the contour lines are dense. As derived by Bowser *et al.* [122], the slope of a contour line for a specific net electrophoretic mobility of an analyte is determined by:

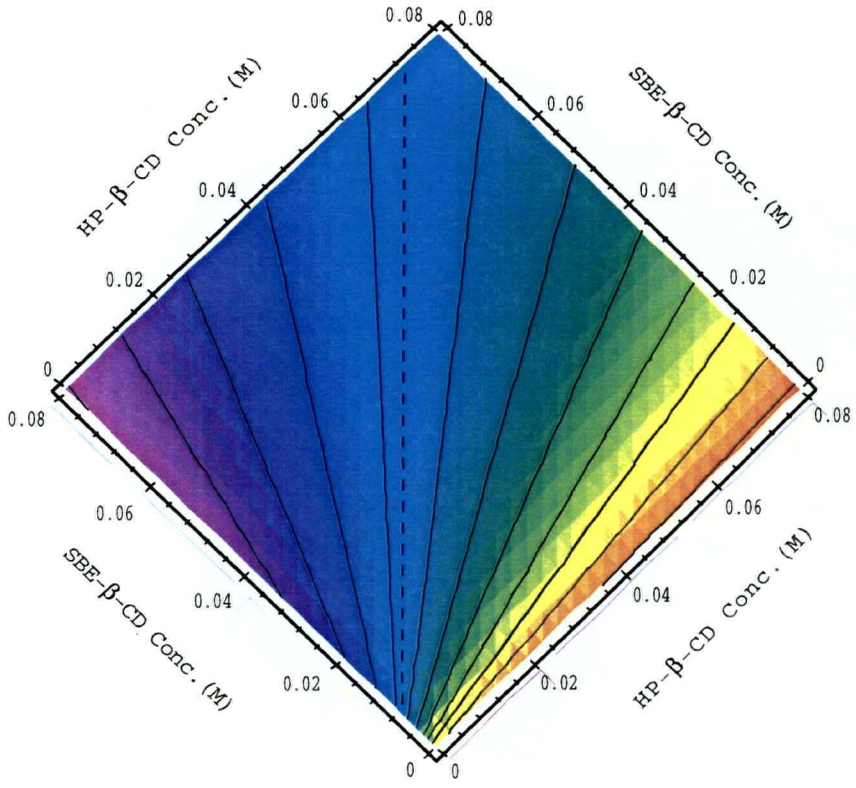

(a)

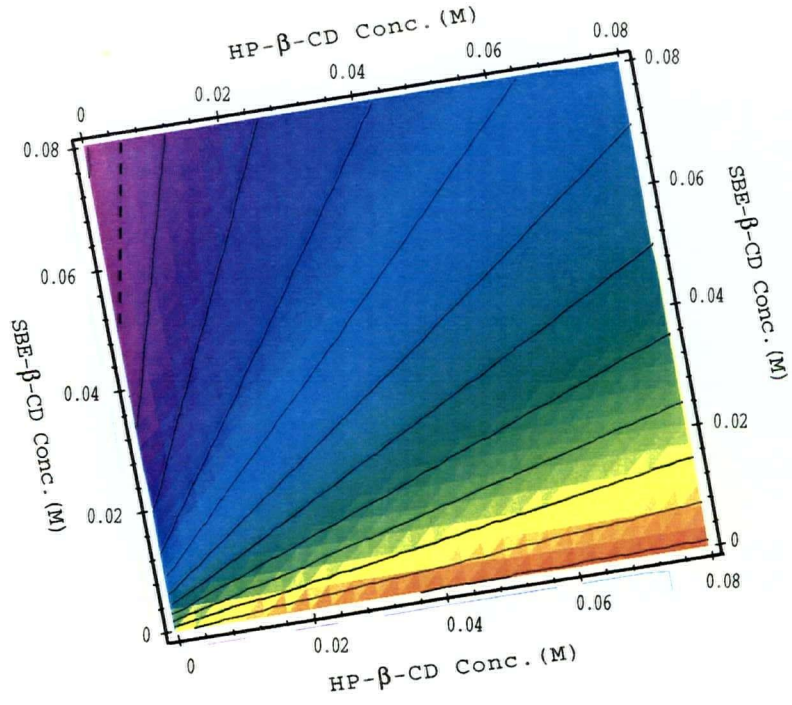

(b)

Figure 4.6 A top view with contour lines of the net electrophoretic mobility surface (a) phenol, rotated from Figure 4.4a, (b) phenol, rotated from Figure 4.4a.

$$\frac{\partial[D]}{\partial[C]} = -\frac{K_{AC}(\mu_{ep}^{A} - \mu_{ep,AC})}{K_{AD}(\mu_{ep}^{A} - \mu_{ep,AD})} \quad (4.12)$$

Using the values listed in Table 4.1, when the slope is equal to 1, as shown in Figure 4.5, the net electrophoretic mobilities of the analytes, phenol, 2-naphthol and 1-naphthol are 1.54×10^{-4} $cm^2V^{-1}s^{-1}$, -1.75×10^{-4} $cm^2V^{-1}s^{-1}$ and -1.82×10^{-4} $cm^2V^{-1}s^{-1}$, respectively. Once the net electrophoretic mobility of each analyte is calculated at various angles of observation (which determines the values of the contour line slope), the intercept of the concentration axes for both SBE-β-CD and HP-β-CD can be determined using equation 1.16, where k' = K[C] and by setting the other additive concentration to zero.. Table 4.3 tabulates the waist position of the net electrophoretic mobilities and the corresponding contour line intercepts of each additive at the different angles of observation.

In theory, contour lines exist for all possible mobility values, ranging from the maximum negative mobility of the complex (due to the binding of an analyte with SBE-β-CD) to the minimum negative mobility of the complex (due to the binding with HP-β-CD). Hence, no matter which way the graphs are rotated, contour lines can be observed. Figure 4.7 (a, b, c, d) shows the binding isotherm surface of phenol with the two additives when viewed from different angles. The waists of these projected surfaces are the locations where a contour line is observed. These contour lines can be used to keep the mobility of one analyte constant, while moving the other analytes away from this analyte by changing the two additive concentrations along the contour curve.

4.5 Conclusion

It has been demonstrated that multicomponent additives can be studied as single component additives using the theory of DCCE. By first understanding how a single multicomponent additive affected the mobility of various analytes, the analyte migration behavior of the analytes under the influence of a mixture of differently charged additives was examined. The ability to

Table 4.3 Waist position of net electrophoretic mobilities and the corresponding contour line intercepts of each additive at the different angles of observation

angle	analyte	net electrophoretic mobility μ_{ep}^{A} (x 10^{-4} $cm^2V^{-1}s^{-1}$)	concentration of SBE-β-CD (mM)	concentration of HP-β-CD (mM)
	phenol	-1.54	7.9	72
45°	2-naphthol	-1.75	0.84	79
	1-naphthol	-1.82	0.55	80
	phenol	-2.31	50	5.4
80°	2-naphthol	-2.40	5.6	13
	1-naphthol	-2.42	4.1	13
	phenol	-1.75	12	48
55°	2-naphthol	-1.94	1.3	55
	1-naphthol	-2.00	0.87	55
	phenol	-1.20	4.1	50
30°	2-naphthol	-1.42	0.40	47
	1-naphthol	-1.49	0.22	46
	phenol	-0.382	6.7	3.5
5°	2-naphthol	-0.515	6.9	1.2
	1-naphthol	-0.496	6.8	1.8

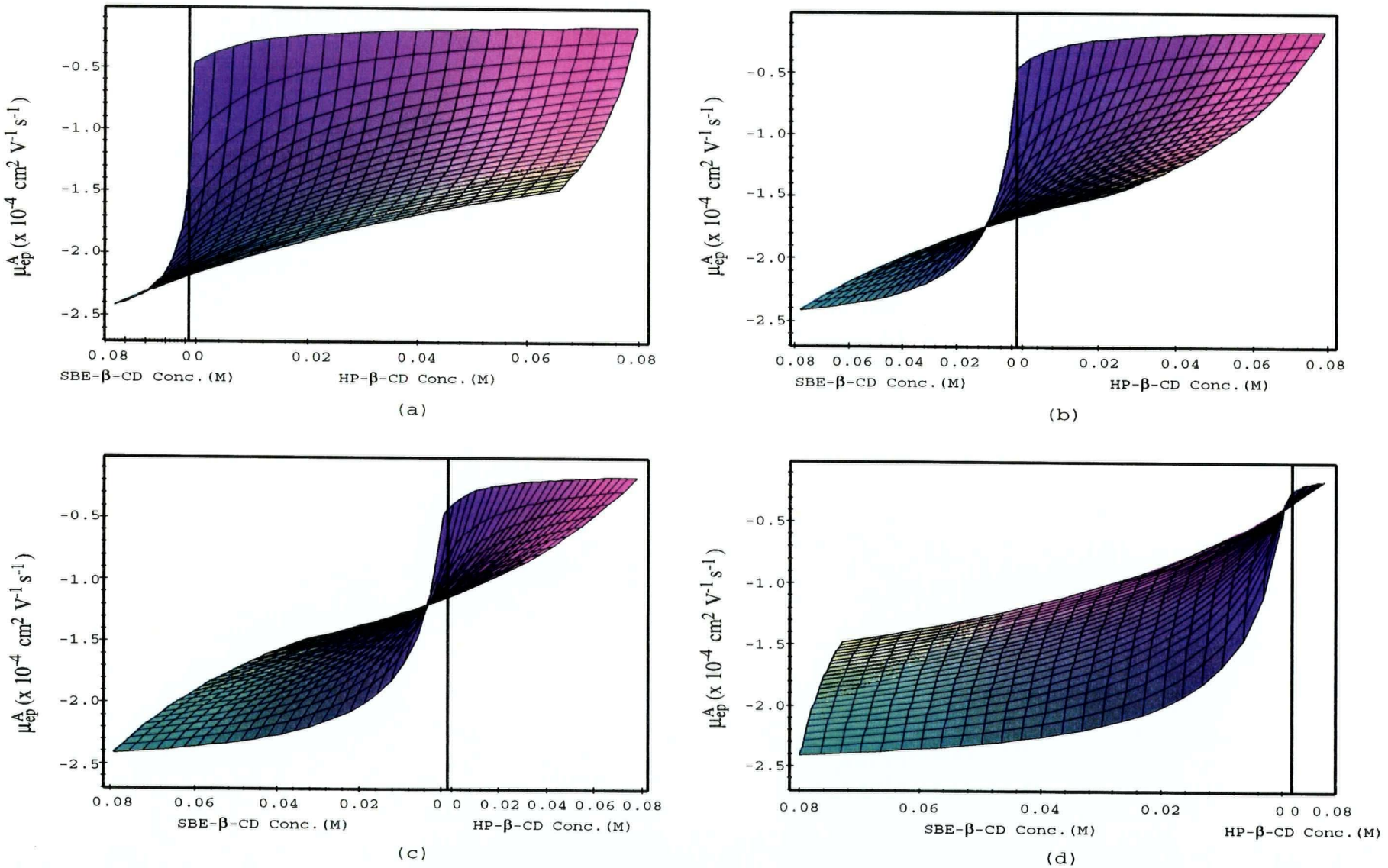

Figure 4.7 A plot of mobility versus the two additive concentrations for phenol at angle rotations of (a) $\theta = -100$, $\Phi = 90$, (b) $\theta = -125$, $\Phi = 90$, (c) $\theta = -150$, $\Phi = 90$, (d) $\theta = -175$, $\Phi = 90$. θ is the rotation angle from left to right and Φ is the rotation angle up and down.

keep the net analyte mobility at a constant concentration of one additive through the adjustment of the concentration of another additive was discussed and the existence of contour lines was introduced. The locations where the contour lines cross the two concentration axes at a 45° angle (the waist) was also presented. It has been determined that by using the individual micro and macro capacity factors in multiple additive CE systems, chemical separations can be designed from the fundamental properties of each component.

Glossary

- capillary electrophoresis (CE)
- electroosmotic flow (EOF)
- cyclodextrin (CD)
- β-cyclodextrin (β-CD)
- high performance liquid chromatography (HPLC)
- liquid chromatography (LC)
- gas chromatography (GC)
- mass spectrometry (MS)
- micellar electrokinetic capillary chromatography (MECC)
- mass-to-charge ratio (m/z)
- dodecyltrimethylammonium bromide (DTAB)
- tetramethylammonium bromide (TMAB)
- adenosine (A)
- adenosine monophosphate (AMP)
- adenosine diphosphate (ADP)
- adenosine triphosphate (ATP)
- critical micelle concentration (CMC)
- sulfobutylether-β-cyclodextrin (SBE-β-CD)
- hydroxypropyl-β-cyclodextrin (HP-β-CD)
- degree of substitution (DS)

References

(1) Landers, J. P., "*Handbook of Capillary Electrophoresis*", CRC Press, Inc., Boca Raton, 1994.

(2) Hjerten, S., *Chromatogr. Rev.* 1967, *9*.

(3) Tiselius, A., *Trans. Faraday Soc.* 1937, *33*.

(4) Heiger, D. N., "*High Performance Capillary Electrophoresis - An Introduction*", 2nd ed., Hewlett-Packard Company, 1992.

(5) Rasmussen, H. T., Goebel, L. K., McNair, H. M., *J. Chromatogr. A* 1990, *517*, 549-555.

(6) Little, E. L., Foley, J. P., *J. Microcol. Sep.* 1992, *4*, 145-154.

(7) Otsuka, K., Terabe, S., *J. Liq. Chromatogr.* 1993, *16*, 945-953.

(8) Lurie, I. S., Klein, R. F., Dal Cason, T. A., LeBelle, M. J., Brenneisen, R., Weinberger, R. E., *Anal. Chem.* 1994, *66*, 4019-26.

(9) Ye, B., Hadjmohammadi, M., Khaledi, M. G., *J. Chromatogr. A* 1995, *692*, 291-300.

(10) Rundlett, K. L., Armstrong, D. W., *Anal. Chem.* 1995, *67*, 2088-2095.

(11) Peng, X. J., Bowser, M. T., Britz-McKibbin, P., Bebault, G. M., Morris, J. R., Chen, D. D. Y., *Electrophoresis* 1997, *18*, 706-716.

(12) Terabe, S., Otsuka, K., Ichikawa, K., Tsuchiya, A., Ando, T., *Anal. Chem.* 1984, *56*, 111.

(13) Terabe, S., Otsuka, K., Ando, T., *Anal. Chem.* 1985, *57*, 834.

(14) Peng, X. J., Bebault, G. M., Sacks, S. L., Chen, D. D. Y., *Can. J. of Chem.* 1997, *75*, 507-517.

(15) Bowser, M. T., Sternberg, E. D., Chen, D. D. Y., *Electrophoresis* 1997, *18*, 82-91.

(16) Britz-McKibbin, P., Chen, D. D. Y., *J. Chromatogr.* 1997, *781*, 23-34.

(17) Bowser, M. T., Chen, D. D. Y., *submitted* 1997.

(18) Bowser, M. T., Chen, D. D. Y., *submitted* 1997.

(19) Connors, K. A., "*Binding Constants - The Measurement of Molecular Complex Stability*", John Wiley & Sons, New York, 1987.

(20) Deming, W. E., *Phil. Mag.* 1931, *11*.

(21) Deming, W. E., *Phil. Mag.* 1935, *19*.

(22) Deming, W. E., *Phil. Mag.* 1934, *17*.

(23) Laidler, K. J., Meiser, J. H., "*Physical Chemistry*", The Benjamin/Cummings Publishing Company, Inc., Menlo Park, CA, 1982.

(24) Terabe, S., Ozaki, H., Otsuka, K., Ando, T., *J. Chromatogr.* 1985, *332*, 211-217.

(25) Guttman, A., Paulus, A., Cohen, A. S., Grinberg, N., Karger, B. L., *J. Chromatogr.* 1988, *448*, 41-53.

(26) Wren, S. A. C., Rowe, R. C., *J. Chromatogr.* 1992, *603*, 235-241.

(27) Shibukawa, A., Lloyd, D. K., Wainer, I. W., *Chromatographia* 1993, *35*, 419-429.

(28) Wren, S. A. C., *J. Chromatogr.* 1993, *636*, 57-62.

(29) Rawjee, Y. Y., Staerk, D. U., Vigh, G., *J. Chromatogr.* 1993, *635*, 291-306.

(30) Rawjee, Y. Y., Williams, R. L., Vigh, G., *J. Chromatogr.* 1993, *652*, 233-245.

(31) Penn, S. G., Goodall, D. M., Loran, J. S., *J. Chromatogr.* 1993, *636*, 149-52.

(32) Penn, S. G., Bergstrom, E. T., Goodall, D. M., Loran, J. S., *Anal. Chem.* 1994, *66*, 2866-73.

(33) Copper, C. L., Davis, J. B., Cole, R. O., Sepaniak, M. J., *Electrophoresis* 1994, *15*, 785-92.

(34) Penn, S. G., Bergstrom, E. T., Knights, I., Liu, G., Ruddick, A., Goodall, D. M., *J. Phys. Chem.* 1995, *99*, 3875-3880.

(35) Rundlett, K. L., Armstrong, D. W., *J. Chromatogr.* 1996, *721*, 173-186.

(36) Gyimesi, J., Szoko, E., Magyar, K., Barcza, L., *J. Include. Phenom.* 1996, *25*, 253-256.

(37) Ferguson, P. D., Goodall, D. M., Loran, J. S., *J. Chromatogr.* 1996, *745*, 25-35.

(38) Ingelse, B. A., Claessens, H. C., Vanderwal, S., Duchateau, A. L. L., Everaerts, F.M., *J. Chromatogr.* 1996, *745*, 61-71.

(39) Lee, Y. H., Lin, T. I., *Electrophoresis* 1996, *17*, 333-340.

(40) Ferguson, P. D., Goodall, D. M., Loran, J. S., *J. Chromatogr.* 1997, *768*, 29-38.

(41) Bose, S., Yang, J., Hage, D. S., *J. Chromatogr. B* 1997, *697*, 77-88.

(42) Barone, G., Castronuovo, G., Elia, V., Muscetta, M., *Thermochim. Acta* 1985, *85*, 443-446.

(43) Barone, G., Castronuovo, G., Di Ruocco, V., Elia, V., Giancola, C., *Carbohydr. Res.* 1989, *192*, 331-341.

(44) Paduano, L., Sartorio, R., Vitagliano, V., Castronuovo, G., *Thermochim. Acta* 1990, *162*, 155-161.

(45) Andini, S., Castronuovo, G., Elia, V., Gallotta, E., *Carbohydr. Res.* 1991, *217*, 87-97.

(46) Castronuovo, G., Elia, V., Fessas, D., Giordano, A., Velleca, F., *Carbohydr. Res.* 1995, *272*, 31-39.

(47) Castronuovo, G., Elia, V., Fessas, D., Velleca, F., Viscardi, G., *Carbohydr. Res.* 1996, *287*, 127-138.

(48) Liu, Y., Sturtevant, J. M., *Biophys. Chem.* 1997, *64*, 121-126.

(49) Torgerson, P. M., Drickamer, H. G., Weber, G., *Biochem.* 1979, *18*, 3079-3083.

(50) Cox, G. S., Turro, N. J., *Photochem. Photobiol.* 1984, *40*, 185-188.

(51) Bright, F. V., Keimig, T. L., McGown, L. B., *Anal. Chim. Acta* 1985, *175*, 189-201.

(52) Orstan, A., Ross, J. B. A., *J. Phys. Chem.* 1987, *91*, 2739-2745.

(53) Sanchez, F. G., Lopez, M. H., Gomez, J. C. M., *Analyst* 1987, *112*, 1037-1040.

(54) Nelson, G., Patonay, G., Warner, I. M., *Anal. Chem.* 1988, *60*, 274-279.

(55) Catena, G. C., Bright, F. V., *Anal. Chem.* 1989, *61*, 905-909.

(56) Hamai, S., *J. Phys. Chem.* 1989, *93*, 2074-2078.

(57) Hamai, S., *J. Am. Chem. Soc.* 1989, *111*, 3954-3957.

(58) Munoz de la Pena, A., Duran-Meras, I., Salinas, F., Warner, I. M., Ndou, T. T., *Anal. Chim. Acta* 1991, *255*, 351-357.

(59) Duran-Meras, I., Munoz de la Pena, A., Salinas, F., Caceres, I. R., *Analyst* 1994, *119*, 1215-1219.

(60) Park, J. W., Park, K. H., *J. Include. Phenom.* 1994, *17*, 277-290.

(61) Aaron, J. J., Laassis, B., Mahedro, M. C., Munoz de la Pena, A., Salinas, F., *J. Include. Phenom.* 1994, *18*, 69-79.

(62) Maafi, M., Laassis, B., Aaron, J. J., Mahedero, M. C., Munoz de la Pena, A., Salinas, F., *J. Include. Phenom.* 1995, *22*, 235-247.

(63) Letellier, S., Maupas, B., Gramond, J. P., Guyon, F., Gareil, P., *Anal. Chim. Acta* 1995, *315*, 357-363.

(64) Duran-Meras, I., Munoz de la Pena, A., Salinas, F., Caceres, I. R., *Applied Spectroscopy* 1997, *51*, 684-688.

(65) Lin, M., Jayawickrama, D. A., Rose, R. A., DelViscio, J. A., Larive, C. K., *Anal. Chim. Acta* 1995, *307*, 449-457.

(66) Gelb, R. I., Schwartz, L. M., Cardelino, B., Fuhrman, H. S., Johnson, R. F., Laufer, D. A., *J. Amer. Chem. Soc.* 1981, *103*, 1750-1757.

(67) Matsui, Y., Mochida, K., *Bull. Chem. Soc. Jpn.* 1979, *52*, 2808-2814.

(68) Sebille, B., Thuaud, N., Piquion, J., Behar, N., *J. Chromatogr.* 1987, *409*, 61-69.

(69) Uekama, K., Hirayama, F., Nasu, S., Matsuo, N., Irie, T., *Chem. Pharm. Bull.* 1978, *26*, 3477-3484.

(70) Debowski, J., Sybilska, D., Jurczak, J., *J. Chromatogr.* 1982, *237*, 303-306.

(71) Fujimura, K., Ueda, T., Kitagawa, M., Takayanagi, H., Ando, T., *Anal. Chem.* 1986, *58*, 2668-2674.

(72) Blyshak, L. A., Dodson, K. Y., Patonay, G., Warner, I. M., *Anal. Chem.* 1989, *61*, 955-960.

(73) Mohseni, R. M., Hurtubise, R. J., *J. Chromatogr.* 1990, *499*, 395-410.

(74) Moeder, C., O'Brien, T., Thompson, R., Bicker, G., *J. Chromatogr. A* 1996, *736*, 1-9.

(75) Sadlej-Sosnowska, N., *J. Include. Phenom.* 1997, *27*, 31-40.

(76) Penn, S. G., Goodall, D. M., Monnig, C. A., Loran, J. S., *43rd ASMS Conference on Mass Spectrometry and Allied Topics.*

(77) Nishi, H., Tsumagari, N., Kakimoto, T., Terabe, S., *J . Chromatogr.* 1989, *465*, 331-43.

(78) Nishi, H., Tsumagari, N., Kakimoto, T., Terabe, S., *J . Chromatogr* . 1989, *477*, 259-70.

(79) Kaneta, T., Tanaka, S., Taga, M., Yoshida, H., *Anal. Chem.* 1992, *64*, 798-801.

(80) Terabe, S., *J. Pharm. Biomed. Anal.* 1992, *10*, 705-15.

(81) Bjergegaard, C., Moller, P., Sorensen, H., *J. Chromatogr.* 1995, *717*, 409-414.

(82) Walbroehl, Y., Jorgenson, J., *Anal. Chem.* 1986, *58*, 479-481.

(83) Wallingford, R. A., Ewing, A. G., *J. Chromatogr.* 1988, *441*, 299-309.

(84) Nashabeh, W., el Rassi, Z., *J. Chromatogr.* 1991, *536*, 31-42.

(85) Jones, W. R., Jandik, P., *J. Chromatogr.* 1991, *546*, 445-458.

(86) Romano, J., Jandik, P., Jones, W. R., Jackson, P. E., *J. Chromatogr.* 1991, *546*, 411-421.

(87) Chen, S., Pietrzyk, D. J., *Anal. Chem.* 1993, *65*, 2770-2775.

(88) Harakuwe, A. H., Haddad, P. R., Buchberger, W., *J. Chromatogr.* 1994, *685*, 161-165.

(89) Okafo, G. N., Birrell, H. C., Greenaway, M., Haran, M., Camilleri, P., *Anal. Biochem.* 1994, *219*, 201-6.

(90) Haddad, P. R., Harakuwe, A. H., Buchberger, W., *J. Chromatogr.* 1995, *706*, 571-578.

(91) Okafo, G. N., Vinther, A., Kornfelt, T., Camilleri, P., *Electrophoresis* 1995, *16*, 1917-1921.

(92) Greve, K. F., Hughes, D. E., Karger, B. L., *J. Chromatogr.* 1996, *749*, 237-245.

(93) Bjornsdottir, I., Hansen, S. H., Terabe, S., *J. Chromatogr.* 1996, *745*, 37-44.

(94) Weldon, M. K., Arrington, C. M., Runnels, P. L., Wheeler, J. F., *J. Chromatogr.* 1997, *758*, 293-302.

(95) Govindaraju, K., Ahmed, A., Lloyd, D. K., *J. Chromatogr.* 1997, *768*, 3-8.

(96) Walbroehl, Y., Jorgenson, J. W., *J. Chromatogr.* 1984, *315*, 135.

(97) Okada, T., *J. Chromatogr.* 1995, *695*, 309-317.

(98) Bowser, M. T., Kranack, A. R., Chen, D. D. Y., *Trends in Analytical Chemistry* , *accepted.*

(99) Evans, D. F., Wennerstrom, H., "*The Colloidal Domain: Where Physics, Chemistry, Biology and Technology Meet*"" VCH Publishers, New York, 1994.

(100) Bowser, M. T., Bebault, G. M., Peng, X., Chen, D. D. Y., *Electrophoresis* 1997, *18*, 2928-2934.

(101) Tswett, M. S., *Tr. Protok. Varshav. Obshch. Estestoispyt Otd. Biol.* 1903, *14*, 20-39.

(102) Martin, A. J. P., Synge, R. L. M., *Biochem. J.* 1941, *35*, 1358-1368.

(103) Svedberg, T., Rinde, H., *J. Amer. Chem. Soc.* 1924, *46*, 2677-2693.

(104) Tiselius, A. *The moving boundary method of studying the electrophoresis of proteins (Thesis)*, Almqvist & Wiksell, Uppsala, 1930.

(105) Jorgenson, J. W., Lukacs, K. D., *Anal. Chem.* 1981, *53*, 1298-302.

(106) Armstrong, D. W., Fendler, J. H., *Biochimica et biophysica Acta* 1977, *478*, 75-80.

(107) Armstrong, D. W., Terrill, R. Q., *Anal. Chem.* 1979, *51*, 2160-2163.

(108) Armstrong, D. W., Nome, F., *Anal. Chem.* 1981, *53*, 1662-1666.

(109) Terabe, S., Ozaki, H., Otsuka, K., Ando, T., *J. Chromatogr.* 1985, *332*, 211-217.

(110) Hinze, W. L., Armstrong, D. W., *Anal. Letters* 1980, *13*, 1093-1104.

(111) Armstrong, D. W., DeMond, W., Alak, A., Hinze, W. L., Riehl, T. E., Bui, K. H., *Anal. Chem.* 1985, *57*, 234-237.

(112) Hinze, W. L., Riehl, T. E., Armstrong, D. W., DeMond, W., Alak, A., Ward, T., *Anal. Chem.* 1985, *57*, 237-242.

(113) Guttman, A., Paulus, A., Cohen, A. S., Grinberg, N., Karger, B. L., *J. Chromatogr.* 1988, *448*, 41-53.

(114) Fanali, S., *J. Chromatogr.* 1989, *474*, 441-446.

(115) Snopek, J., Soini, H., Novotny, M., Smolkova-Keulemansova, E., Jelinek, I., *J. Chromatogr* . 1991, *559*, 215-22.

(116) Nishi, H., Fukuyama, T., *J. Chromatogr.* 1991, *553*, 503-516.

(117) Wren, S. A. C., Rowe, R. C., *J. Chromatogr.* 1992, *603*, 363-367.

(118) Bjørnsdottir, I., Hansen, S. H., *J. Chromatogr.* 1995, *711*, 313-322.

(119) Luna, E. A., Bornancini, E. R. N., Thompson, D. O., Rajewski, R. J., Stella, V. J., *Carb. Res.* 1997, *299*, 103-110.

(120) Tait, R. J., Thompson, D. O., Stella, V. J., Stobaugh, J. F., *Anal. Chem.* 1994, *66*, 4013-4018.

(121) Szolar, O. H. J., Brown, R. S., Luong, J. H. T., *Anal. Chem.* 1995, *67*, 3004-3010.

(122) Bowser, M. T., Kranack, A. R., Chen, D. D. Y., *Anal. Chem.* 1998, *in press*.